

DEVELOPMENT OF A REFERENCE ELECTRODE FOR
APPLICATION IN LOW TO MID TEMPERATURE AQUEOUS
SOLAR ENERGY ENVIRONMENTS

by

Bruce R. Lanning



June 4, 1981

CLOSED RESERVE

ARTHUR LAKES LIBRARY
COLORADO SCHOOL of MINES
GOLDEN, COLORADO 80401

ProQuest Number: 10782288

All rights reserved

INFORMATION TO ALL USERS

The quality of this reproduction is dependent upon the quality of the copy submitted.

In the unlikely event that the author did not send a complete manuscript and there are missing pages, these will be noted. Also, if material had to be removed, a note will indicate the deletion.



ProQuest 10782288

Published by ProQuest LLC (2018). Copyright of the Dissertation is held by the Author.

All rights reserved.

This work is protected against unauthorized copying under Title 17, United States Code
Microform Edition © ProQuest LLC.

ProQuest LLC.
789 East Eisenhower Parkway
P.O. Box 1346
Ann Arbor, MI 48106 – 1346

A thesis submitted to the Faculty and the Board of Trustees of the Colorado School of Mines in partial fulfillment of the requirements for the degree of Master of Science (Metallurgical Engineering).

Golden, Colorado

Date June 4, 1981

Signed: *Bruce Lanning*
Bruce Lanning

Approved: *William A. Averill*
William A. Averill
Thesis Advisor

Golden, Colorado

Date June 4, 1981

William D. Copeland
William D. Copeland
William D. Copeland v
Professor/Head
Department of Metallurgical
Engineering

ABSTRACT

The uniqueness of solar energy systems precludes the transfer and application of the existing technology used in conventional energy conversion systems such as nuclear and fossil fuel systems. In low to mid temperature environments between 25-300C, solar containment materials are subjected to high thermal gradients and applied stresses, asymmetric heat fluxes, high ultraviolet radiation, diurnal duty cycles, and thermal cycling that will effect both the mechanical and chemical properties of the containment materials. With the combined synergistic effects of solar systems on accelerating corrosion rates and the economics for using low cost containment materials with extended service lives, field inspection and monitoring are needed during actual operation of these systems. Therefore, the three electrode system was chosen as an appropriate monitor to understand the corrosion and electrochemical mechanisms in solar systems. Since the reference electrode is quite often the limiting factor in the three electrode monitor, the research objective was to design and develop or adapt a new or existing reference electrode to solar energy systems.

The documented solid-solution type reference electrodes were reviewed for specific application in solar systems. Conventional or commercial electrodes, electrode adaptations with junctions or membranes, and also electrode innovations were tested for thermodynamic (or non-thermodynamic) stability and reversibility in mid temperature, thermally cycled environments. Stability measurements were made in a glass-lined, stainless steel autoclave and potentiodynamic measurements were made with a Model 350 PAR potentiostat.

Cu/CuSO₄, calomel, and Ag/AgCl electrodes were tested in neutral, H₂SO₄, HCl, and ethylene glycol-water solutions and the Ag/AgCl and new Pd-H electrodes were thoroughly tested in 0.01 M HCl. Below 120C, the Cu/CuSO₄, satd. calomel, and Ag/AgCl were reasonably stable and predictable in the neutral, H₂SO₄, HCl, and ethylene glycol-water solutions. Above 150C, both the thermal and electrolytic-type Ag/AgCl electrodes with zirconia junctions were unstable. Thermal-type Ag/AgCl electrodes were not only sensitive to light but impurities, such as borosilicate from high alkali glassware. A new palladium-hydride membrane electrode with black platinum coating on the inside (gas) and outside (solution) surfaces behaved well at temperatures up to 260C in 0.01 M HCl solutions. The potential determining

reaction and hence, behavior, was shown to be identical to the standard hydrogen electrode and also reversible ± 50 mv from the rest potential. Although this Pd-H membrane electrode behaves well under thermally cycled conditions, it can be contaminated by silver and possibly other noble cationic impurities which are reduced by atomic hydrogen. Also, the type of impurities which poison the platinum substrate such as sulfur, arsenic, and antimony, may impair the performance of this Pd-H electrode. As a candidate reference in a three electrode solar monitor, however, the versatility, predictability, and stability of the Pd-H membrane electrode tested in this research make this electrode a viable choice.

TABLE OF CONTENTS

	PAGE
ABSTRACT	iii
TABLE OF CONTENTS	vi
LIST OF FIGURES	x
LIST OF TABLES	xiii
ACKNOWLEDGEMENTS	xiv
CHAPTER 1 INTRODUCTION	1
1.1 Purpose of this Study	5
1.2 Organization of Thesis	6
CHAPTER 2 CRITERIA FOR A GOOD REFERENCE ELECTRODE	7
CHAPTER 3 SURVEY OF REFERENCE ELECTRODES	12
3.1 Internal Reference Electrodes ...	12
3.1.1 Hydrogen Electrode	12
3.1.2 Metal/Metal Oxide Electrodes	17
3.1.3 Sulfate Electrodes	19
3.1.4 Calomel or Mercury/Mercurous Chloride Electrode	21
3.1.5 Semiconductor Electrodes ..	22
3.1.6 Silver/Silver Halide Electrodes	22
3.1.7 'Thalamid' Electrode	25
3.2 Adaptations to the Internal Electrode	26
3.2.1 External Reference Electrodes	26
3.2.2 Junctions or Membrane Arrangements	28

TABLE OF CONTENTS

(Cont.)

		PAGE
3.3	Innovative Electrodes	29
	3.3.1 Platinum Substrate	30
	3.3.2 Palladium Substrate	32
	3.3.2(a) Background on Palladium Hydride	32
	3.3.2(b) Proposed Design for Pd-H Electrode	47
CHAPTER 4	EXPERIMENTAL	50
4.1	Apparatus	50
4.2	Polarization Measurements	54
	4.2.1 Palladium Hydride	54
	4.2.2 Silver Metal	54
4.3	Electrode Design	55
4.4	Materials (Reagents) and Electrode Preparation	59
	4.4.1 Ag/AgCl Preparation	60
	4.4.2 Pd-H Preparation	62
CHAPTER 5	RESULTS AND DISCUSSION	65
5.1	Preliminary Tests of Commercial Reference Electrodes	65
5.2	Thermal Type Ag/AgCl	71
5.3	Electrolytic Type Ag/AgCl	76
5.4	Palladium Hydride Electrode	84
	5.4.1 Membrane Methodology	85
	5.4.2 Initial Tests of a Pure Pd Tube	87

TABLE OF CONTENTS

	(Cont.)	PAGE
5.4.3	Response of Pd-H Electrode at Higher Temperatures and Pressures with Various Surface Conditions	88
5.4.4	Observations of the Influence of Pre-treatment on Electrode Behavior	92
5.4.5	Performance of a Suitable Pd-H Electrode	96
5.4.5(a)	Thermodynamic Stability	97
5.4.5(b)	Effect of pH	104
5.4.5(c)	Reversibility	107
5.4.5(d)	Pd-H Performance in Various Solutions ...	108
5.4.5(e)	Thermal Cycling	110
5.4.5(f)	Determination of a Reaction Mechanism at the Pd-H Electrode	111
CHAPTER 6	Summary	117
REFERENCES CITED	121
APPENDIX	127
A1	Estimation of Gibbs Free Energies at Elevated Temperatures for the Ag/AgCl - H ⁺ /H ₂ System	127
A2	Estimation of Potential Difference for the Ag/AgCl - Pd-H System	129
A2.1	Calculation of the Standard Electrode Potential (E _T ⁰)	129
A2.2	Calculation of Potential Difference Assuming a Constant Hydrogen Pressure	131

TABLE OF CONTENTS

	(Cont.)	PAGE
A2.3	Calculation of Potential Difference Assuming Hydrogen Pressure Varies with α_{\max}	132
A3	Estimation of Activity Coefficients with the Debye-Huckel Limiting Law	134
A4	Determination of Pd-H Rate Determining Step	136
A5	Polarization Measurements	139

LIST OF FIGURES

FIGURE		PAGE
1.1	A Schematic of the Three Electrode System with a Standard Hydrogen Electrode Reference	3
2.1	A) A Circuit Representation of the Electrical Double Layer B) Typical Polarization Scan; 1) Non-reversibility and 2) Reversibility	9
3.1	A Schematic of the Potential Drops (excluding liquid junctions or membranes) Across the Measurement Circuit	13
3.2	Relationship Between R/R_0 (and E) and H/Pd	33
3.3	Pressure-Composition (P-C) Relationships at Higher Temperatures and Pressures	35
3.4	Hysteresis of P-C Relationships ..	37
3.5	A) Dimensional Changes as a Function of Electrolytic Hydrogen Absorption Cycles B) Relative Length and Width Changes After 92 Cycles	40
3.6	A) Potential vs Composition for Pd-H Electrode at 25C B) Cell Potential Isobars for the Pd-H Electrode	46
3.7	A Schematic of the Pd-H Membrane Electrode Used in this Study	48
4.1	A Half Section of the Autoclave Assembly	51
4.2	A) Schematic of the Measurement Circuit and B) Top View of the Blast Shield and Autoclave Assembly	52

LIST OF FIGURES
(Cont.)

FIGURE		PAGE
4.3	A Schematic Drawing of the A) Ag/AgCl Electrode and B) Cu/CuSO ₄ Electrode Used in this Study	56
4.4	A Schematic of the Pd-H Electrode	58
5.1	Standard Electrode Potentials of the 0.1 N KCl Calomel Electrode (vs Ag/AgCl) as a function of Temperature for Various Electrolytes	66
5.2	Standard Electrode Potentials of the S.C.E. Electrode (vs Ag/AgCl) as a Function of Temperature for Various Electrolytes	67
5.3	Standard Electrode Potentials of the Cu/CuSO ₄ Electrode (vs Ag/AgCl) as a function of Temperature for Various Electrolytes	68
5.4	The Effect of Cl ⁻ Concentration on the Standard Electrode Potential of the 0.1 M KCl and Satd. Calomel and Cu/CuSO ₄ Electrodes (vs Ag/AgCl)	70
5.5	Optical Micrographs of AgCl Electrodes	75
5.6	Potential Difference Between Two Identical Ag/AgCl Electrodes in 0.01 M HCl at Elevated Temperatures	78
5.7	Potential Difference Between Two Identical Ag/AgCl Electrodes in 0.01 M HCl at Elevated Temperatures	79
5.8	Potential Difference Between Two Identical Ag/AgCl Electrodes in 0.01 M H ₂ SO ₄ at Elevated Temperatures	80
5.9	A Schematic of the Pd-H Membrane Electrode used in this Study	86
5.10	Measured Potentials of the Ag/AgCl - Pd-H/H ₂ System in 0.01 M HCl at Elevated Temperatures	90

LIST OF FIGURES
(Cont.)

FIGURE		PAGE
5.11	Measured Potentials of the Ag/AgCl - Pd-H/H ₂ System in 0.01 M HCl at Elevated Temperatures	91
5.12	Optical Micrographs of Palladium	93
5.13	Optical Micrographs of Palladium	94
5.14	Measured Potentials of the Ag/AgCl - Pd-H/H ₂ System in 0.01 M HCl at Elevated Temperatures (variable α_{max})	99
5.15	Potential versus Temperature for the Pd-H Electrode in 0.01 M HCl Solution (satd. Calomel Reference)	102
5.16	Measured Potentials of the Ag/AgCl - Pd-H/H ₂ System in 0.01 M HCl at Elevated Temperatures (constant H ₂)	103
5.17	Measured Potentials of the Ag/AgCl - Pd-H/H ₂ System in 0.01 M HCl at Elevated Temperatures (zirconia junction)	105
5.18	pH Dependence of the Pd-H Electrode	106
5.19	Typical Linear Polarization Scan of the Pd-H Electrode	109
5.20	Cathodic Current Density versus Potential for the H ⁺ /Pd-H Redox Reaction at 25C	115

LIST OF TABLES

TABLE		PAGE
5.1	Preparation and Description of Optical Micrographs	95
5.2	Results of X-Ray Diffraction Analysis of Pd-H	95

ACKNOWLEDGMENTS

The author is grateful for all the help and assistance rendered by a number of people in the department of Metallurgy at the Colorado School of Mines. The committee members Dr. Gerard Martins and Dr. David Olson were particularly patient and helpful and should be acknowledged. My advisor, Dr. William Averill should, of course, be acknowledged in this context.

Many business and personal friends were very understanding and generous throughout our interactions. N.E. Bedner, in the Ceramic Products Division of Corning Glass Works, not only put forth the extra time and effort to help this distraught graduate student, but also donated his zirconia products to our research cause. Steve Pohlman and Pat Russel at the Solar Energy Research Institute, were the inspiration and added responsibility that this graduate student needed to try and meet those deadlines. Hence, I am very grateful for all of their services.

I would also like to acknowledge the Colorado School of Mines for its teaching assistantship, the Mining and Mineral Resource Research Center for their Fellowship, and SERI for their project funds.

Finally, I'd like to extend my thanks and appreciation to Bob Watson. In research, it's the day to day problems and solutions that make or break the idea. Mr. Watson's guidance and optimism helped put those ideas to work.

CHAPTER 1

INTRODUCTION

The practicality of solar energy systems is determined by the total energy production for a given capital investment and hence, there is a need to use lower cost materials with extended service lives. In comparison to other energy conversion systems such as geothermal and nuclear, the operating conditions for the solar energy systems are more demanding on the containment materials. Subjected to the diurnal, thermal cycling conditions of solar energy systems in the mid-temperature range of 25-300C, containment materials (receiver tubes, tanks, pipes) are vulnerable to a wide range of aggressive attack due to solar heat flux, impurities, and decomposition products from organic heat transfer fluids. Corrosion fatigue, stress corrosion cracking, and general localized corrosion and pitting are the primary forms of attack encountered in these systems. Knowledge of the corrosion and electro-chemical mechanisms involved in the above forms of attack are crucial in the performance of a viable solar energy system.

With the emphasis on low cost materials, the

performance of these materials in aggressive solar energy environments will have to be monitored continuously. Bench scale tests are used initially to determine service life of materials, but to avoid unexpected failure in a system with marginal material tolerances, on-line corrosion monitoring is necessary. The most frequent types of corrosion monitors used today make use of 1) weight-loss coupons, 2) pressure sensitive hydrogen probes, 3) hydrogen penetration measurements (electrochemical reduction of H^+), 4) electrical resistance (decrease area \rightarrow increase electrical resistance), 5) optical methods (e.g. laser measurement of oxide layers), and 6) electrochemical methods (linear polarization and potentiodynamic measurements) (1,2,3,4). These techniques are used to quantitatively monitor corrosion rates and indicate trends in the corrosion behavior of a material. In solar energy systems, however, an understanding of the corrosion and electrochemical mechanisms are just as important as a continuous monitor of the corrosion rate. Therefore, since the electrochemical methods are still the most complete and informative corrosion monitors today, this type of monitor is a logical choice for solar applications.

Although a basic three electrode system, as shown in Figure 1.1, is used for precise electrochemical

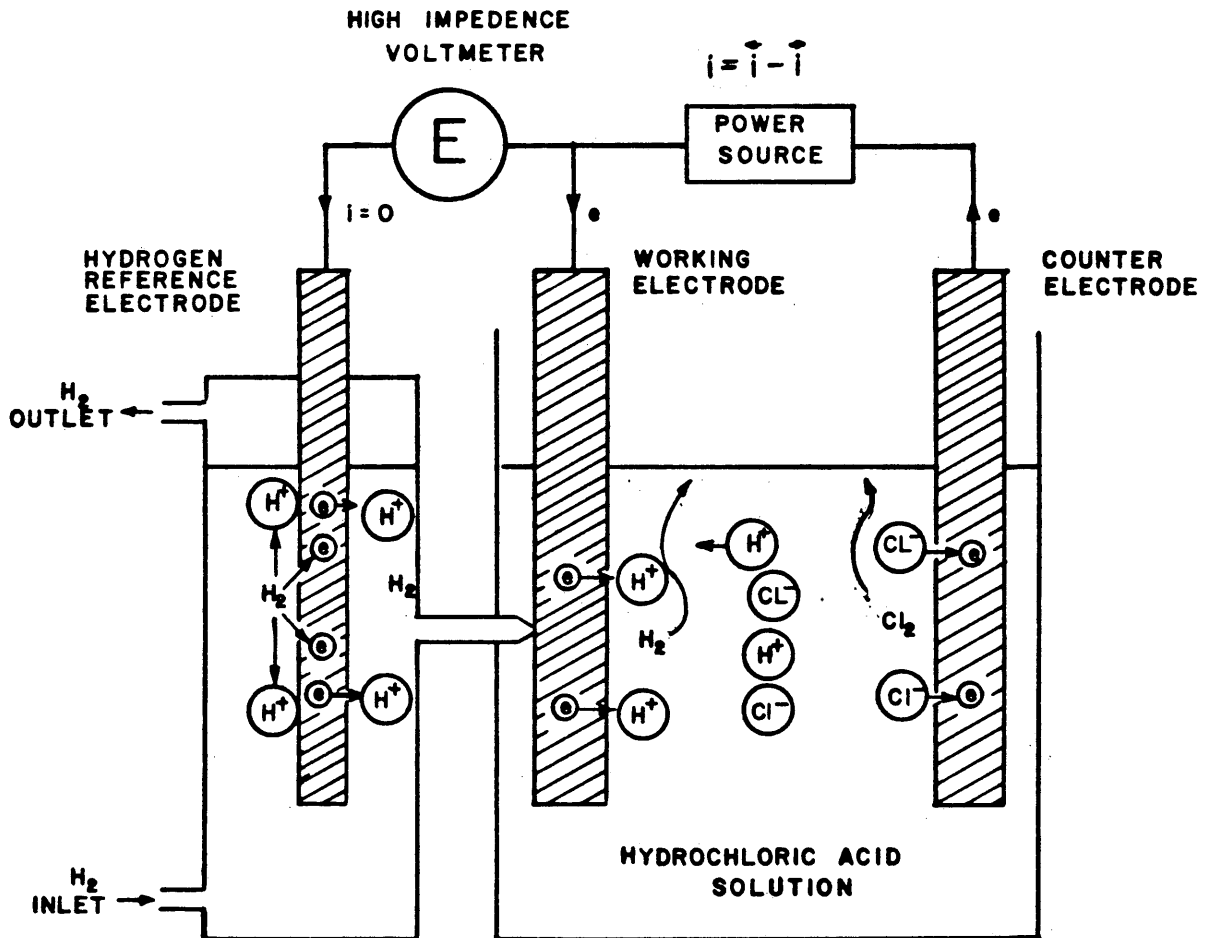


FIGURE 1.1 - A SCHEMATIC OF THE THREE ELECTRODE SYSTEM WITH A STANDARD HYDROGEN ELECTRODE REFERENCE

measurements, a two electrode system has replaced the three electrode system in some polarization resistance or low current applications. In a two electrode system, the counter electrode functions as both the counter and reference electrode. If the conductivity of the solution varies appreciably as a result of process changes, then the accuracy of the two electrode system is poor. The accuracy for this system, however, is limited to ± 20 mv (4). Since a three electrode system is a more complete monitor than a two electrode system, the three electrode system was the only system considered in this research.

A three electrode system then, consists of a working electrode, a counter electrode, and a reference electrode. The working, or test electrode, the counter electrode, the power source, and the aqueous solution, or environment, are collectively referred to as the corroding system. A counter electrode is either a source or a sink of the electrons in the overall electrochemical reaction. To insure that just electrons are consumed in the half cell reaction at the counter electrode and not the actual counter electrode, the counter electrode should be inert to the media under consideration. While a counter electrode is an integral part of this corrod-

ing system, the reference electrode is isolated from any electron flow and measures the corresponding electromotive force (emf) at the working electrode surface. In high temperature, high pressure media, the reference is quite often the limiting factor in the overall accuracy of the measuring circuit. The focus of this research was to define the established criteria for a 'good' reference electrode, survey the possible high temperature, high pressure reference electrodes, and finally, design and test prospective reference electrodes.

1.1 Purpose of this Study - The proposed objectives for this research were broad in scope, yet specific in nature. All of the documented solid-solution type reference electrodes were to be reviewed for specific application in solar energy conversion systems. Once a viable candidate(s) had been identified and thoroughly tested, it would be used to monitor the corrosion of containment materials in various service environments.

The aim of this study has been;

- 1) To select several candidate electrodes for service in solar energy collector systems (i.e. environments of 300C and 7.0×10^6 pascals and a pH range of 2-11),

- 2) To construct a high pressure autoclave system with stable material characteristics for testing the electrodes,
- 3) To evaluate the performance of promising reference electrodes within the guidelines of a 'good' reference electrode,
- 4) To establish the performance of a viable reference electrode(s) in various service environments.

1.2 Organization of Thesis - The material has been organized in the following logical manner; first restating the previously established criteria that will be used to characterize a 'good' reference electrode, then surveying the prospective electrodes in the literature, and finally evaluating the performance and viability of prospective or innovative candidate(s) in high temperature, high pressure environments.

CHAPTER 2

CRITERIA FOR A GOOD REFERENCE ELECTRODE

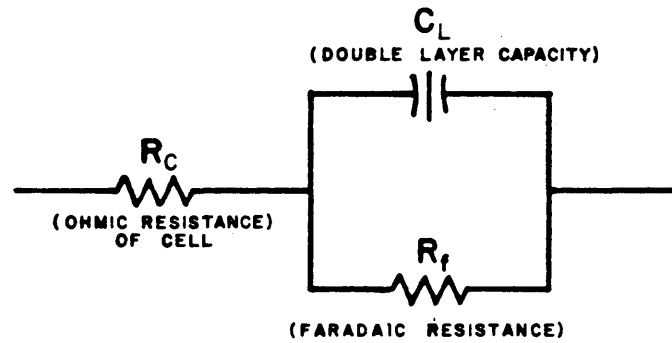
.... if for a given electrode in equilibrium all but one of the components are in standard states, the chemical potential of the component which is not in a standard state may be obtained by 'reference' to the measured potential difference. (5)

This description by Ives and Janz establishes the purpose of a 'reference' electrode. An electrode, containing both the solid and solution phase components in equilibrium with known chemical potentials, ideally maintains a stable potential difference across its solid-solution interface. In turn, this intrinsic, invariant potential of an electrode is used as a reference to determine the unknown potentials at other solid-solution interfaces. If external influences alter the equilibrium of the reference electrode, the electrode must be able to quickly re-establish equilibrium and this fixed emf value across the solid-solution interface. Even though this description pertains to the ideal thermodynamic electrode, other non-equilibrium, non-thermodynamic electrodes can be used as a reference electrodes.

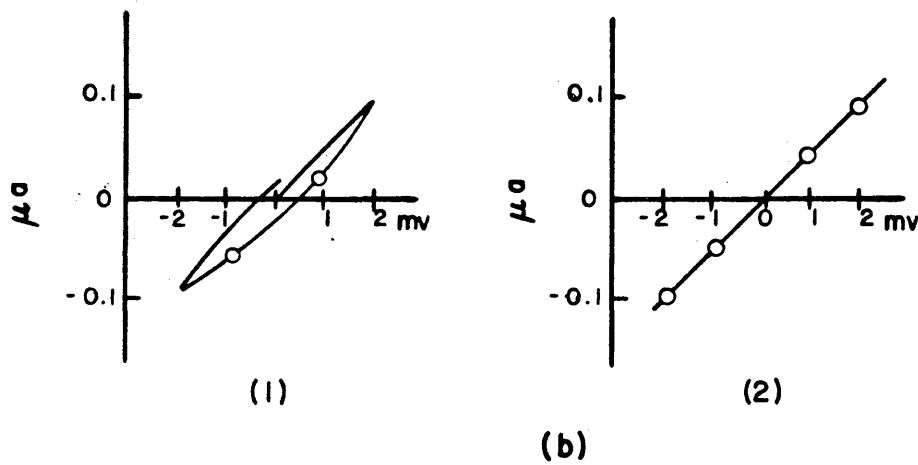
Any thermodynamic or non-thermodynamic electrode must not only be stable but compatible with the test

solution. For a given set of conditions, the potential drop across the solid-solution interface must be predictable and invariant. An unstable, unpredictable electrode would obviously not serve as a suitable reference or control. To measure the stability of an electrode however, the electrode is placed in a high impedance measuring circuit. Since an infinite or high impedance circuit is often unattainable, current may pass across the solid-solution interface and polarize the electrode. If an electrode is subjected to small polarizing currents and becomes unstable, then this type of electrode would not be considered a 'good' reference electrode. This non-polarizable or reversible criteria of a 'good' reference electrode will be discussed in a little more detail.

An ideally non-polarizable, or reversible electrode will allow infinite electron (or positive charge carrying current) transfer without upsetting the fixed potential difference across the solid-solution interface. A circuit analogy, presented in Figure 2.1(a), will help to explain the polarizable and non-polarizable surfaces. The bulk of the solution is situated at the left edge of the schematic and the solid surface is situated at the right edge. From the bulk of the solution up to the fixed, hydrated ions at the outer Helmholtz



(a)



(1)

(2)

(b)

FIGURE 2.1 - A) A CIRCUIT REPRESENTATION OF THE ELECTRICAL DOUBLE LAYER
 B) TYPICAL LINEAR POLARIZATION SCAN;
 1) NON-REVERSIBILITY AND 2) REVERSIBILITY

plane of the double layer, the average resistance of the cell is given by R_c . The resistor, R_f , and capacitor, C_L , in parallel, represent the double layer at the solid-solution interface. An ideally non-polarizable electrode would have a value of $R_f = 0$, and a fixed capacitance, whereas, an ideally polarizable electrode would have a value of $R_f = \infty$ (high impedance) and a variable voltage drop across the capacitor. This circuit also explains why a non-polarizable electrode has a large exchange current density; since the magnitude of R_f is small, a large current can pass undeterred through the double layer. Therefore, to determine whether an electrode is polarizable, small cathodic and anodic currents are applied to the electrode and the corresponding potential response is observed. An electrode must be reversible at voltages ± 10 mv from the rest potential(5). Non-reversible and reversible behavior are shown in Figure 2.1(b).

It has been established that a 'good' reference electrode must be stable and reversible, yet this assumes that the electrode is compatible with the test solution. Use of a reference electrode in a non-compatible test solution may create a significant concentration gradient across the junction material. As the concentration gradient decreases with time, a

junction potential is created, causing the electrode potential to drift. At low temperatures, the ionic diffusion rates in the junction material may be so low that the electrode may falsely exhibit a stable response, yet at higher temperatures, and accelerated diffusion rates the junction potential may significantly influence the measured emf. Any type of thermodynamic or non-thermodynamic electrode, isolated from the system behind a junction material, is susceptible to these junction effects.

Finally, the following criteria were used to assess the viability of a 'good' reference electrode. For a given set of conditions, all thermodynamic and non-thermodynamic electrodes must be 1) stable and 2) reversible at potentials ± 10 mv from the rest potential. A thermodynamic electrode, used for thermodynamic measurements, must respond to changes in temperature and specie activity according to the Nernst equation;

$$E = E^{\circ} + RT/nF \ln(\Pi a_i^{\nu}).$$

Though most reference electrodes used in corrosion studies are steady state rather than equilibrium electrodes, the solid-solution reference electrodes, considered in this study, were reviewed according to the above criteria for a 'good' thermodynamic reference electrode.

CHAPTER 3

SURVEY OF REFERENCE ELECTRODES

3.1 Internal Reference Electrodes - Any electrode in direct contact with, or enclosed within, the test environment has been classified as an internal reference electrode for this study. The following discussion of the documented internal electrodes does not consider possible junctions, membranes, or similar configurations.

3.1.1 Hydrogen Electrode - The basic configuration for measuring the emf of a system is shown in Figure 3.1. It should be noted here that while a general treatment would consider any conducting solid, only the metal/solution interface will be considered.

The overall potential consists of:

$$E_{S/M_1} + E_{M/M_1} + E_{M/M_2} + E_{M_2/S} + (IR)_{\text{solution}}$$

Assuming the solution is highly conductive, then the overall potential of the above cell will consist of the potential drop across two metal/solution interfaces and the two metal/metal junctions. The potential drop across one Metal(1)/solution interface, however, cannot be determined without the presence of another Metal(2)/

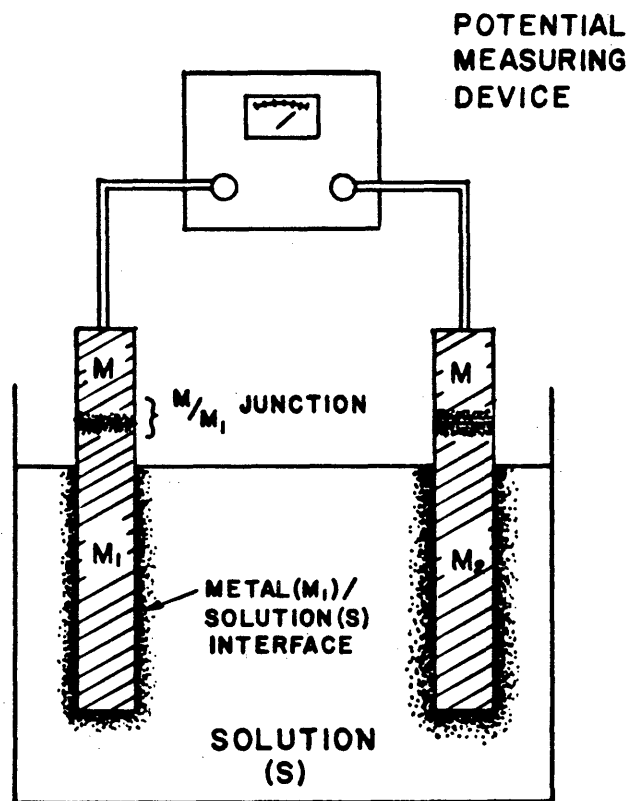
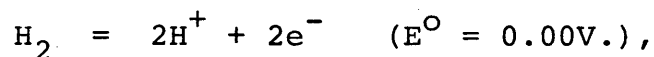


FIGURE 3.1 - A SCHEMATIC OF THE POTENTIAL DROPS (EXCLUDING LIQUID JUNCTIONS OR MEMBRANES) ACROSS THE MEASUREMENT CIRCUIT

solution interface, Since the emf of a single electrode cannot be determined (i.e. the Galvani or Inner potential), a standard half cell reaction at one electrode, with known chemical potentials, has been established as a reference. The standard half cell reaction is;



or otherwise known as the standard hydrogen electrode (SHE). Referring back to the above schematic, the 0.00 V. emf pertains to the M(1)/S interface or the above half cell reaction, and both the Metal/Metal junction potentials. Therefore, the measured potential would refer to the remaining M(2)/S interface or the other half cell reaction. The designation of a reference standard, such as the hydrogen reaction, was essentially arbitrary.

Theoretically, a standard hydrogen electrode must maintain equilibrium between an activity of hydrogen ions equal to one and a partial pressure of dissolved molecular hydrogen equal to one atmosphere. The reaction is generally catalyzed by a solid substrate such as platinum, or platinoids. A good substrate should actively adsorb hydrogen molecules, reduce the activation energy barrier for hydrogen atomization, and finally dislodge the atom from its adsorbed state. This particular sequence of steps is known as ionization. Although the hydrogen reaction on platinum is exothermic, the catalytic

activity of platinum diminishes with time. One theory, concerning the catalytic activity of platinum, suggests deep and shallow sites for the discharging ($H^+ + e \rightarrow H_{(ads)}$) and ionization ($H_{(ads)} \rightarrow H^+ + e$) processes respectively(6). A local galvanic couple is established between the deep cathodic sites and the shallow anodic sites on the platinum surface which ultimately destroys the catalytic properties in a fashion not unlike galvanic corrosion. Surface heterogeneity, associated with a high surface area coating though, is crucial for the kinetics of a rapid hydrogen evolution reaction. Just mentioning a few characteristics of hydrogen catalysts reveals the complexity of the overall reaction scheme and yet, the theoretical premise is simple; activity of hydrogen ions equal to one in equilibrium with dissolved molecular hydrogen at a pressure of one atmosphere.

Ideally, the hydrogen electrode would be an optimum reference electrode. It is the standard, or reference, for all electrochemical reactions. The H_2 and H^+ components are relatively stable at high temperatures, the hydrogen evolution reaction on platinum and platinoids is fairly well known, and the electrode is known to exhibit reversible behavior. Realistically though, the standard hydrogen reaction is an impractical and cumbersome equilibrium reaction to achieve.

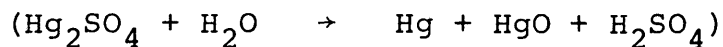
Assuming an inert, catalytic substrate is available, the activity of hydrogen atoms ($a_{\text{H}}^+ = 1$) and the hydrogen partial pressures are difficult quantities to measure. At hydrogen ion activities or concentrations above 0.01 M, a concentration gradient develops across the junction material, and the liquid junction potentials become significant in the measured potential. Because of this, the Bureau of Standards has established a known, practical pH range between 2-12(7). Also, with increasing temperature and hence, total pressure, the partial pressure of hydrogen is again difficult to determine. There are also concentration gradients and diffusion barriers between the surface and the bulk of the solution which alter the ideal activities at the electrode surface. A standard hydrogen electrode would be an optimum high temperature-pressure electrode to strive for, but the inherent problems of the actual electrode render this type of electrode impractical.

Now that the standard hydrogen electrode has been outlined, having been a logical place to start in the evaluation of reference electrodes, the various types of reference electrode systems reported in the literature will be discussed. Each electrode 'type' will be reviewed according to their performance in aqueous systems

at elevated temperatures and increased pressures (300C and 6.9×10^6 pascals) for a pH range of 2-12. Special emphasis will be given to the electrodes chosen for this study and a detailed background on the palladium system will be reviewed last.

3.1.2 Metal/Metal Oxide Electrodes - According to Ives(5), the metal for a metal/metal oxide electrode must be sufficiently noble to resist chemical attack and it should also be present in a reproducible stable state of minimum free energy. If the standard potential of the electrode is positive, then there will be no tendency for the metal phase to oxidize. Finally, the oxide should possess an adequate exchange current density. Though silver is perhaps the most widely used metal/metal oxide electrode, other possible metal electrodes are presented.

Since mercury salt disproportionates at high temperatures to give HgO, the Hg/HgO electrode may therefore be a possible electrode for high temperature systems.



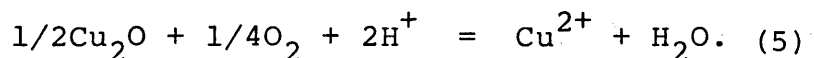
The thermodynamic viability of this electrode though, breaks down at temperatures greater than 150C (423K) in systems which contain partial pressures of hydrogen greater than 0.1 MPa(9). Also, with the Hg/HgO electrode,

there is a possible danger of mercury gas contamination. Case and Bignold(8) showed that the Hg/HgO electrode functions well in alkaline solutions. Mercury oxide showed no evidence of decomposition when electrodes were heated in 0.1 M NaOH up to 280C and the emf's were reproducible to within \pm 1 mv. They also found that if a porous polytetrafluoroethylene (PTFE) plug is used, this electrode is stable up to 250C. Because this electrode is limited to alkaline solutions, it would not be a 'good' electrode for acid solutions.

The Ag/AgO electrode behaves well up to 160C(9), but above this temperature, the AgO decomposes into Ag. Therefore, this type of reference electrode would obviously be temperature limited.

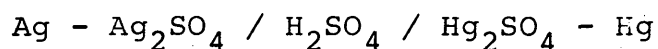
Other less noted electrodes were reviewed. The behavior of the Pt/PtO₂, Ir/IrO₂, Rh/Rh₂O₃, and Zr/ZrO₂ electrodes in HCl/NaCl, and NaOH/NaCl electrolytes have been reported by Dobson, Snodin, and Thirsk(10). All of these electrodes though, exhibited considerable temperature hysteresis on thermal cycling to 250C. As a reference electrode, antimony and bismuth have been used in some biological applications(5). According to Myers and Bonilla(11), however, the Sb/SbO electrode, used in pH measurements, behaves irregularly between 100-300C. The authors maintained that the instability

in the electrode was due to hydrate formations. Although a freshly plated copper electrode will behave like a theoretical copper-cuprous oxide electrode in the pH range of 4.7 to 8.0, the electrode potentials will deviate positively from predicted response in aerated systems. The deviation is caused by the oxidation of the film followed by the dissolution reaction;

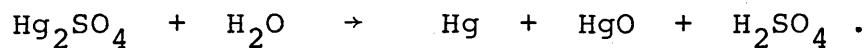


Since the solubility of Cu^{2+} is high and the metal phase can be present in two stable oxidation states, this electrode was not considered for this research.

3.1.3 Sulfate Electrodes - All of the sulfate electrodes considered for high temperature-pressure applications are limited to acid solutions (i.e. H_2SO_4). Lietzke and Stoughton(12) studied the mercury/mercurous sulfate and the silver/silver sulfate electrodes in the cell;



at temperatures up to 200C. The Hg_2SO_4 was found to hydrolyze in 0.05 M H_2SO_4 at 250C to form HgO by the following reaction;



Silver/Silver sulfate, on the other hand, is suitable for use in 0.5-0.05 M sulfuric acid at temperatures up to 250C. Since Pb/PbSO_4 appears to be serviceable in

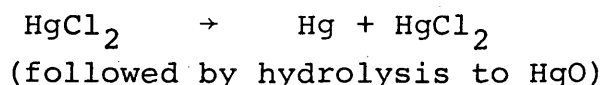
acidic solutions up to 250C, this electrode was also considered. Its activity depends only on the activity of the SO_4^{2-} ions because of the low solubility of PbSO_4 . Like the mercury/mercury sulfate and silver/silver sulfate electrodes, this reference electrode is limited to acidic solutions and the maximum temperature cited(9) is for a particular acid concentration. Finally, the Cu/CuSO_4 electrode has been used for corrosion monitoring, but it has been adopted primarily for underground corrosion work and not for high temperature-pressure conditions(13).

The Cu/CuSO_4 is one of the most widely used electrodes in field applications, it is simple to construct, and will maintain a stable potential although little research has been done at higher temperatures. Ives treatment on sulfate electrodes will explain this dilemma. An ideal sulfate electrode, according to Ives(5), should contain a sparingly soluble salt in equilibrium with the liquid phase. There are some discrepancies, however, in the basic mechanisms of the Cu/CuSO_4 electrode that should be noted. First, the solubility of CuSO_4 is high at room temperature ($K_{\text{sp}} = 1000$) and decreases appreciably with increased temperature ($K_{\text{sp}} = 1.14$ at 100C and $K_{\text{sp}} = 0.025$ at 150C) and second, the Cu/CuSO_4 system represents a fixed potential of Cu metal in equilibrium with Cu^{++} . The potential of a sulfate

electrode should consist of a sulfate salt in equilibrium with a fixed SO_4^{2-} concentration in solution. Though solubility problems may limit the usefulness of this electrode, the simplicity of design and reported stability at low temperatures warrant further investigation of the electrode at higher temperatures and pressures.

3.1.4 Calomel or Mercury/Mercurous Chloride Electrode -

Although this reference electrode is used quite extensively at room temperature and temperatures slightly above room temperature, it is not serviceable at higher temperatures(5). The main problem is the rapid loss of calomel at temperatures above 200C. Also, with the increased solubility of Hg_2Cl_2 at higher temperatures, significant junction potentials may arise. Since the calomel electrode has a rather large temperature coefficient caused chiefly by the changes in solubilities of potassium and mercurous chloride, the mercurous chloride disproportionates at higher temperatures to yield mercury and HgCl_2 by the following reaction;



Upon abrupt cooling, the electrode is no longer at equilibrium with regard to the solubility of the calomel, and the return to equilibrium is slow. Temperature hysteresis is characteristic of an electrode unable to

maintain equilibrium(5). The more concentrated the solution or electrolyte, however, the higher the critical temperature. In 0.1 M, 0.5 M, and 1.0 M $[\text{Cl}^-]$, the corresponding upper temperature limits for the calomel electrode are 80C, 200C, and 230C(5). For use as an internal reference electrode, the standard calomel electrode (SCE) is not stable at temperatures around 300C even after altering the electrolyte concentration.

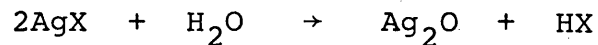
3.1.5 Semiconductor Electrodes - Semiconductor electrodes are used primarily as pH sensitive electrodes. McKaveney and Byrnes(51) have made a survey of semiconductor electrodes for use as analytical monitors at 30C. In this survey, germanium was shown to be highly sensitive to acids and bromine oxidants, indium-antimonide was 'good' in acid solutions as a pH monitor, and silicon was a 'good' sensor for acids, hydrogen peroxide oxidants, and fluorides in an acid media. Applications for the semiconductor electrodes though, appear to be confined to room temperature and these types of electrodes have not been used as a potential determining devices since their standard potentials vary at higher temperatures and pressures.

3.1.6 Silver/Silver Halide Electrodes - According to MacDonald(9), the Ag/AgBr and Ag/AgI electrodes have

been studied at temperatures to 200C. The Ag/AgI electrode appears to be unstable at temperatures above 145C; indicated by a marked deviation from a normal E_T^O versus temperature plot above this point. This instability in the silver iodide electrode was attributed to the $\alpha \rightarrow \beta$ phase modification in the structure (Ag \rightarrow AgI). Since the solubility of AgBr at room temperature and also at 100C is an order of magnitude lower than that of AgCl, this electrode appears promising. Of the tests performed with the AgBr electrode, most of the deviations in the standard potential have been attributed to the variation in electrode preparation technique. Both the AgBr and AgI electrodes though, are very sensitive to ultraviolet light. When carefully prepared and kept in the dark, the AgBr appears to be a serviceable electrode.

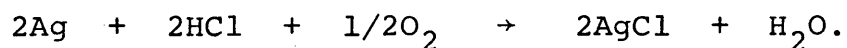
Provided the AgCl surface was sufficiently well protected from hydrogen contamination, the Ag/AgCl electrode has been the most popular and widely used reference electrode for high temperature-pressure applications. Greeley, et al(14), have measured the standard potentials of the silver/silver chloride electrode (vs SHE electrode) at temperatures to 275C. These potentials were determined in acidic solutions since the Ag/AgCl electrode is not stable in basic solutions at elevated temperatures. This limitation on the Ag/AgCl electrode is probably due to hydrolysis

effect;



where X is the halide ion(9). Depending on the type of preparation (i.e. thermal, electrolytic, or thermal-electrolytic), this reference electrode could perform very well at temperatures below 300C. Because thermal cycling at high temperatures leads to hysteresis effects, the Ag/AgCl electrode must be carefully constructed. A series of identical electrodes would have to be constructed for each set of experiments since the thermal shock of cooling down to room temperature embrittles certain components (i.e. the Ag or AgCl phases) of the electrode and is the direct cause of temperature hysteresis(9). Conventionally, a series of electrodes are first constructed with an identical design and tested for a mean standard potential at room temperature. The electrodes which are within a certain deviation from the mean standard potential are then selected for use in the experiment.

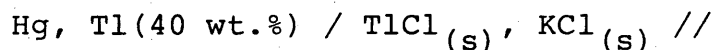
Along with the problem of hydrogenation, the silver/silver chloride electrode is very sensitive to oxygen impurities. This effect can be shown by the following reaction;



For this project, the oxygen content of the electrolyte

may be substantial and hence, oxidize the Ag metal. Although not as critical as the problem of oxygen contamination, the silver/silver chloride electrode must be allowed to age properly(5). This process may take anywhere from a few hours to several days. With careful preparation and control, the silver/silver chloride electrode is the most well known and stable reference electrode for high temperature-pressure applications and would be a good choice for this project.

3.1.7 "Thalamid" Electrode - Janaer Glaswerk(5) has developed an electrode that demonstrated apparent stability up to 135C. The electrode, dubbed 'Thalamid', half cell consists of a 40 percent thallium amalgam in contact with solid thallos chloride and a solution saturated with 3.5 m potassium chloride.



Because of the uncertainties introduced into the evaluation of the standard potential by the high solubility of thallos chloride, this cell is not used in combination with the Pt/H electrode. One favorable consequence of thallos chloride though, is its low tendency to combine with the common anion. As a result of this and unlike the calomel and even the silver/silver chloride systems, the Thalamid electrode

is free from temperature hysteresis. Though Baucke(15,16,17) has reported the standard potentials of the Thalamid electrode in aqueous solutions between 5 and 90C, this reference electrode appears to be limited to temperatures below 150C.

3.2 Adaptations to the Internal Electrode - The limitations of the internal electrodes, discussed in the previous section, may be overcome by adapting or fixing the original electrode arrangement of function in apparently unserviceable environments. These adaptations will be discussed in this section.

3.2.1 External Reference Electrodes - There is only one basic requirement in the design of an external reference electrode; the chosen reference electrode must be compatible with the external solution at 25C (298K). The pressure reducing bridge and the pressure balanced electrolytic bridge are the two necessary designs for external reference electrode bridges(9). In the pressure reducing bridge technique, the external electrode is at atmospheric pressure and is connected to the solution in the autoclave by a bridging tube. Using a water-jacketed porous asbestos, cellulose, or birchwool plug in the bridge should locate the temperature gradient in a well defined region. Care

must be taken in the selection of the materials though, since silica and silica-containing materials are soluble and the wood and the cellulose release adverse acids. Streaming potentials as high as 70 mv have been encountered using this technique(9). The second technique, pressure balanced electrolytic bridge, appears to be satisfactory. For this process, the electrode is placed in a pressure vessel at room temperature. The reference electrode is connected to the autoclave by a bridging tube which does not contain a plug (uses sand, glass, or a balanced-pressure glass KCl bridge). Stainless steel and corundum have been used for the water-cooled bridging tubes. Due to solution changes within the bridging tube, gas bubbles may form, inhibit the flow of electrolyte, and ultimately alter the measured emf. In one instance(18), an asbestos wick was used in the bridging tube and the temperature difference between the autoclave and the reference electrode was as great as 65C. The pressure balanced electrolytic bridge appears to be a practical alternative to the internal reference electrode.

The problems associated with any reference electrode, used externally, are the streaming potentials and the thermal junction potential. The streamin potential is caused by the flow of electrolyte which is brought about by a pressure drop between the autoclave and reference

electrode. In most cases, this streaming potential has been reduced to a negligible value of around \pm 0.5-1.0 mv. The thermal junction potential, which arises from the metallic thermocouple effect, the electrode temperature effect, and any thermal diffusion gradient (Soret effect), has not been adequately reduced. Although the contribution from the metallic thermocouple emf can be neglected, the other two components of the thermal junction emf are subtracted from the external measured potential to yield the corrected standard potential.

$$E_T = E_{\text{ext}} - E_{\text{therm}}$$

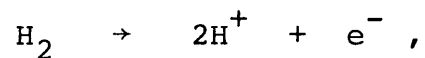
E_{therm} is given by MacDonald (9, eqn. 24). Depending on the magnitude of thermal junction effects and the accountability of these effects, an external arrangement may be acceptable in cases where internal electrodes are severely impaired.

3.2.2 Junctions or Membrane Arrangements - The most typical types of reference electrodes have either a static membrane (junction) or a direct contact with the electrolyte. With a static membrane, differential expansion at higher temperatures may lead to mixing or dilution of the electrode solutions. Also, the container material of the membrane may contaminate the electrolyte. Derek Lewis(19,20,21) has designed a cell with a flowing liquid junction where diffusion across the

laminar boundary layer is eliminated by pumping the electrolytes at sufficiently high flow rates. This type of continuously regenerating liquid junction makes possible a variety of electrochemical measurements with solutions having a closely controlled and readily variable composition. In conjunction with an external reference electrode, this flowing liquid junction was used to temperatures of 374C.

3.3 Innovative Electrodes - The innovative electrodes considered here present the most promising alternatives to conventional electrode design. This section provides the background for the palladium hydride membrane electrode and a restatement of the standard hydrogen electrode, and hopefully extends some insight into possible future electrode innovations.

Having reviewed all of the current, documented reference electrodes, including external arrangements and junction considerations, it is appropriate that the hydrogen electrode is again considered in a little more detail. When referred to as an electrode, this implies that the standard hydrogen electrode (SHE) consists of the hydrogen reaction;



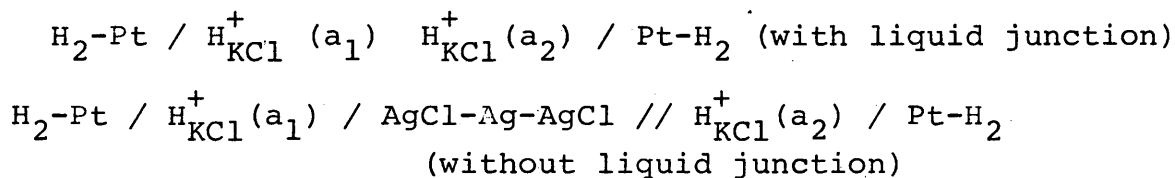
and an active substrate to catalyze the above reaction.

The crucial element in this electrode's performance is the substrate material. Conventionally, platinum is used to catalyze the reaction, although palladium and its various alloys are also possible, documented, substrate materials. Platinum, including bright platinum, platinized platinum, and platinum black, will be considered first and then a detailed discussion of the Pd-H electrode will follow.

3.3.1 Platinum Substrate - Platinum is the most common and stable metal used for the hydrogen electrode reaction. The mechanism of the hydrogen evolution reaction at the surface of platinum has been studied quite thoroughly(5). According to Nernst, however, the hydrogen electrode will fail in neutral solutions. Nernst contends that this electrode will not only fail to maintain an invariant solution phase, but the hydrogen discharge mechanism must, at some point, change from the hydrogen ion to the water molecule. Both of these theoretical problems are for neutral solutions. Although the hydrogen electrode can be used over a wide variety of hydrogen pressures, hydrogen must still be bubbled over the platinum surface at all times. Introducing hydrogen into the system in this manner will ultimately contaminate the working electrode. To eliminate the need for bubbling hydrogen over the surface of the electrode, Greeley, et

al(14,22), have devised a floating electrode which 'sees' both the aqueous and gas phases. Hydrogen in the solution will therefore come into equilibrium more quickly with the hydrogen in the vapor phase.

One of the main problems with this electrode is the estimation of the fugacity of hydrogen in the presence of high solvent vapor pressures. The fugacity of hydrogen is the difference between the total pressure and the solvent vapor pressure (at 200C, the uncertainty in the cell potential from these calculations is of the order of \pm 10-20 mv). Studies have been done using twin hydrogen electrodes in concentration cell such as;



In this manner, the cell potential, as given by the Nernst equation is independent of the pressure of hydrogen in the system.

Another possible method for determining the hydrogen pressure would be to use a palladium diffuser. Palladium has the unique property of freely absorbing hydrogen atoms into its lattice structure. Also, the resistance of a palladium wire is known to be sensitive to the amount of hydrogen absorbed into its lattice (23,24,25). Assuming the hydrogen pressure could be maintained in

in the linear range of the resistance versus hydrogen content plot (Refer to Figure 3.2), then the partial pressure of hydrogen in the gas phase could be accurately determined. By carefully monitoring the resistance of the palladium diffuser, the partial pressure of hydrogen in the system can be controlled. With these possible methods for simplifying the determination of hydrogen partial pressure, the range of the hydrogen electrode could be extended to higher temperatures and pressures.

3.3.2 Palladium Substrate - After presented a fairly complete background on the palladium hydride electrode, a proposed palladium hydride membrane electrode will be presented.

3.3.2(a) Background on Palladium Hydride - Palladium was mentioned above as a possible tool for determining the partial pressure of hydrogen in a system. As hydrogen is selectively absorbed into the interstitial octahedral sites of the Pd lattice(28), the overall structure will proportionately expand and consequently alter the physical properties of the Pd metal. Many functional relationships between palladium's chemical or physical properties and the H/Pd atom ratio have been discovered (28). A review of these physical and chemical properties, in the presence of hydrogen, will hopefully establish a precedence for a

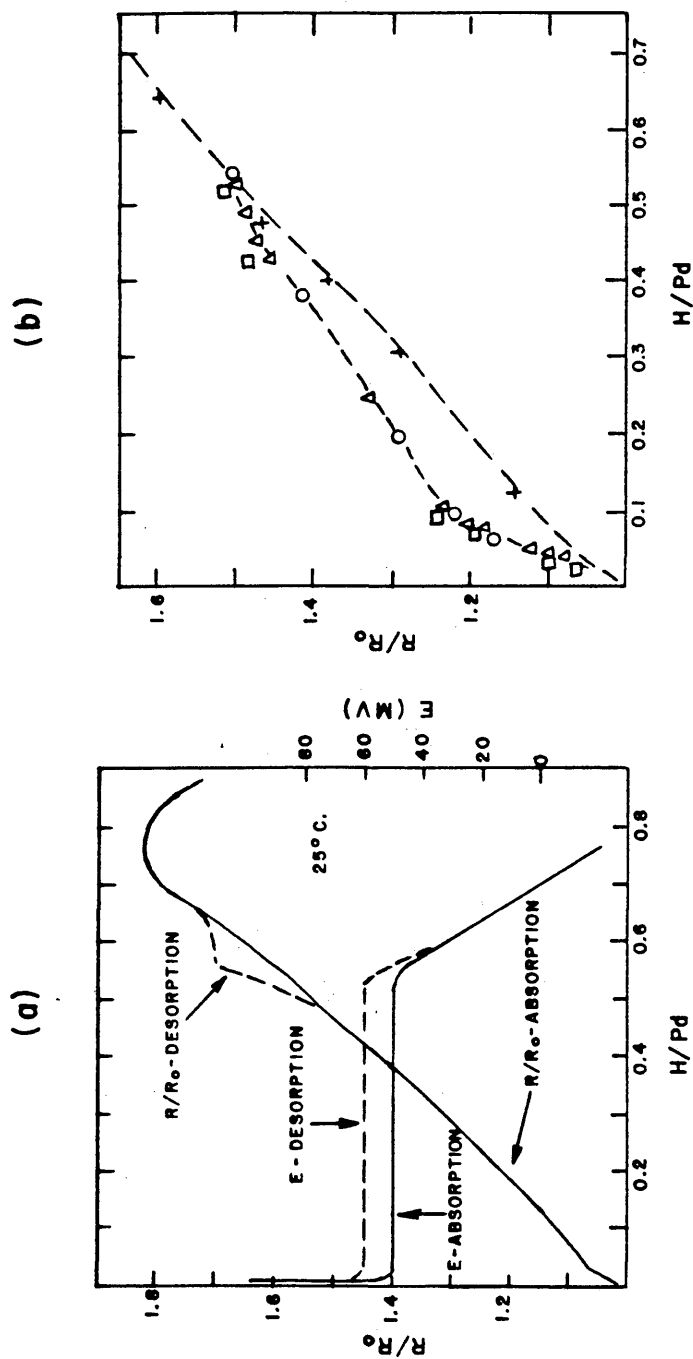


FIGURE 3.2 - RELATIONSHIP BETWEEN R/R_0 (AND E) AND H/Pd
 A) ACCORDING TO BARTON AND LEWIS(26) AT 25°C AND
 B) ACCORDING TO FLANAGAN AND LEWIS(27) AT 55°C (+) AND
 BRUNING AND SIEVERTS(27) AT 160C (o), 180C (Δ),
 AND 200C (\square).

later discussion of the electrochemical aspects.

An optimum substrate for the hydrogen reaction should possess enough absorption energy to overcome the activation barrier for atomization of molecular hydrogen and still be able to dislodge the hydrogen ion. For the reverse reaction, a substrate should have sufficient adsorption energy to discharge an ion and still be able to combine hydrogen atoms and release the hydrogen molecule. This is why platinum is the optimum choice. The mechanism for the hydrogen evolution reaction on palladium is analogous to platinum though subtly different.

Palladium forms a stable hydride phase in the presence of hydrogen gas. Many researchers have studied hydrogen absorption in Pd at various temperatures and have constructed 'pressure-composition-temperature' diagrams similar to those in Figure 3.3(28). Note that these are gas-solid absorption isotherms. At low H/Pd atom ratios less than 0.025 on the 25C isotherm, the stable phase is α , and at high H/Pd ratios greater than 0.6, the stable phase is β . Between these two limits there lies a 'plateau' region of invariant pressure where the $\alpha + \beta$ phases coexist. This 'plateau' region is present in all of the isotherms up to a critical temperature of about 295C and corresponds to a pressure of 19.87 atm and $H/Pd = 0.27$.

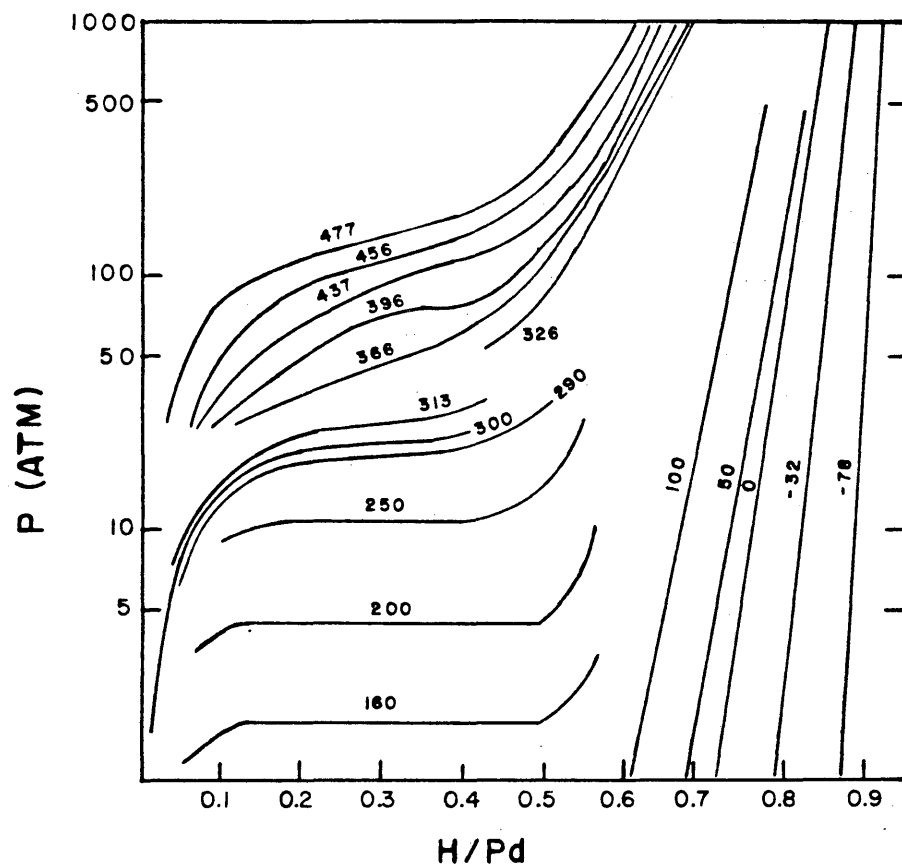


FIGURE 3.3 - PRESSURE-COMPOSITION (P-C) RELATIONSHIPS AT HIGHER TEMPERATURES AND PRESSURES ACCORDING TO LEVINE AND WEALE (1960) (32).

These isotherms reveal two important advantages in using the Pd-H electrode as a hydrogen electrode. First, for a given temperature, there is a region in which the pressure is constant and the limit of this plateau region is $\approx 300^\circ\text{C}$. Second, since Pd absorbs hydrogen into its lattice, it would be unnecessary to bubble hydrogen over the surface of this electrode. The 'plateau' regions of the absorption isotherms merely suggest a possible scheme to maintain known stable partial pressures, though the pure α and β regions outside of this 'plateau' should not be excluded.

Referring again to Figure 3.3, it would appear that each 'absorption' isotherm represents true equilibrium or just one unique isothermal condition. The results in Figure 3.4 show the actual absorption-desorption isotherms and reveal the marked hysteresis of the Pd-H system(30). There is some uncertainty among researchers as to whether the absorption or desorption curves represent true equilibrium. It could be said that this hysteresis reflects the failure of the system to achieve 'true' equilibrium, though structural (i.e. states of stress and strain) changes should also be considered. During absorption, the Pd lattice expands in the transition from the α to the β phase, straining the lattice a certain degree. In the desorption cycle though, the transition is from the β to the α phase and

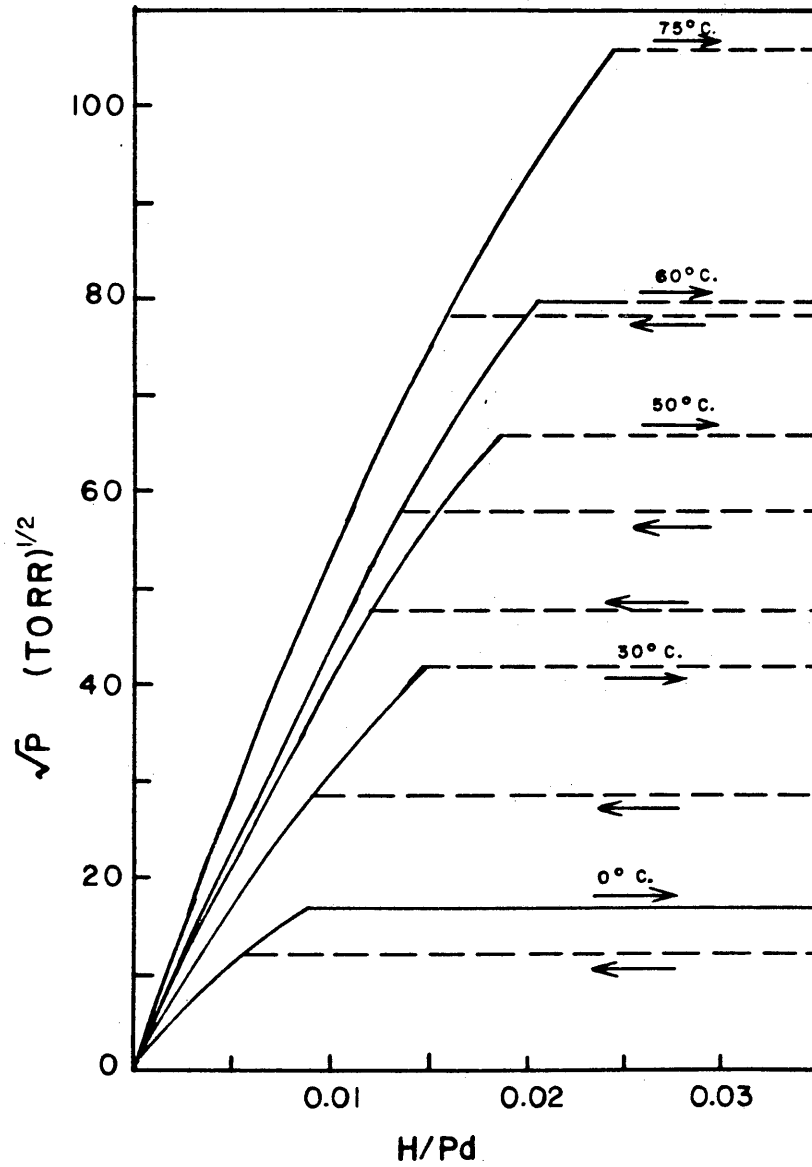


FIGURE 3.4 - HYSTERESIS OF P-C RELATIONSHIPS ACCORDING TO WICKE AND NERNST(3)

the degree of desorption strain will differ from the absorption strain. Most Pd-H electrodes would, however, be used in the desorption cycle. It is not the intent here to explain these isotherms, but point out the various facets of the Pd-H system since the activity of hydrogen at the Pd-H/solution interface will influence the thermodynamic and controlling mechanisms of the hydrogen reaction.

Before reviewing the proposed mechanisms governing the Pd-H electrode reactions and the observed potential responses, the pertinent physical properties will be presented first. Electrical resistance of Pd metal increases proportionally with the hydrogen content or H/Pd atom ratio as shown in Figure 3.2. Electrical resistance for the Pd-H is usually presented as R/R_0 , where R is the measured resistance and R_0 is the resistance of pure Pd metal. R_0 is approximately 10.7×10^{-6} ohm·cm⁻¹ at 25C. There is a change of slope at a H/Pd ratio around 0.015-0.025, corresponding to α_{\max} , a maximum in the curve at 0.7-0.8, and a linear portion in between corresponding to the two-phase region. At higher temperatures, the linear relationship still holds although the position and slope of each curve is different (Refer to Figure 3.2(b)). The 'knee' in the curve at lower H/Pd ratios refers to the maximum of the α phase.

Not only have many researchers (18, 23, 24) used this 'knee' to determine α_{\max} at various temperatures, but the entire curve has been used to correlate atom ratios with the presence of α and β phases. When using resistance measurements to continuously monitor the hydrogen content of palladium in an aqueous solution, the effects of co-conduction may screen the true resistance and therefore, should be minimized.

Other physical properties dependent on the hydrogen content in Pd are 1) shape 2) hardness, 3) lattice parameter, 4) elastic constants, and 5) paramagnetism(28). Contrary to electrical resistance, paramagnetism decreases linearly with increasing hydrogen content, and analogous to electrical resistance, hardness increases with increased hydrogen content in the pure α phase. The changes in the shape and lattice parameters though, are important practical considerations. Assuming Pd-H performs as a reference electrode, gross changes in shape may lead to mechanical problems in the system (Refer to Figure 3.5). Significant shape changes occur predominantly during the cyclical desorption and absorption of hydrogen. Alloying Pd with ≈ 25 percent Ag, however, seems to stabilize the shape of massive palladium(28). Not only will the overall shape of the metal change during expansion and contraction of the FCC lattice, but the lattice parameter will also vary. The lattice parameter(34)

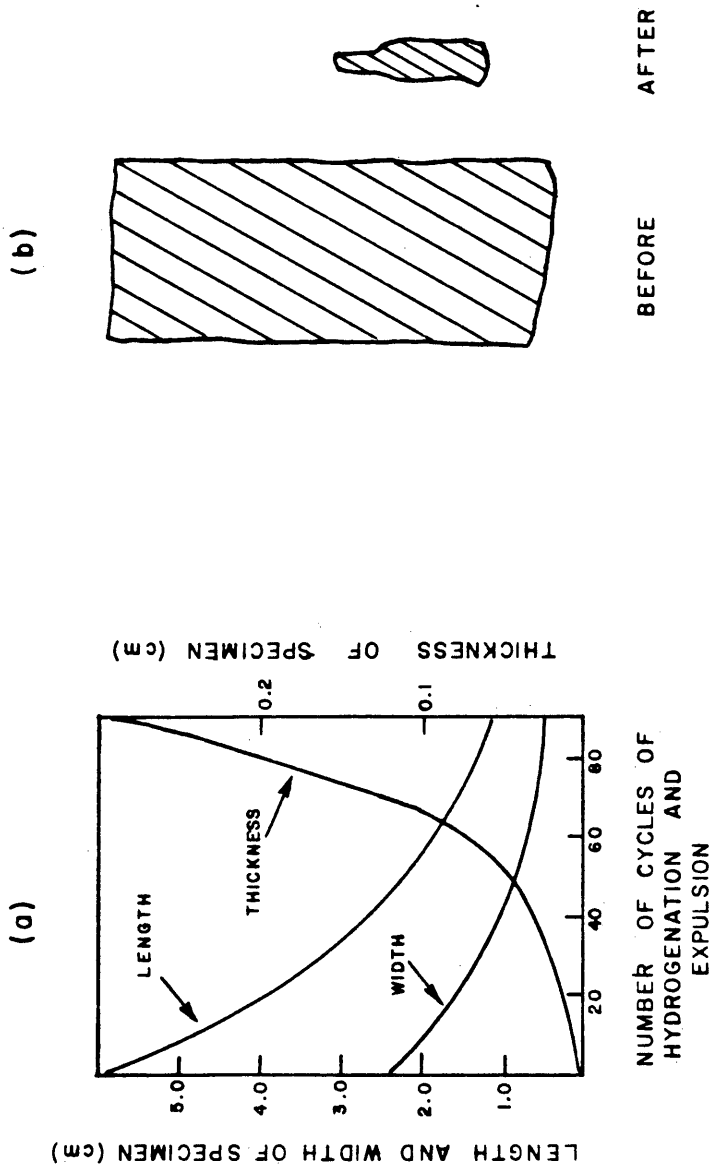


FIGURE 3.5 - A) DIMENSIONAL CHANGES AS A FUNCTION OF ELECTROLYTIC HYDROGEN ABSORPTION CYCLES (EXPULSION BY HEATING IN A FLAME)
 B) RELATIVE LENGTH AND WIDTH CHANGES AFTER 92 CYCLES - KRAUSE AND KAHLENBERG(1965)(33).

increases slightly in the pure α region from 3.882 to 3.886 KX, has two constant values of 3.886 (α_{\max}) and 4.017 KX (β_{\min}) in the 'plateau' region, and again increases from 4.017 to 4.032 KX in the high H/Pd region. For a given Pd-H reference electrode, the lattice parameter could be used to establish the phases present in that electrode under actual operating conditions and further correlate reaction mechanisms and potential responses with Pd-H phases. Hence, the physical properties of palladium would certainly aid in the development of the Pd-H as a viable reference electrode.

The focus of the discussion thus far has been the basic phenomenon of absorption of hydrogen in the Pd lattice. Now, with a little knowledge of the Pd-H, the Pd-H electrode can be reviewed as a viable reference electrode. Perhaps not totally apparent at this point, the response of the Pd-H electrode is strongly dependent on the design and preparation of the Pd metal. Also, the actual configuration of the test system has to be considered in evaluating this electrode. Most systems reviewed here consist of a pure 0.25 mm dia. Pd wire in contact with a hydrogen-stirred acid solution of known hydrogen partial pressure. The electrode potential response will be reviewed with an acute awareness of the system configuration and specimen preparation.

It has been well established(35,36,37,38) that a two-phase Pd-H electrode, in hydrogen-stirred acid solutions has an emf of (+) 0.050 V. vs. SHE at 25C. This positive potential shift is apparantly due to non-equilibrium between the chemical potential of hydrogen in solution and the metal phase. If palladium absorbs hydrogen in excess of $H/Pd \approx 0.57$, a thermodynamic 'equilibrium' condition is established and the measured potential should be 0.00 V. (vs. SHE). At H/Pd ratios less than 0.025, equivalent to α_{max} , the standard potential will be greater than 0.05 V.; potential increases or becomes more noble as the hydrogen content of the metal decreases. The above observations pertain to work done at 25C and $\frac{1}{2}$ 1 atm hydrogen pressure and should not be confused with later discussions of high temperature Pd-H work.

Below 200C, equilibrium between a hydrogen gas phase or dissolved hydrogen in solution, and the Pd metal is difficult to obtain(39). In the pure α phase, there exists a homogeneous solid solution of Pd-H which has been shown to follow Sieverts law; $C = Kp^{1/2}$, where C is the dissolved hydrogen concentration and p is the equilibrium pressure. The mechanisms for hydrogen ebsorption in the Pd lattice are not necessarily explained by a homogeneous solid solution of Pd-H.

Some researchers(31) believe hydrogen diffuses rapidly along minute fissures in the slip planes and by a secondary mechanism into the undistorted lattice. They theorize the presence of a complex 'rift' network within the Pd metal. If hydrogen were to occlude within this complex 'rift' network, then it would be logical to assume that a defect structure with a high dislocation density would preferentially absorb more hydrogen than an annealed structure, or a lattice with a lower dislocation density. Pre-treatment of the Pd metal would therefore, be critical. C.G. Shull at Oak Ridge Laboratories though, found hydrogen atoms in the β phase solution will occupy the octahedral interstitial sites of the Pd lattice, and thereby supports the idea of a solid-solution phase(28). For this study, the activity of hydrogen in the Pd metal at the surface will be considered constant and not a function of the fissures, nooks, or channels a few atomic diameters from the surface. This also assumes a fairly uniform diffusion gradient normal to the Pd surface. These proposed mechanisms of the Pd-H phase are complex and unresolved, though an important basis for the development of a hydrogen reference electrode.

Depending of whether hydrogen is charged into the Pd from diatomic molecules of the gas phase or from the hydronium ions of the solution phase, the response of

the electrode in solution may be different. A gas-charged Pd-H electrode will exhibit a 0.0 V. potential (vs. SHE) difference; whereas, an electrolytically charged electrode will attain a 0.05 V. potential after several hours in a 2.0 N H_2SO_4 solution at 1 atm H_2 pressure. Many investigators(35,36,37) have observed the (+) 0.05 V. potential with an electrolytic-type electrode because the electrode has not been fully charged. If the α phase is present, the electrode has not attained equilibrium(18,28,35). An electrolytic-type electrode has either selectively absorbed hydrogen from a hydrogen-stirred solution, an electrochemical process, or both. In contrast to the electrolytically charged electrode, a gas-charged Pd-H electrode forms a passive layer of hydrogen atoms at the metal-solution interface and will maintain a stable 0.00 V. potential. Anodic polarization will destroy this 'passive layer' and the gas-charged electrode will respond similarly to an electrolytic electrode. Regardless of the charging procedure, if the hydrogen content of the hydride is in the plateau region of the absorption isotherm, the measured emf will be (+) 0.05 V. at 25C.

Pd-H electrodes, like Pt electrodes, can be poisoned by certain impurities in solution(28,38). Sulfur, arsenic, bromine, iodine, and related compounds have been known to poison the palladium-hydride surface.

Slight anodization of the Pd-H electrode will remove trace impurities assuming the impurity species can be reduced by hydrogen. Also, hydrogen may reduce compounds of a higher oxidation state to a lower, more harmful state. Such behavior could account for the limited absorption of hydrogen (i.e. $H/Pd = 0.025$) by palladium, found by Schuldiner in 2 N H_2SO_4 solutions(35). The sulfur in the sulfate ion may have been reduced to a state which suppressed the absorption process in palladium. Unless fresh palladium surface sites can be regenerated, by such means as atomic hydrogen reduction of impurities, then the Pd-H electrode may be limited by certain impurities in the system.

The discussion of the Pd-H electrode at low temperatures or 25C, incorporates most of the work on the Pd-H systems and establishes the basis for reviewing work at higher temperatures and pressures. Dobson and Thirsk(18,40,41) have done the primary research on potential measurements of Pd-H at elevated temperatures between 25 and 195C. Dobson established the absorption isotherms in hydrogen-stirred aqueous media using relative resistance measurements and compared his results to known absorption isotherms for the gas-solid system. According to Dobson (see Figure 3.6(b)), equilibrium, and hence a 0.00 V. potential difference, is re-established rapidly at higher temperatures. Whether an α_{max} phase

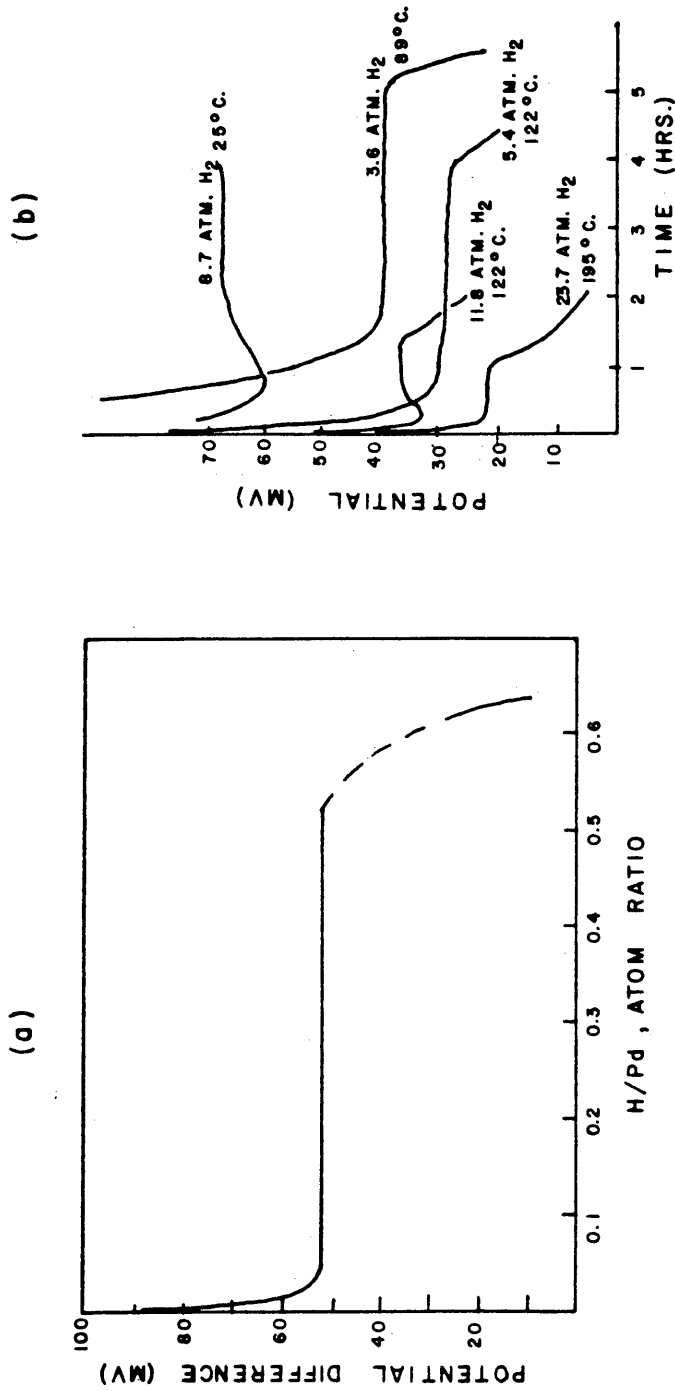


FIGURE 3.6 - A) POTENTIAL VS COMPOSITION FOR PD-H ELECTRODE AT 25C -
VASILE AND ENKE(42)
B) CELL POTENTIAL ISOBARS FOR THE PD-H ELECTRODE -
DOBSON(49)

or β_{\min} phase is established depends on the equilibrium pressure at the surface of the electrode; pressures below the 'plateau', invariant pressure region, correspond to the α phase. Although the potential response of the Pd-H electrode is sluggish at lower temperatures, the viability of this electrode as a reference electrode appears to improve significantly at higher temperatures.

3.3.2(b) Proposed Design for a Pd-H Electrode - The present configuration for a Pd-H electrode consists of a pure, 0.25 mm dia., wire charged 1) in a hydrogen-stirred 2 N H_2SO_4 , or HCl solution; 2) cathodically in a 2 N H_2SO_4 solution; or 3) in a hydrogen gas atmosphere. Without the presence of dissolved hydrogen or hydrogen ions in solution, this electrode is limited to the 'plateau' life of the Pd-H. The typical 'plateau' life for a Pd-H electrode lasts approximately 6 hours(38). Since membranes have been used to measure diffusion rates and diffusion constants of hydrogen through Pd(43,44), the same type of configuration could be incorporated into a reference electrode design. The schematic in Figure 3.7 is an illustration of this idea; hydrogen gas on one side of the membrane and a solution or electrolyte on the other side. The hydrogen would be effectively removed from the system and carefully controlled on the inside of the membrane. This design

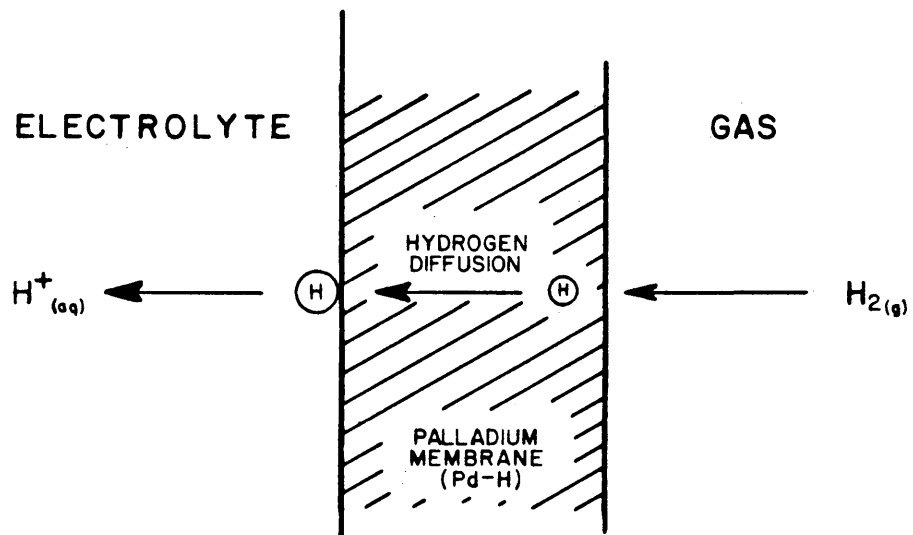


FIGURE 3.7 - A SCHEMATIC OF THE PD-H MEMBRANE ELECTRODE USED IN THIS STUDY

has many interesting advantages over the SHE. First, assuming a steady state diffusion of hydrogen is established in the membrane, a constant source of pure hydrogen could be supplied to the electrode; impurities may even be fortuitously reduced and removed from the solution side of the electrode. Second, the entrance (gas) and exit (electrolyte) sides of the membrane could be treated to enhance absorption into the metal and to catalyze the hydrogen reaction mechanisms respectively. In the event a gas-charge on the 'entrance side' is inadequate, an electrolytic charging mechanism could be devised with cathodic polarization out of a 2 N H_2SO_4 solution. Regardless of the configuration on the entrance side of the membrane, the pre-treatment of the Pd metal will be carefully controlled to insure maximum catalytic surface sites for the hydrogen reaction.

CHAPTER 4

EXPERIMENTAL

4.1 Apparatus - The experimental tests performed above 90C were all done in a 2-liter autoclave from Autoclave Engineers (See Figure 4.1). Although the body of the autoclave was made of the standard 316L S.S., the head was specially machined out of 304 S.S.. A glass liner was used inside the autoclave. For more severe environments, a Ryton coated, titanium autoclave, with the identical dimensions of the S.S. vessel, had been prepared. A series VF- 500 Autoclave Engineer furnace externally heated the vessel up to a maximum of 732C. In the furnace shell, an imbedded K-type thermocouple was used to monitor the furnace temperature. Surrounding the entire autoclave assembly, a 10-gauge steel blast shield was built, containing any leaks or explosions to the immediate area. A schematic of the blast shield and surrounding area is given in Figure 4.2(b).

Wire leads and/or tubing, leading into and out of the vessel, were sealed in the head in one of two ways. The two possible seals are shown in Figure 4.1. Standard Conax fittings were used for the single or

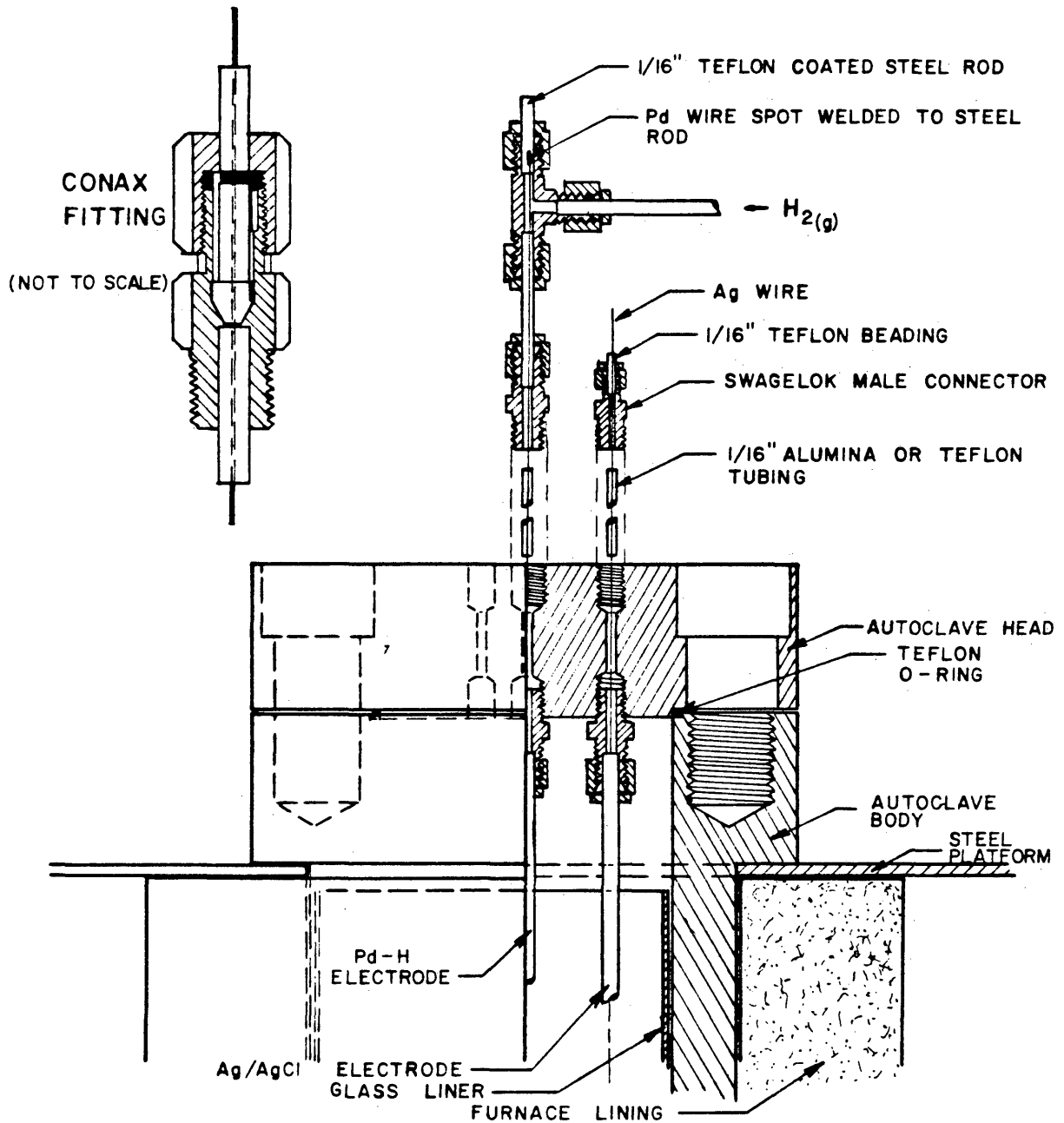
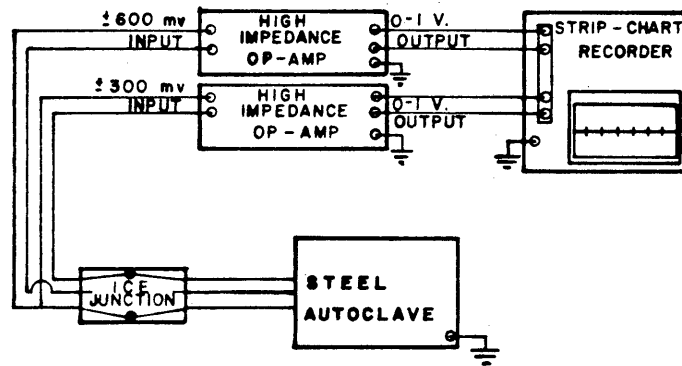
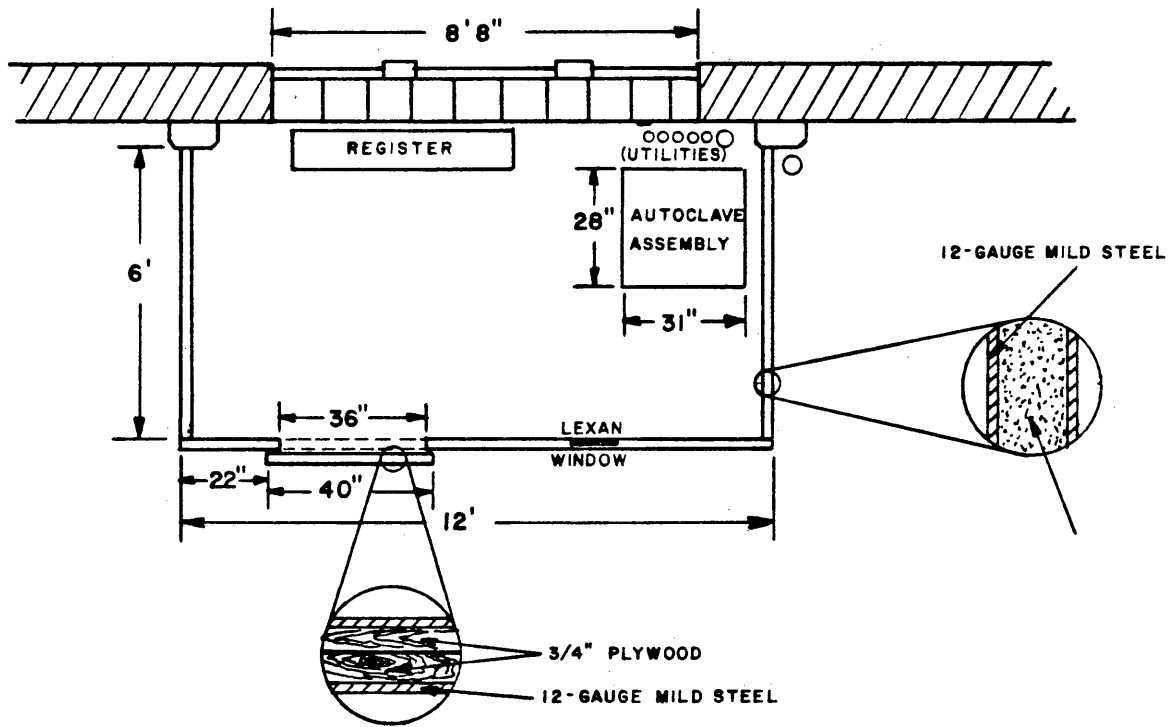


FIGURE 4.1 - A HALF SECTION OF THE AUTOCLAVE ASSEMBLY (SCALE: 0.5 = 1.0)



(a)



(b)

FIGURE 4.2 - A) SCHEMATIC OF THE MEASUREMENT CIRCUIT AND
 B) TOP VIEW OF THE BLAST SHIELD AND AUTOCLAVE ASSEMBLY

multiple wire leads in excess of 1/32" dia.. For the small 0.25 mm dia. Ag wire leads, a carefully bored 1/16" teflon beading encased the Ag wire and the teflon sheathed wire assembly was sealed with a Swagelok fitting inside the head.

Within the autoclave head, 1/16" Alumina (Al_2O_3) and teflon tubing insulated the wire leads from the steel autoclave. Swagelok fittings were not only used within and around the vessel, but for connections throughout the system.

The schematic in Figure 4.2(a) shows the measurement circuit for the system. Wire leads from the electrodes are joined at a solder junction to the copper leads and placed in contact with an ice bath. Situated in series, the 10- megaohm impedance operational amplifier minimizes current flow and possible electrode polarization. The input to this 'high' impedance Op-amp will receive either a \pm 300 mv or a \pm 600 mv signal and send out the signal in a 0-1 volt or 0-5 volt range. These special range selections were designed to interface with either the 0-1 volt input of a Leeds and Northrup multipoint strip-chart recorder or the 0-5 volt input of an Apple II computer and thus incorporate flexibility into the data acquisition process. An externally grounded pipe was hooked into the system

to eliminate the occasional stray potentials or fields.

4.2 Polarization Measurements - Two sets of measurements were made with the potentiostat/galvanostat arrangement.

4.2.1 Palladium Hydride - All of the polarization measurements were tested with a Model 350 PAR potentiostat/galvanostat. Before placing in solution, the Pd electrodes were internally charged with $H_2(g)$ for approximately one hour. A saturated calomel electrode with Luggin probe was used as the reference and a Pt gauze was used as the counter electrode. As in other Pd-H tests, the test solutions for the potentiodynamic measurements were not purged and therefore, contained dissolved oxygen, carbon dioxide, and other dissolved gases present in the atmosphere. Solutions for these tests were prepared with de-ionized water. The actual operation of the Pd-H electrode in these dynamic tests was identical to the Pd-H operation in the static high temperature-pressure autoclave tests.

4.2.2 Ag Metal - The Ag metal potentiodynamic scans were also tested with a Model 350 PAR potentiostat. In these tests, carbon counter electrodes were used.

Before mounting the pure Ag specimen in a sample holder which exposes approximately 1 cm^2 of sample surface area, the Ag metal surface was ground and polished. It was necessary to complete the polishing with the 1μ particles or smaller. Once ground and polished, a tested sample was reused in a new fresh solution.

4.3 Electrode Design - The configuration for the Pd-H, Ag/AgCl (Ag/AgBr), and Cu/CuSO₄ electrodes were all different and the schematics are presented in Figures 4.3 and 4.4. In Figure 4.3(b), the drawing of the Cu/CuSO₄ electrode exemplifies its simplistic and practical design. Although this design limits the Cu/CuSO₄ electrode to temperatures below 90C, the basic Cu/CuSO₄ reaction mechanisms also limit this electrode to 90C. The Ag/AgCl electrode design on the other hand, is specially suited for high temperature-pressure service. This Ag/AgCl electrode is patterned after the Ag/AgCl electrode designed by Agrawal and Staehle(45) (Refer to Figure). A teflon body, the soaked and packed zirconium oxide sand(-35 to 100 mesh), a magnesium stabilized zirconia plug, and a buffer compartment enable this electrode to function at high temperatures and pressures in almost all test solutions. The pre-

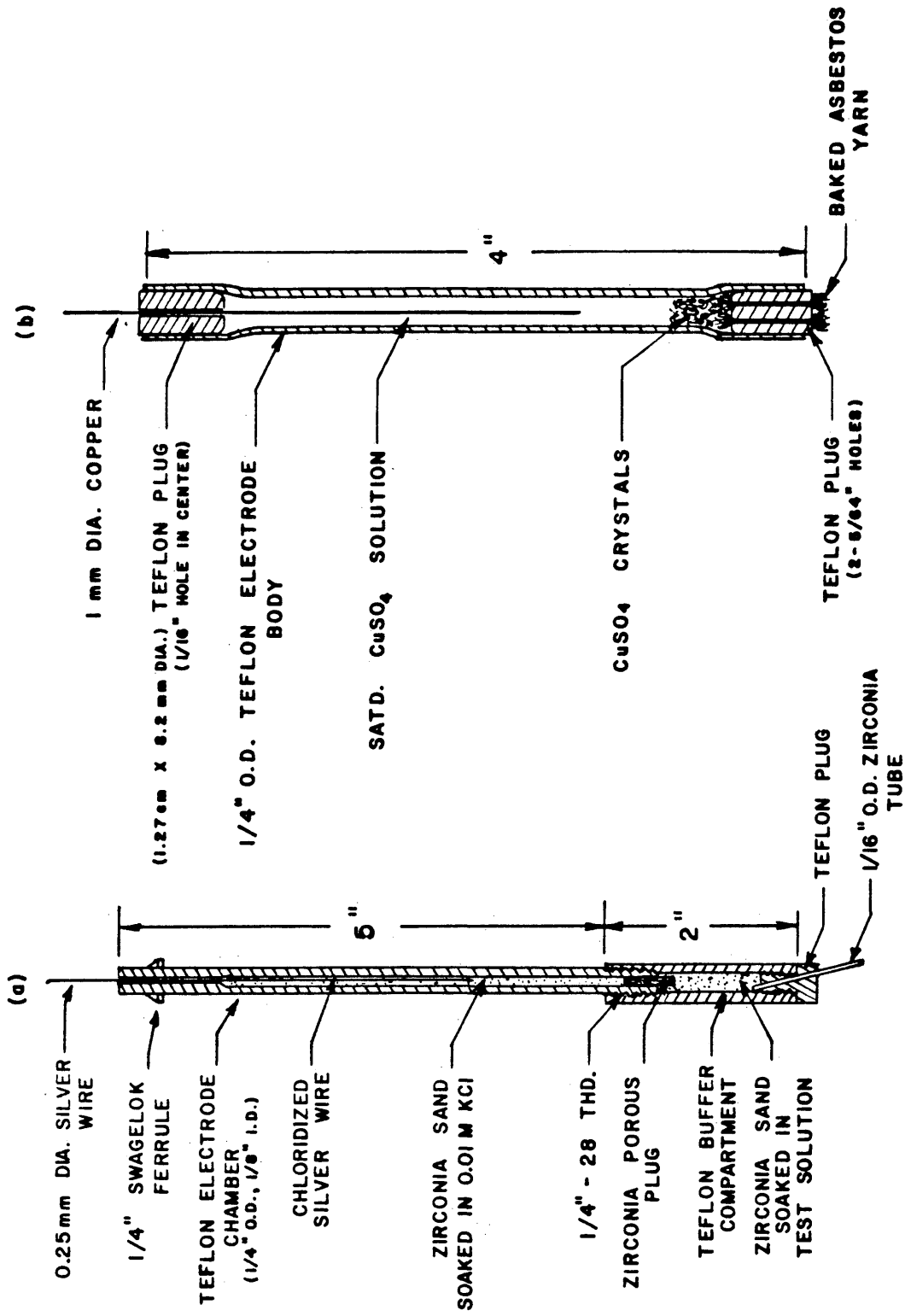


FIGURE 4.3 - A SCHEMATIC DRAWING OF THE A) AG/AGCL ELECTRODE AND B) CU/ $CuSO_4$ ELECTRODE USED IN THIS STUDY

paration procedure for these electrodes will be discussed later.

The Pd-H electrode is shown in Figure 4.4. Many electrode configurations were tried before this final design was established. This design facilitates quick and easy replacement of the Pd sample tube and brazed steel plug, insures an effective hydrogen seal, and establishes a good electrode response. The Pd tube is the only conductive material in contact with the solution since all the other components are teflon sheathed. Note that the hydrogen gas on the inside of the tube is static rather than flowing. To minimize contaminants and insure ample hydrogen availability, the original atmosphere was drawn out with a vacuum and then purged with hydrogen. This draw-purge cycle was repeated several times to obtain a fairly pure $H_2(g)$ atmosphere. Finally, the 0.005" wall thickness of the Pd tube was essentially the practical limit for Englehard Industry's fabrication process. Wall thickness may influence the performance of a Pd-H electrode, yet Wahlin(28) states that the 'transmission in Pd is insensitive to the thickness and dependent on the exposed surface area'. Wahlin arrived at this observation by electrolytically transmitting hydrogen through Pd. The above Pd-H electrode design was used in nearly all

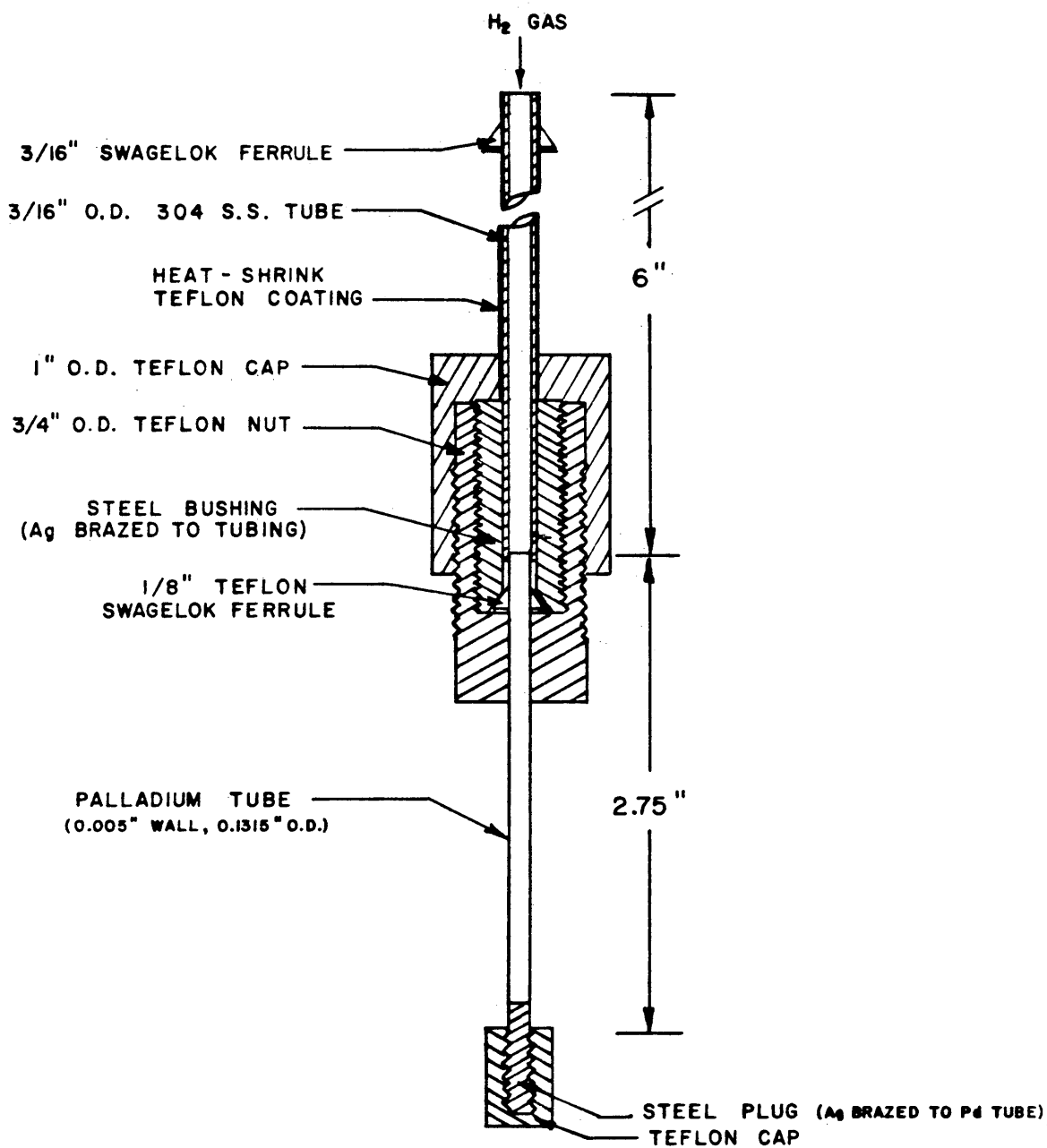


FIGURE 4.4 - A SCHEMATIC OF THE PD-H ELECTRODE

of the tests.

4.4 Materials (reagents) and Electrode Preparation -

All of the chemicals were reagent grade purity or better. In the preparation of the Ag/AgCl electrode, high purity KCl crystals were used since Br and other impurities, present in the manufacturing of lower grade crystals, may impair the performance of the Ag/AgCl electrode(5). Also, 99.9 percent high purity hydrogen gas, with 2 ppm O₂ and 4 ppm H₂O_(v), was used in the Pd-H electrode to reduce the known poisoning effects of O₂ and H₂O vapor. An inline 7μ filter and a molecular sieve in series were used to trap these and other impurities. The solutions in the electrode compartments and plating operations, and the actual test solutions were prepared with triply distilled ($\approx 1.0 \times 10^{-6}$ mho·cm⁻²) and singly distilled water ($\approx 3.0 \times 10^{-6}$ mho·cm⁻²) respectively. The Ag(5Nt), Pd(3Nm), and Cu(5Nt) wire were purchased from the Ventron Corp. and the 0.1315" dia. Pd tube, with 0.005" wall, was special ordered from Englehard Industries. Also, Corning supplied the magnesium stabilized zirconia 1/8" dia. rod ($\approx 8\%$ porosity) and 1/16" O.D. tubing. The compartment or body of the Ag/AgCl and Cu/CuSO₄ electrodes were machined out

of T.F.E. teflon rods, or tubing. After machining, the teflon was ultrasonically cleaned in 50 percent aqua regia, then in acetone, and finally rinsed in distilled water. These parts were not annealed to liberate fluorine or low molecular weight fluorocarbons. Because of the inherent sensitivity of reference electrode measurements, all electrodes were carefully prepared and tested with the intent to eliminate or minimize adverse contaminants.

4.4.1 Ag/AgCl Preparation - A schematic of the Ag/AgCl electrode is shown in Figure 4.3(a). Prior to testing, the zirconia sand in the electrode body was soaked in 0.01 M KCl for at least 24 hours and the zirconia plugs were boiled in a KCl solution for at least 2 hours. Both zirconia sand and plugs were stored in 0.01 M KCl solutions. After a test, a 'contaminated' electrode, showing significant deviation from original rest potential, could be re-generated by rinsing the electrode compartment with 0.01 M KCl solution and replacing the zirconia plug. A saturated calomel electrode was used to measure the rest potential of new Ag/AgCl electrodes. A new Ag/AgCl electrode was used if the measured rest potential was within ± 1 mv of the mean rest potential of previous Ag/AgCl

electrodes. Agrawal(45) reports a value of 99 mv (vs. SCE) although electrodes were used with potentials of 89 mv (vs. SCE).

Two methods, thermal and electrolytic, were used to coat or deposit a AgCl solid onto the Ag wire. A thermal AgCl preparation merely consisted of melting pure AgCl powder, drawing up the molten AgCl into a pasteur pipette, and allowing the molten AgCl, within the confinements of the pipette, to freeze around a 0.25 mm dia. Ag wire. This entire procedure was carried out in a darkroom. The pipette was then carefully broken and detached from the light purple-blue, or 'plum' colored, AgCl deposit. The electrolytic Ag/AgCl wires were prepared by placing the Ag wire (anode) in a 1.0 M HCl solution, surrounding this wire with another Ag wire (cathode) in a helical configuration and imposing a current density of 1.0 ma/cm^2 for approximately 4 hours on this system. The whole Erlenmeyer flask, or cell, was enshrouded in aluminum foil. In contrast to the relatively thick, thermal AgCl coating, the thinner electrolytic AgCl coating was less sensitive to light and more adherent to the metal surface.

4.4.2 Pd-H Preparation - Although initial Pd tubes were first oxidized in KMnO_4 or KClO_4 solutions and then reduced in a H_2 atmosphere, the corresponding performance of these electrodes were sporadic and a new standard pre-treatment procedure was adopted. Cleary and Green(46,47), in their research on Pd-H membrane fuel cells, have stressed the importance of Pd pre-treatment and its corresponding influence on electrode behavior. They have found that 1) annealing Pd in an oxidizing atmosphere below 875°C , the decomposition temperature of PdO , produces a blue oxide which enhances electrode performance and 2) initial surface abrasion exposes fresh active surface sites which also improve electrode performance. Over a period of several months, ageing occurred in Pd samples and reduced the efficiency of an electrode. Therefore, in lieu of this information, Pd tubes were first abraded with 320 grit emery cloth on the inside and outside surfaces, oxidized (O_2 atmosphere) at 500°C for 45 minutes, and then immediately reduced (H_2 atmosphere) at 500°C for another 45 minutes. The Pd tube displayed a blue color after the oxidizing stage and then transformed to a bright metallic luster after H_2 reduction, indicative of the pure Pd-H. After heat treatment, Pd tubes were plated with Cu,

Pd, or Pt on the inside and/or Pd or Pt on the outside. The configuration for externally plating Pd tubes was analagous to the AgCl deposition set-up. To internally plate the Pd tubes, a Pt wire, wrapped with paper towel to avoid short circuiting, was suspended down the center of the Pd tube. Pd tubes were Pt plated in a 0.072 F chloroplatinic acid and 1.3×10^{-4} F lead acetate solution at 30 ma/cm^2 for approximately 5-10 minutes. It should be noted that in the presence of hydrogen in the Pd lattice, the Pt was readily reduced even before the start of an applied current.

The Pd plating conditions were identical to Pt plating. To prepare the Pd plating solution, a 500 ma current, with frequent polarity reversals, was first passed through a 'grade 1', 0.1 mm dia. Pd wire in a 37 percent HCl solution. This process was continued until approximately 0.5 grams of Pd was dissolved. At this point lead acetate was added. Then, this solution volume was reduced to approximately 10 ml by evaporation and finally diluted with distilled water to a 50 ml total volume.

Cu was plated out of a standard acid copper plating solution. The bath consisted of 1.32 M copper sulfate, 0.612 M sulfuric acid, and 3.3×10^{-4} M hydrochloric acid. A bright copper plate was the

result of an applied current density of 21.5-53.8 ma/cm² for approximately 5-10 minutes. A black, highly particulate deposit, however is probably a more desirable plate(30).

CHAPTER 5

RESULTS AND DISCUSSION

5.1 Preliminary Tests of Commercial Reference Electrodes -

Although the materials used in constructing commercial reference electrodes limit the working environments for these electrodes, various Ag/AgCl and standard calomel electrodes were tested in HCl, H₂SO₄, NaCl, and neutral solutions. Along with these electrodes, a Cu/CuSO₄ electrode, constructed in the lab, was also tested. A commercial electrode is convenient, exhibiting reproducible and stable responses and hence, an appropriate point to begin a reference electrode research. The results of these tests are presented in the following figures.

In Figures 5.1, 5.2, and 5.3, are shown the potential response of 0.1 N Calomel, satd. Calomel, and satd. Cu/CuSO₄ at increasing temperatures in 1.0 N NaCl, 1.0 N H₂SO₄, distilled water, and a 50-50 ethylene glycol-water mix. At equilibrium, the standard rest potential is a function of temperature and the activity of the participating ions in the electrode half cell reaction (i.e. Nernst relationship). An electrode potential should not be a function of

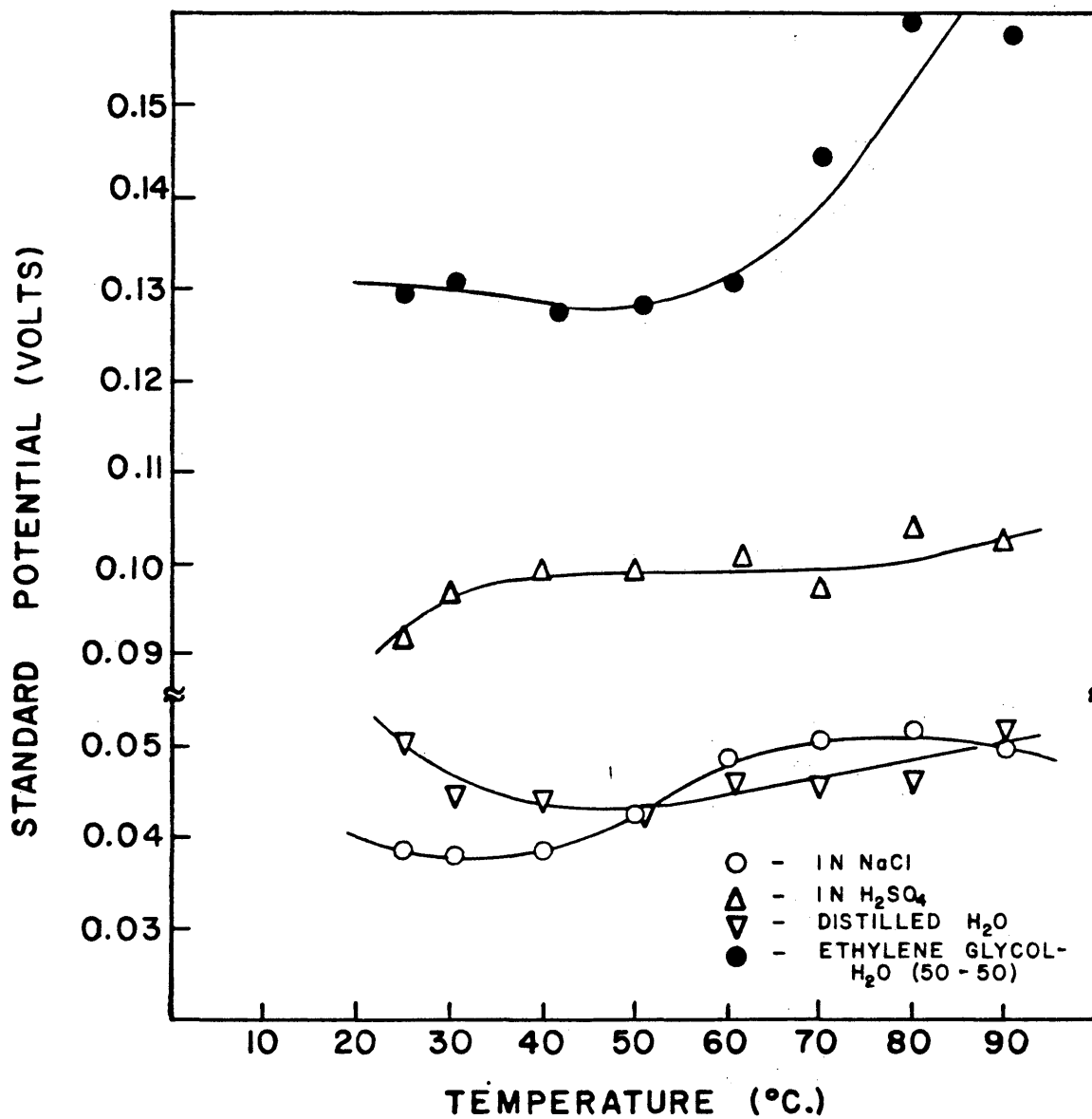


FIGURE 5.1 - STANDARD ELECTRODE POTENTIALS OF THE 0.1 N KCL CALOMEL ELECTRODE (VS AG/AGCL) AS A FUNCTION OF TEMPERATURE FOR VARIOUS ELECTROLYTES

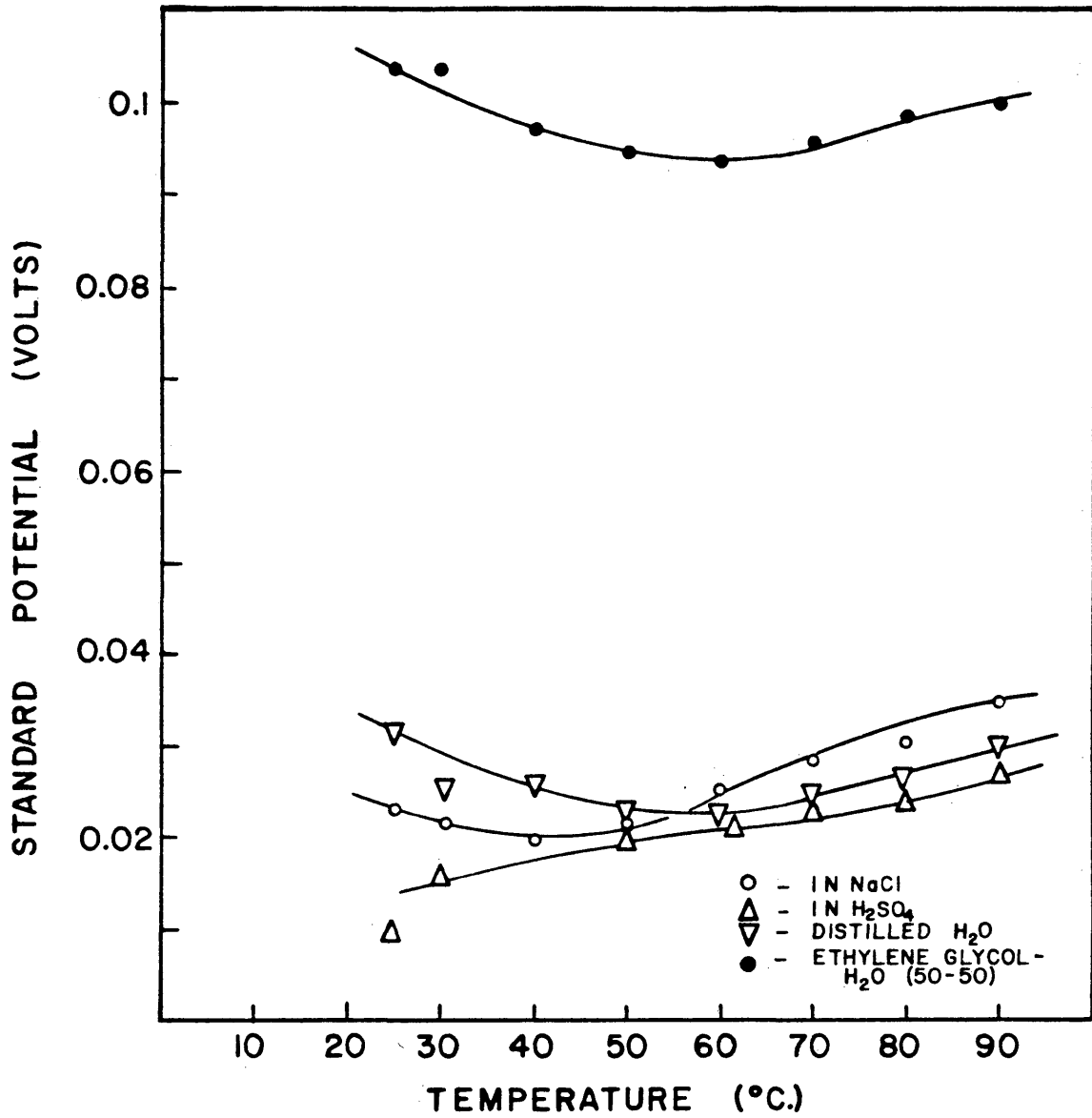


FIGURE 5.2 - STANDARD ELECTRODE POTENTIALS OF THE SATD. CALOMEL ELECTRODE (VS AG/AGCL) AS A FUNCTION OF TEMPERATURE FOR VARIOUS ELECTROLYTES

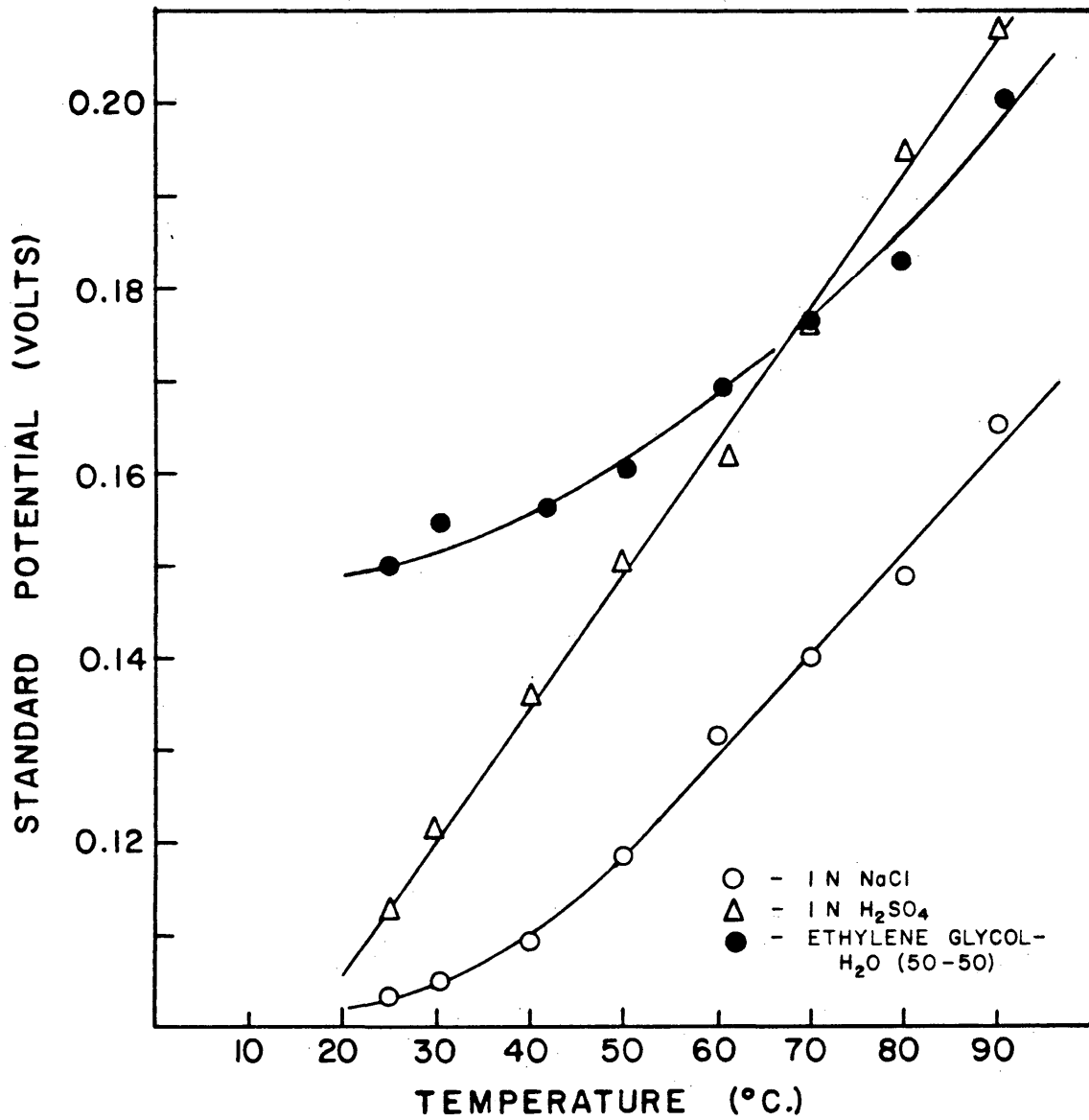


FIGURE 5.3 - STANDARD ELECTRODE POTENTIALS OF THE CU/CUSO₄ ELECTRODE (VS AG/AGCL) AS A FUNCTION OF TEMPERATURE FOR VARIOUS ELECTROLYTES

the test solution. Unless a liquid junction effectively protects an electrode half cell reaction, then the non compatibility between a reference electrode and electrolyte may cause significant deviations from ideal, thermodynamic behavior. The results in Figure 5.2 illustrate the responses for a satd. calomel electrode in 1.0 N NaCl, 1.0 N H₂SO₄, and approximately neutral solutions. Although the curve for the ethylene glycol-water mix is shifted ≈ 70 mv above the other curves, the parabolic shape of the curve is consistent. A 0.1 N KCl calomel electrode exhibited similar behavior.

In a sulfuric acid solution, the Cu/CuSO₄ rest potential increased linearly with temperature, but the results were quite different in aqueous NaCl and ethylene glycol solutions. A Cu/CuSO₄ may be functional in an ethylene glycol-water solution, yet the viability of this electrode in the absence of sulfate ions at higher temperatures is questionable. For reasonable compatibility between the electrode and test solution, the Cu/CuSO₄ and commercial satd. calomel electrodes are suitable for work at temperatures less than 90C.

The results in Figure 5.4 effectively illustrate this compatibility criteria for a good reference electrode. Ideally, an increasing ion activity in the test solution

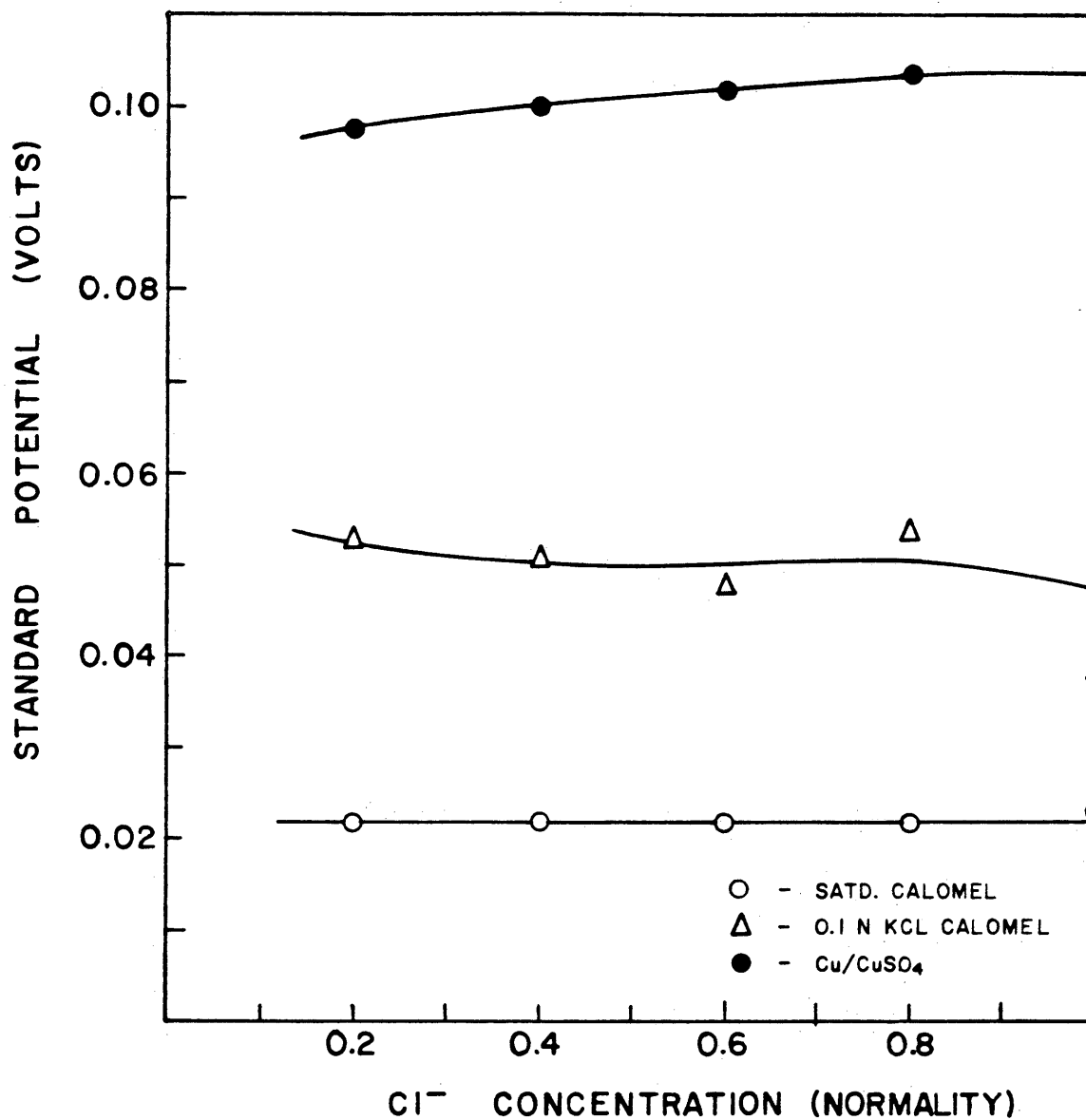


FIGURE 5.4 - THE EFFECT OF Cl^- CONCENTRATION ON THE STANDARD ELECTRODE POTENTIAL OF THE 0.1 M KCL AND SATD. CALOMEL AND $Cu/CuSO_4$ ELECTRODES (VS $Ag/AgCl$)

should not have an effect on the electrode rest potential. Notice that the satd. calomel electrode is unaffected by the chloride ion concentration, yet this is not too surprising since the calomel electrode is reversible to the chloride ion. More importantly, the Cu/CuSO_4 was relatively unaffected by the activity of the chloride ions with fluctuations of ± 5 mv. These results confirm the known stability of the satd. calomel electrode and also present some indication of the stability of a Cu/CuSO_4 electrode in a non-compatible solution. Cu/CuSO_4 though, is not reproducible above 90C.

These preliminary tests not only confirmed known observations, but established the levels of precision in reference electrode measurements. Below 90C, a satd. calomel electrode is excellent in aqueous environments and a Cu/CuSO_4 , though not as reproducible or accurate as a calomel electrode, is satisfactory in aqueous and ethylene glycol-water solutions. Due to these results, the Cu/CuSO_4 will be tested at higher temperatures and the calomel will be limited to temperatures below 120C since calomel is known to disproportionate and HgCl_2 will hydrolyze to HgO .

5.2 Thermal Type Ag/AgCl - The method of preparation for the thermal-type Ag/AgCl was outlined in the

experimental section and the performance and observations of this electrode at higher temperatures-pressures will be discussed. Preparation, light sensitivity, impurity effects, and lattice strain, are critical in the performance of this electrode(5). Though Ives suggest, for a thermal-type electrode, the decomposition of a proper mixture of silver oxide and silver chlorate in the form of a paste, for these tests, pure AgCl was used directly in the preparation of the thermal Ag/AgCl electrode.

Nearly all of the electrodes prepared, exhibited rest potentials below reported values and actual measured values were approximately 86.2 mv and 89.6 mv after thermal cycling. A comment should be made on this thermal cycling phenomenon. When AgCl is heated, the solubility of AgCl increases, and this preferentially allows crystals of high energy states to reprecipitate in lower, more stable, energy states(5). It would seem then, that a thermal cycle would improve the stability of an electrode and explain the observed reproducibility of a thermally cycled electrode at room temperature.

Thermal AgCl coatings are reported(5) to have a low specific resistance and greater porosity in comparison to electrolytic deposits. It is very difficult

to accurately control the thickness or the porosity of a thermal-type deposit and since electrode components must be present in their stable, lowest forms of free energy, a thermal-type electrode is inherently difficult to prepare. According to Ives, the simplicity of a thermal preparation is usually preferred over the electrolytic-type. The variability in AgCl deposition could account for the negative shift in rest potential from known reported behavior(45).

A solid AgCl deposit, cooled from molten AgCl, was very sensitive to light. Even though the electrode was prepared in the dark, the color of the solid deposit would change, or degrade, from a light purple to a much darker, almost black, color in only a few hours. It was difficult to actually attribute a specific shift in electrode response to light sensitivity of the electrode since most of the thermal-type electrodes responded sporadically at higher temperatures and pressures. The poor performance of this type of electrode was the result of other, more detrimental influences.

In preparing a Ag/AgCl electrode, molten AgCl was drawn up into a pasteur pipette and then allowed to cool around a Ag wire. It was found, with the aid of an X-ray diffractometer, that borosilicate was

present in the solid AgCl; in one instance, there appeared to be another phase present (Refer to microtraph). Molten AgCl, at temperatures above 450F, apparently leached borosilicate out of the pipette, thereby contaminating the AgCl phase. Pyrex brand glass has 12.9 percent B_2O_3 and high alkali glassware have even higher borosilicate contents. The presence of other unknown trace impurities, such as dissolved oxygen in the molten AgCl, may have aided in the poor performance of this electrode. It should be mentioned again that these electrodes were carefully prepared, avoiding any possible exposure to contaminating impurities.

This type of thermal Ag/AgCl then, was not recommended for practical high temperature work. Because of the problems encountered with the thermal Ag/AgCl preparation, testing of the more sensitive, thermal Ag/AgBr electrode was never attempted. The difficulty in preparing a pure homogeneous, solid AgCl phase, as shown in the micrograph, was probably a factor in the sporadic behavior of this electrode at higher temperatures. Although these problems could eventually, with careful preparation, have been overcome, it was found that the following type of Ag/AgCl electrode was more practical.

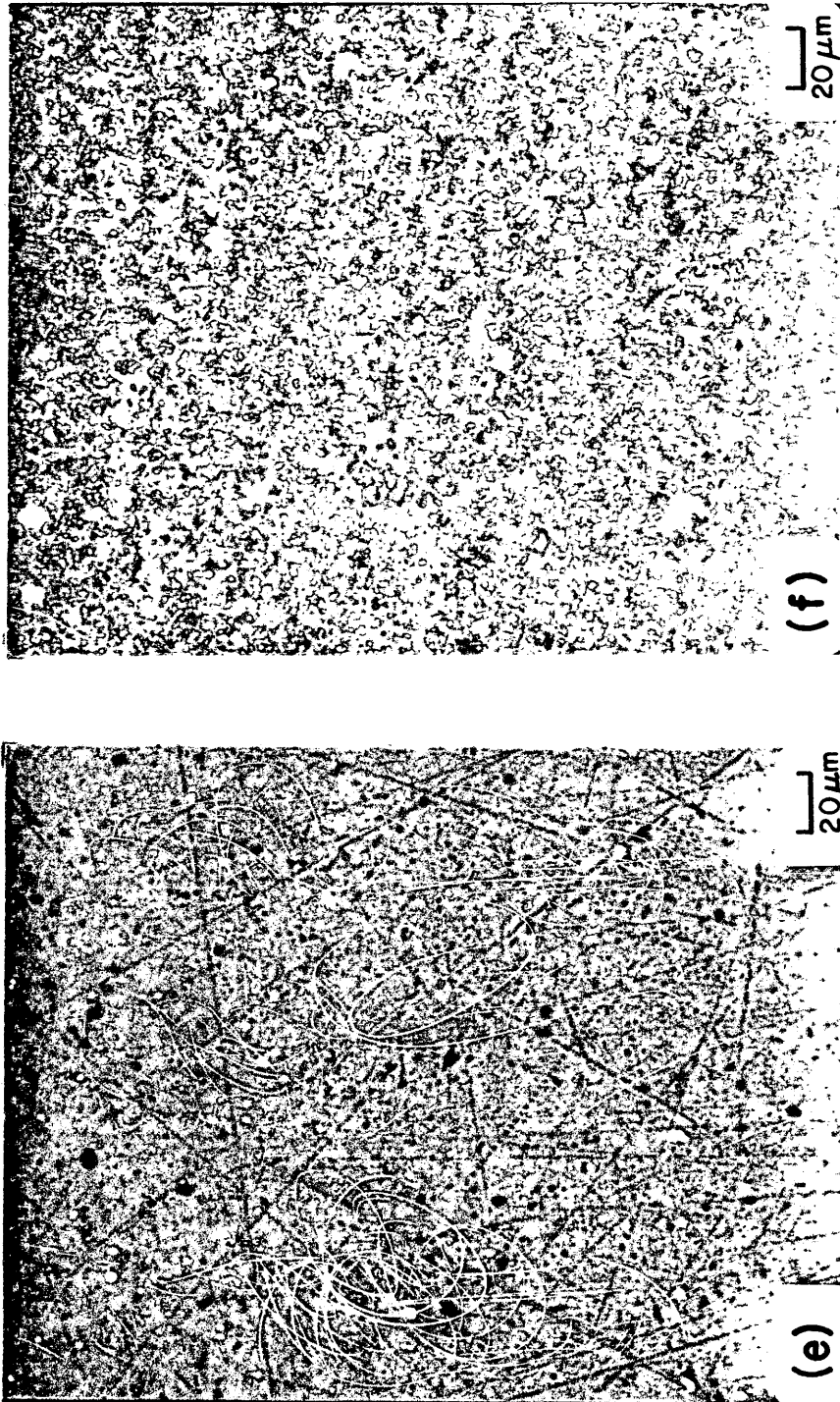


FIGURE 5.5 - OPTICAL MICROGRAPHS OF E) UNCONTAMINATED AND F) CONTAMINATED AGCL ELECTRODES

5.3 Electrolytic-Type Ag/AgCl - After many unsuccessful attempts with the thermal-type electrode, the electrolytic-type Ag/AgCl electrode was suggested and tried. To prepare an electrolytic Ag/AgCl electrode, Ag metal is oxidized to silver ions, and in the presence of chloride ions, AgCl re-precipitates onto the electrode. This forms a stable, adherent, AgCl film on the metal surface. The details of preparation are discussed in the procedure. An electrolytic-type Ag/AgCl electrode is simple to construct and fairly reproducible and was used as the standard reference for measuring other candidate reference electrodes.

The current density for AgCl deposition is known to effect the specific resistance and therefore, the porosity of the AgCl phase(5). Ives stated that current densities between 3-18 ma/cm², in 0.1 N chloride solutions, will yield uniform, coherent, red-brown deposits on the Ag surface with a higher specific resistance the more slowly the layer is formed. In this research, the AgCl was deposited at a current density of 1.0 ma/cm² for 4 hours in 1.0 M HCl. The 'plum' deposit was reasonably adherent and not easily washed or rubbed off. After repeated tests, the purple-blue deposit would transform into an off-white color. This soft white halide layer could perhaps be

the same deposit Ives suggests for deposition current densities in excess of 18 ma/cm^2 . A white AgCl wire was discarded and replaced with a fresh, new purple-blue AgCl wire since the latter type of coating resulted in a more stable electrode.

The results for the 0.01 M KCl Ag/AgCl electrode are presented in Figures 5.6, 5.7, and 5.8. A Ag/AgCl electrode previously thermal cycled, was used as the reference to measure the potential response of another, identical Ag/AgCl electrode. Thermal cycling was observed to reduce instability in the predicted electrode behavior. Referring to the figures, it is apparent that the electrodes are reasonably stable up to 150C in 0.01 M HCl and then behave very erratically at higher temperatures. Although the AgCl wire is tightly packed with 'soaked' zirconia sand to reduce streaming potentials, some solution flow may occur at higher pressures. This would certainly not account for the 100-200 mv fluctuations. Another explanation of this poor stability could be the time differential, between electrodes, in establishing thermal equilibrium. Slight inconsistencies in the AgCl deposit affect the local free energy states and their tendency to equilibrate(5). Thus, equilibration times will vary from sample to sample. Increasing temperature would seem to aid rather than

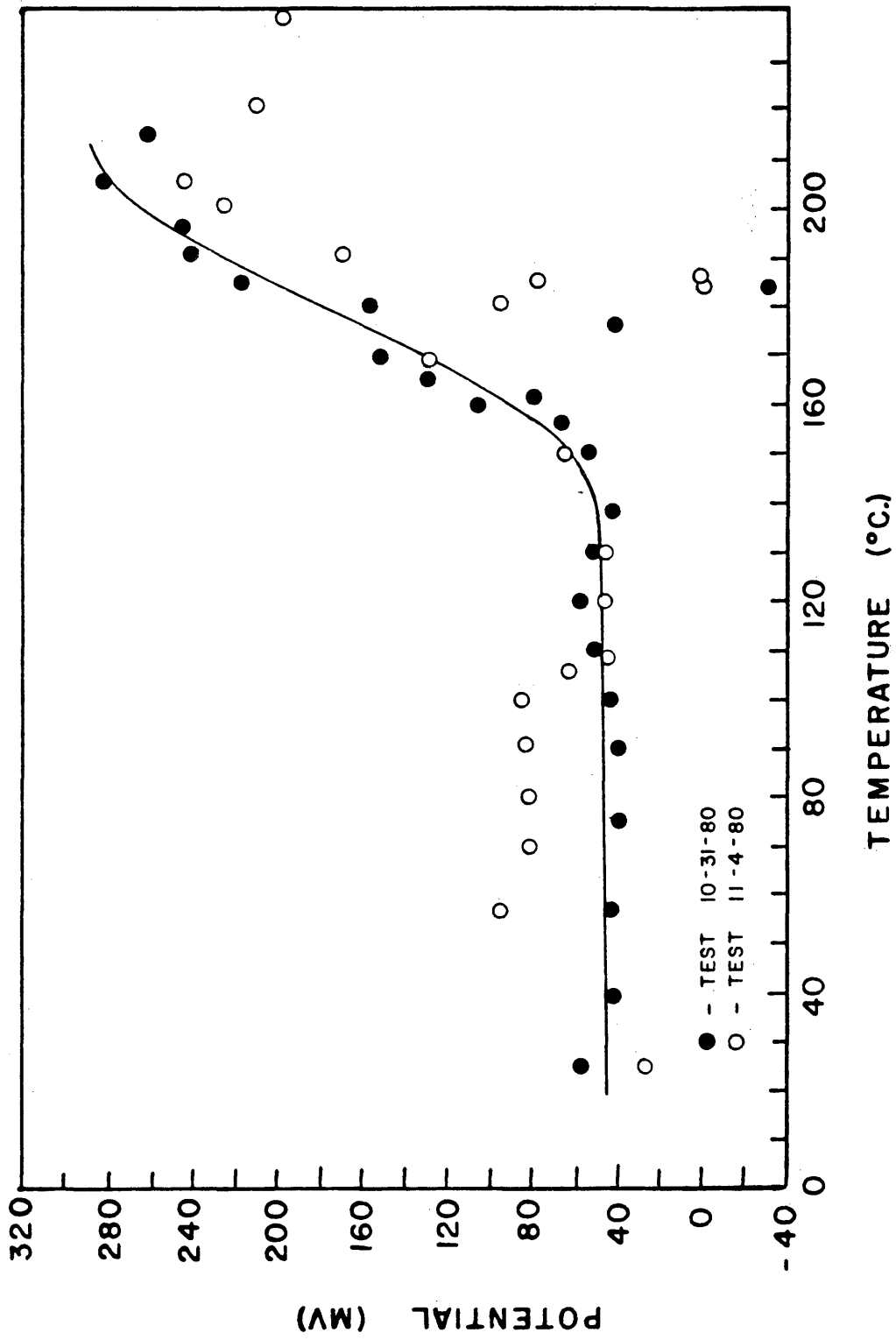


FIGURE 5.6 - POTENTIAL DIFFERENCE BETWEEN TWO IDENTICAL AG/AGCL ELEC-TRODES IN 0.01 M HCL AT ELEVATED TEMPERATURES

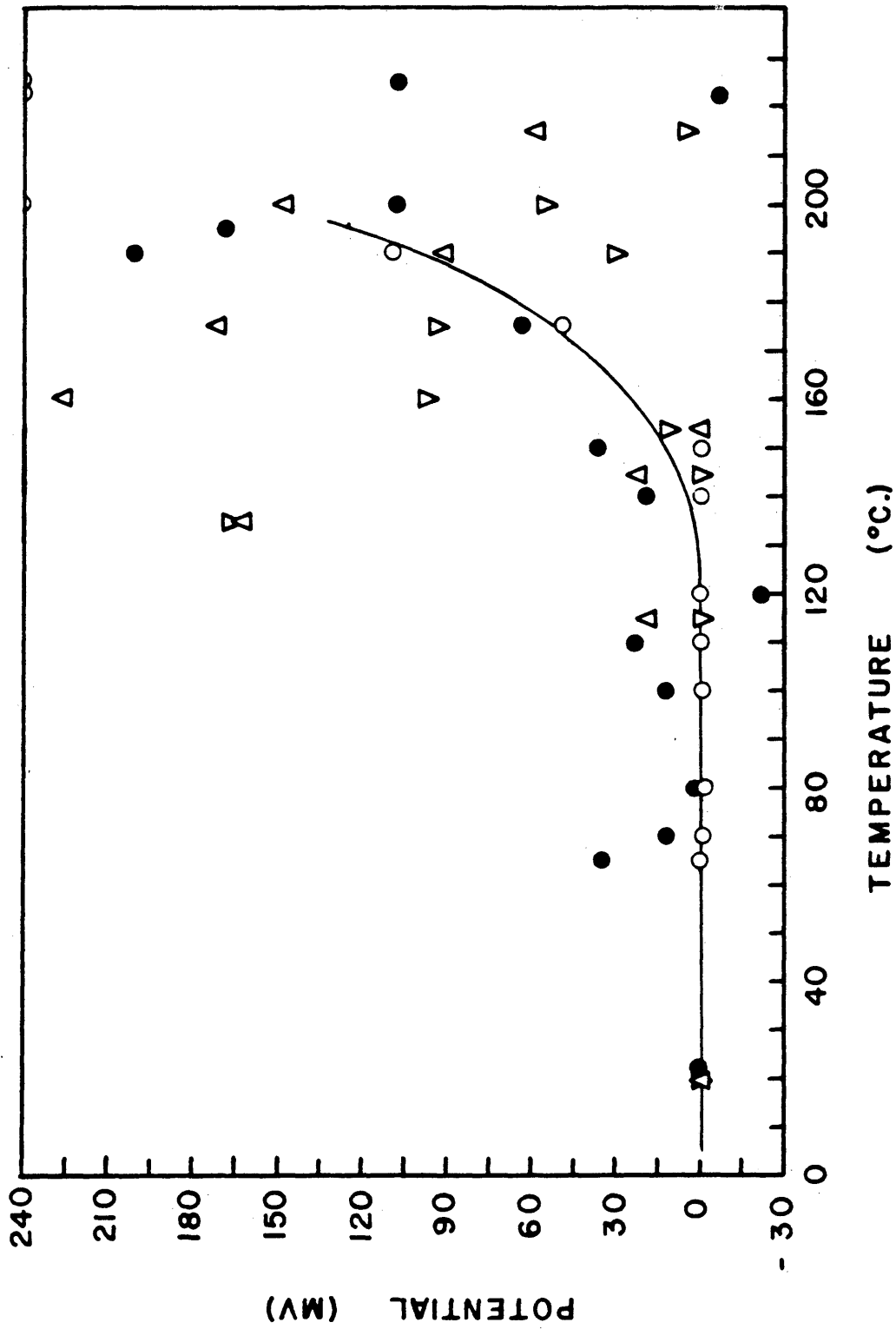


FIGURE 5.7 - POTENTIAL DIFFERENCE BETWEEN TWO IDENTICAL AG/AGCL ELECTRODES IN 0.01 M HCL AT ELEVATED TEMPERATURES

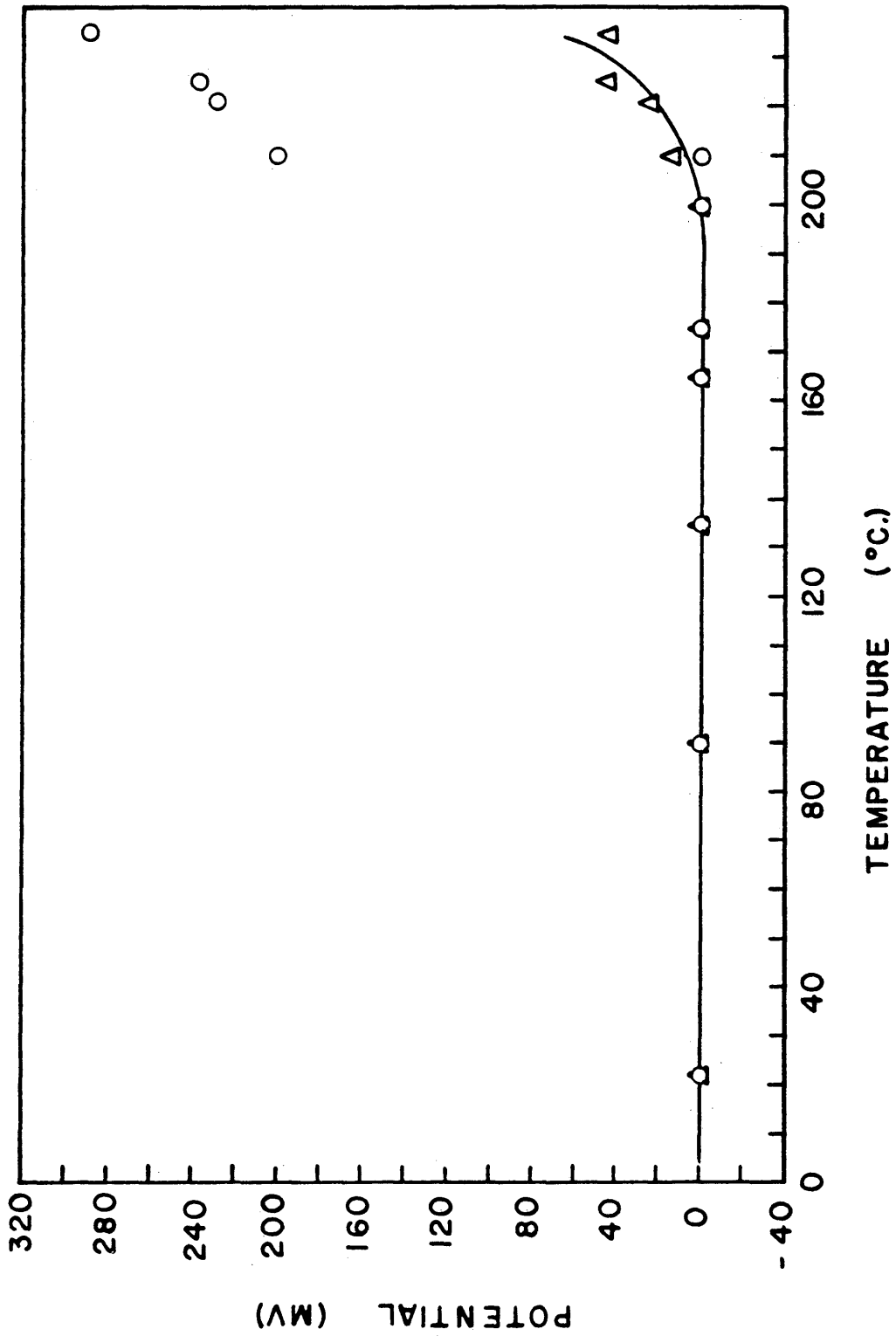


FIGURE 5.3 - POTENTIAL DIFFERENCE BETWEEN TWO IDENTICAL AG/AGCL ELECTRODES IN 0.01 M H₂SO₄ AT ELEVATED TEMPERATURES

hinder thermal equilibration times.

Equilibrium between the electrode and solution is also a function of the measuring circuit. Even though high impedance amplifiers were used to minimize current flow in the measuring circuit, other sources of stray fields may have effected the electrode. Whenever external factors were suspected of impairing an electrode, the problem was either immediately eliminated or minimized. Therefore, the unstable response of the Ag/AgCl electrode above 150C was suspected as a fault of the basic electrode mechanisms rather than the overall system.

The Ag/AgCl was tested in a variety of solutions though most of the tests were run in 0.01 M HCl for a number of reasons. A 0.01 M HCl solution is 1) a good control or standard in which to observe other dependent variables of the system, 2) a source of chloride ions for the AgCl reaction, 3) within the concentration limits for Debye-Huckel calculations of the activity coefficients, 4) widely used by researchers in studying the Ag/AgCl system, and 5) a reasonably simple and manageable solution to handle at higher temperatures-pressures. It should be noted that the actual pH of 2.4 for the system differed from the calculated pH of 2.0 (Refer to appendix and theoretical calculations).

Since the 0.01 M HCl solution was an optimum choice for the Ag/AgCl research, it would seem that other factors were biasing this electrode's behavior.

At the end of each test, the measured electrode rest potentials at 25C were, whenever effected, less positive with respect to a satd. calomel electrode. An electrode, with a 'plum' colored AgCl deposit, could be 're-generated' by rinsing the soaked zirconia sand with fresh KCl and replacing the zirconia plug. The above procedure was used successfully to regenerate the original Ag/AgCl emf. This capacity of the Ag/AgCl electrode to re-establish equilibrium suggests that the instability encountered at higher temperatures is a function of the external system.

Impurities in the system may have contaminated the electrode. Since it was desirable to simulate the actual operating environments of a three electrode corrosion monitor, dissolved oxygen was not removed from the system. Ives(5) reports that dissolved oxygen is known to impair the performance of a Ag/AgCl electrode. The higher the temperature, the higher the overpressure of oxygen, and hence, the higher the probability for contaminating the Ag/AgCl electrode. In later tests with the Pd-H electrode and de-aerated systems, the Ag/AgCl electrode exhibited more stable and predictable behavior.

Note that in the Pd-H system, a Ag/AgCl electrode was possibly exposed to dissolved hydrogen in the system. Overall impurity levels though, were either eliminated or reduced to acceptable concentrations. Though pre-electrolytic reduction of impurities could have been used to reduce impurity levels, high purity reagents and a careful operational control were used in this case.

The electrode design was modeled after Agrawal's (45) electrode, yet this type of configuration may have caused the instability in the Ag/AgCl electrode used in these tests. In later tests, the buffer compartment was removed and the electrode appeared to behave more predictable. The buffer compartment could have been a source for an unnecessary and significant junction potential. A bare AgCl coated Ag wire was tried as a reference in the Ag/AgCl (0.01 M KCl) / H^+ (0.01 M HCl) / Pd-H system and the results were in good agreement with predictable, thermodynamic behavior. Not only might the electrode configuration, with its inherent junction potentials, have caused the observed instability, but the teflon material of the electrode body might have also. Without careful pre-treatment, low molecular weight fluorocarbons or fluorine may have been given off by the teflon

at higher temperatures. The teflon was carefully cleaned although it was not thermally treated before testing. From the above discussion, it is apparent that subtle, seemingly insignificant factors, may have biased the Ag/AgCl electrode response; realizing that experimental procedure was modelled after proven methods in the published literature.

The stability and versatility of the Ag/AgCl electrode has been well documented, yet precaution should still be exercised in its preparation and use. In this research, the Ag/AgCl electrode performed reasonably well and was chosen as the reference for the Pd-H electrode. Thermodynamic considerations have been included in the context of the Pd-H electrode discussion and only the actual measured rest potentials, relative to other Ag/AgCl electrodes at higher temperatures, have been presented here.

5.4 Palladium Hydride Electrode - The emphasis of this research has been the characterization and development of a reference electrode for solar energy environments. From the information presented in section 3.3.2, it is apparent that a Pd wire, charged with atomic hydrogen will maintain a stable potential, and may even undergo the same reaction scheme as the standard

hydrogen electrode(35,36,37,38). Rather than develop an electrode that will have to be calibrated on the SHE scale, it is more convenient and practical to develop an electrode which demonstrates the same reaction scheme as the standard hydrogen electrode. The details of this new Pd-H design and preparation are presented in the procedure, although a brief note will be made on the proposed methodology behind the Pd membrane with special emphasis on the inner and outer surface properties. Therefore, the following discussion will deal with first, the problems and observations in preparing the Pd-H membrane, then, the results for the various Pd-H electrodes, and finally, the performance and viability of the proposed Pd-H reference electrode based on the criteria for a 'good' reference electrode.

5.4.1 Membrane Methodology - A standard hydrogen electrode with platinum substrate will, by its inherent theoretical design, contaminate a solution with one atmosphere of dissolved molecular hydrogen. Hence, a membrane, with the predictable hydrogen absorption behavior of Pd, could be used to isolate the gaseous hydrogen from the test solution and still effectively maintain the overall hydrogen equilibrium reaction (Figure 5.9). The overall membrane must break down, or

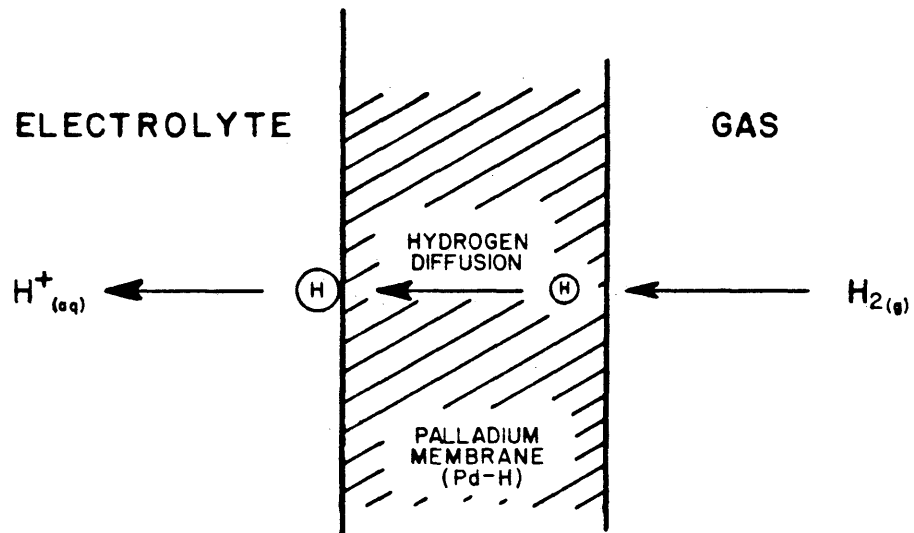


FIGURE 5.9 - A SCHEMATIC OF THE PD-H MEMBRANE ELECTRODE USED IN THIS STUDY

atomize, the molecular hydrogen on the gaseous side and catalyze the ionization process on the solution side. A carrier catalyst, such as powdered copper, uranium, or platinum could be used on the gas side and a black Pd or Pt surface could be used on the solution side. To establish a stable potential, the Pd-H electrode will either have to maintain a steady state mass flow of hydrogen or an equilibrium condition between the activity of hydrogen in the Pd lattice and the activity of hydrogen in solution at the solid-solution interface. Many different types of Pd electrode configurations were attempted in order to simulate the above methodology for a Pd-H electrode. Since each type of electrode configuration gave some insight into the final electrode arrangement, these results are presented in the first part of the discussion of the Pd-H membrane electrode.

5.4.2 Initial Tests of a pure Pd tube - The first test in 0.01 M KCl at 25C, consisted of a pure Pd membrane with no initial pre-treatment other than rising in 1) 50 percent aquaregia, 2) 37 percent HCl, and 3) distilled water. Remember that a Pd membrane is actually a Pd tube, sealed off at one end with a steel plug. With reference to a saturated calomel electrode, the Pd-H electrode exhibited an initial rest potential of

0.310 V., a potential of 0.303 V. after 20 hours, and a potential of 0.2745 V. after approximately 48 hours. The potential drift could either be due to surface contamination of the Pd surface or hydrogen contamination of the calomel electrode. This same Pd-H electrode was removed from the test solution, cleaned in the same manner, and then returned to a new 0.01 M KCl test solution; the measured test potential was 0.28 V. vs. SCE at 25C. Evidently the Pd-H electrode has been contaminated, or altered, to the extent that the original rest potential could no longer be re-established. Though perhaps premature, the electrode was tested at higher temperatures-pressures with a Ag/AgCl reference.

5.4.3 Response of Pd-H Electrode at Higher Temperatures and Pressures with Various Surface Conditions -

The purpose of these initial Pd-H tests was to devise a Pd-H electrode with a stable, possibly thermodynamic, potential. An electrolytic-type Ag/AgCl electrode was used as the reference and in most instances was the primary source of instability in the system; the deviation of the Pd-H electrode response from predicted theoretical behavior coincided with the observed deviation between two identical Ag/AgCl electrodes. The presence of dissolved oxygen and hydrogen may have contaminated

the Ag/AgCl electrode. Initially a pure Pd membrane exhibited a potential of 0.312 V. (vs. Ag/AgCl at 25C) and then leveled off to a rest potential of 0.337 V. after approximately 5 hours. The measured rest potentials were reasonably stable (± 1 mv) although other types of Pd membrane preparations were attempted.

The results of the Pd-H electrode, with various surface preparations and pre-treatments, are shown in Figures 5.10 and 5.11. It is quite apparent from these results that the Ag/AgCl (0.01 M KCl) / zirconia / junction / 0.01 M HCl / H^+ / Pd-H system is unstable. The solid line represents the ideal thermodynamic potential response of a 0.01 M KCl Ag/AgCl electrode vs. a SHE (Refer to appendix for the theoretical calculations). Considering the data on the whole, the ideal thermodynamic curve appears to be an asymptote to the actual system response. Though the ideal curve has some curvature to it, the curvature of the actual test data is quite pronounced, displaying a parabolic shape skewed to the lower temperatures. Surface preparation seems to influence the measured potentials of the system, though a more prominent factor is dominating the overall potential response of the system. Therefore, in lieu of the above results and before presenting the results of a more viable Pd-H electrode configuration, the surface preparation and

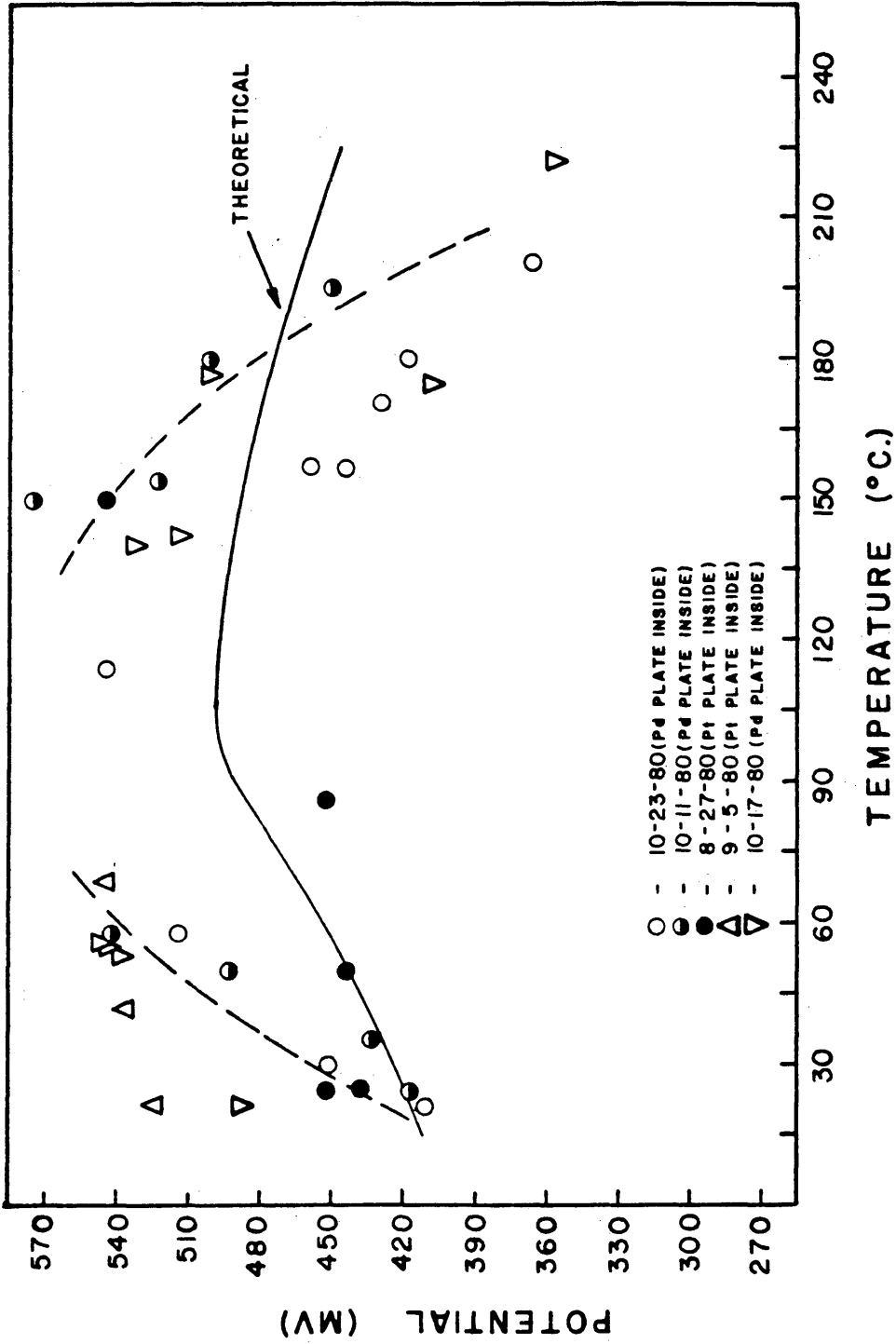


FIGURE 5.10 - MEASURED POTENTIALS OF THE AG/AGCL - PD-H/H₂ SYSTEM IN 0.01 M HCL AT ELEVATED TEMPERATURES

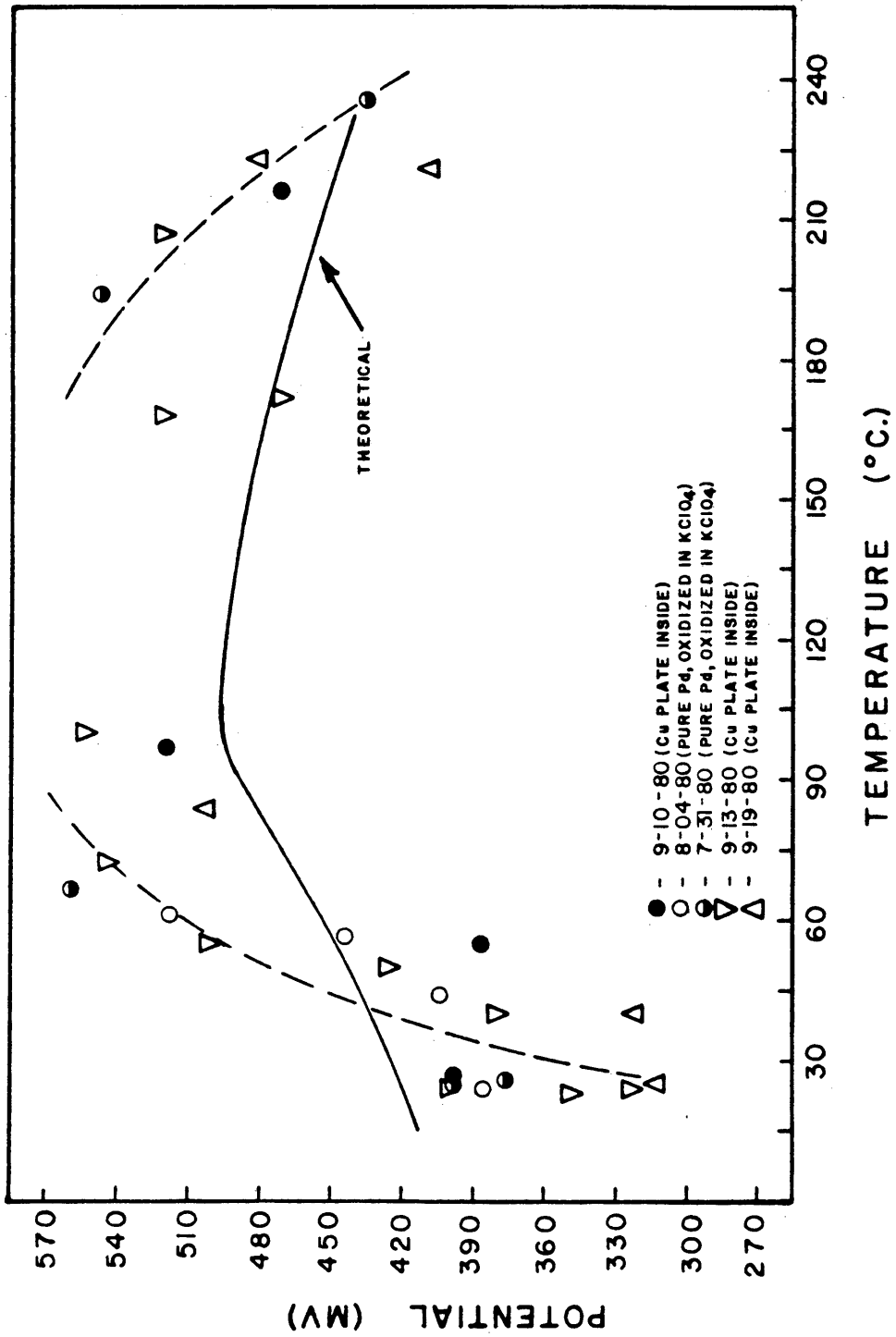


FIGURE 5.11 - MEASURED POTENTIALS OF THE AG/AGCL - PD-H/H₂ SYSTEM IN 0.01 M HCL AT ELEVATED TEMPERATURES

pre-treatment techniques, and observations, will be discussed.

5.4.4 Observations of the Influence of Pre-Treatment on Electrode Behavior - Depending on the type of fabrication of the massive Pd metal, the degree of cold working will effect such properties as the grain size and dislocation density, and hence, may influence the activity of hydrogen occluded, or absorbed, into the Pd lattice. Annealing the sample, to relieve stress concentrated areas, leads to grain growth and reduces the overall grain boundary area. Both of these procedures, annealing and cold working will have an effect on the initial potential at 25C and possibly influence the potential response at higher temperatures and pressures.

Referring to Figures 5.10 and 5.11 and to the Pd micrographs, initial rest potential is observed to be a function of grain size. First, comparing the grain size in the micrographs for test 9-10,13,19-80 and the as received sample, it is apparent that the grain size is larger in the former sample. The sample 9-10,13,19-80 was annealed at 500C for 90 minutes; 45 minutes in an oxygen environment and 45 minutes in a hydrogen environment. This identical treatment of the sample was repeated in three successive tests and after the final test, the

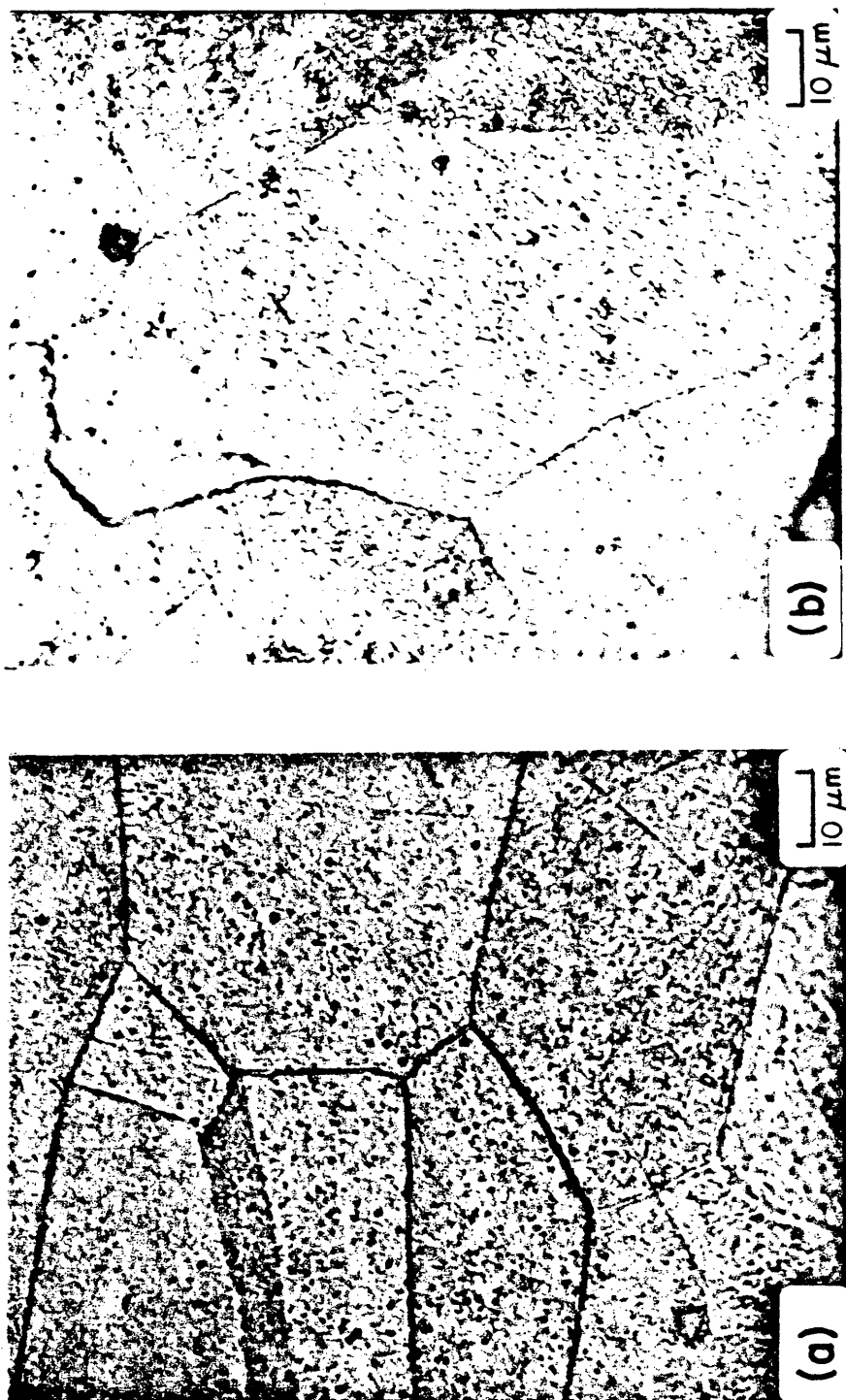


FIGURE 5.12 - OPTICAL MICROGRAPHS OF A) AS-RECEIVED PD METAL AND B) TESTED PD-H ELECTRODE (REFER TO TABLE FOR PREPARATION)

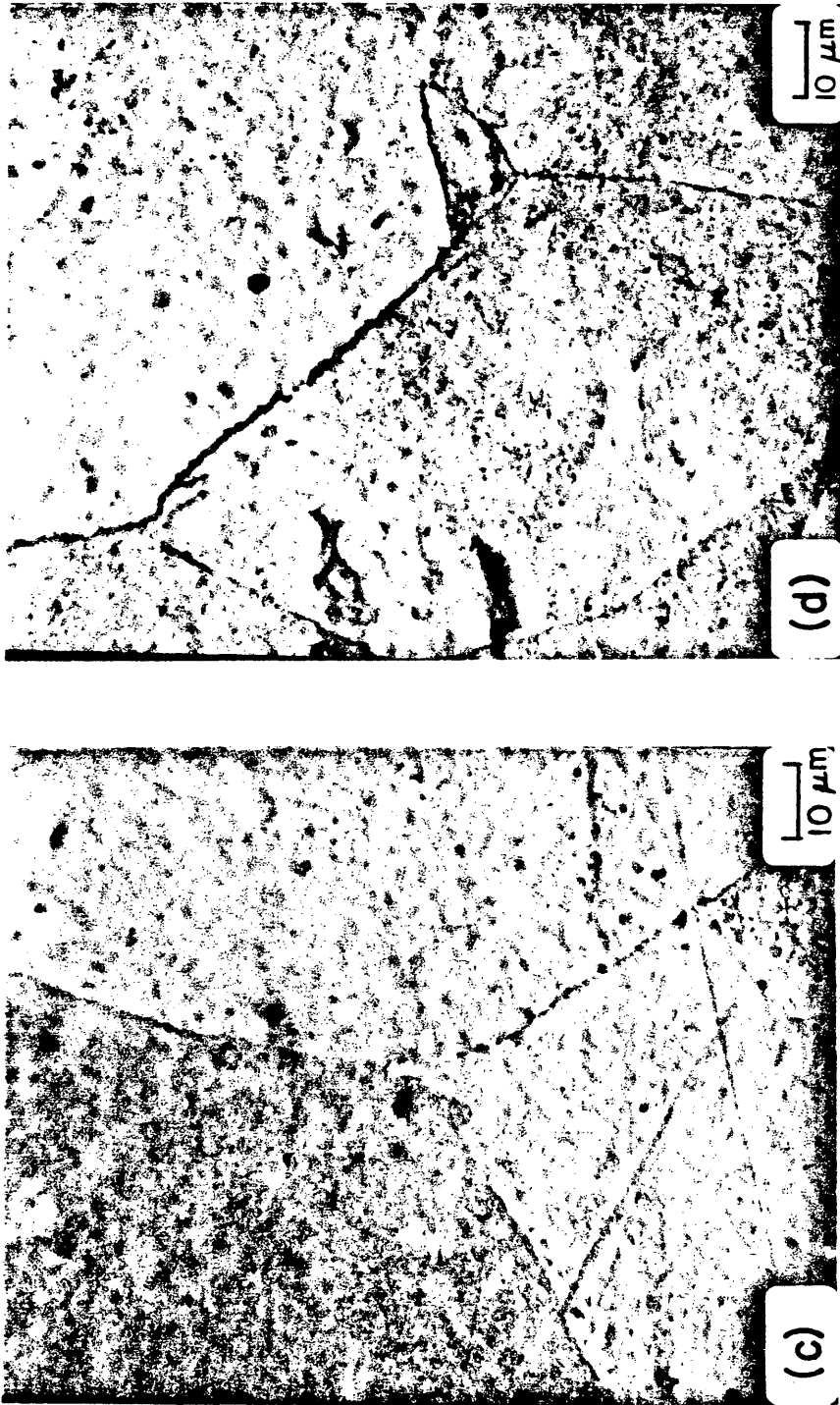


FIGURE 5.13 - OPTICAL MICROGRAPHS OF TESTED PD-H ELECTRODES (REFER TO TABLE FOR PREPARATION)

SAMPLE	TYPE	DESCRIPTION	ETCHANT	ETCH TIME (sec)
a)	Pd metal	as received	40% HNO ₃ , 60% HCl	45
b)	Pd metal	Test 8-27, 9-5-80	40% HNO ₃ , 60% HCl	5
c)	Pd metal	Test 9-10, 13, 1980	40% HNO ₃ , 60% HCl	17
d)	Pd metal	Test 9-10, 13, 1980	40% HNO ₃ , 60% HCl	17
e)	AgCl (s)	untested	-	-
f)	AgCl (s)	tested (contaminated)	-	-

TABLE 5.1 - PREPARATION AND DESCRIPTION OF OPTICAL MICROGRAPHS

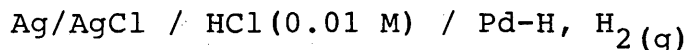
MEASURED		PURE Ag (CUBIC) REFERENCE		
$d\text{\AA}$	I/I_1	$d\text{\AA}$	I/I_1	hkl
2.354	100	2.359	100	111
2.0355	33	2.044	40	200
1.442	23	1.445	25	220
1.23	24	1.231	26	311

TABLE 5.2 - RESULTS OF X-RAY DIFFRACTION ANALYSIS OF PD-H

observed micrograph was prepared. These tests, 9-10, 9-13, and 9-19, are shown in Figure 5.11. In each successive test, the grains became larger, and the measured rest potential became more noble, or negative with respect to the Ag/AgCl electrode. Aben and Burger(34) observed the same effect of grain size on rest potential. The total annealing time for sample 7-31-80 was less and the observed potential response was less noble.

The diamond pyramid hardness (DPH) of each grain also appeared to be a function of the pre-treatment and actual testing procedures. Although the DPH for the as received sample was 140, the DPH was 161 and 195 for test samples 7-31-80 and 9-10,13,19-80 respectively. There is not enough information to suggest solid-solution strengthening, precipitation hardening, or the like, and it was not the intent of this research to explain this phenomenon. It is important though, to emphasize the importance of pre-treatment and its effects on the electrode performance. Therefore, the performance of each Pd-H electrode should be evaluated in the context of the actual pre-treatment and fabrication procedures.

5.4.5 Performance of a Suitable Pd-H Electrode - One electrode configuration appeared to behave in a predictable and repeatable manner. In the pretreatment of this electrode, the Pd-H membrane was 1) abraded inside and out, 2) annealed for 90 minutes at 500C; 45 minutes in a pure $H_2(g)$ atmosphere and 45 minutes in a pure $O_2(g)$ atmosphere, and 3) coated with a Pt plate on the inside and outside of the membrane (Refer to Procedure). The activity of atomic hydrogen in the palladium lattice, for this configuration, was apparently constant at each temperature and the electrode therefore, performed in a stable, predictable manner. Note that in the following discussion of this Pd-H membrane electrode, a bare Ag/AgCl wire was used as the reference and the theoretical calculations pertain to the system;



5.4.5(a) Thermodynamic Stability - To show the thermodynamic stability of the Pd-H electrode, it has to be shown that the activity of atomic hydrogen in the lattice is in equilibrium with the activity of hydrogen ions in solution and both activities vary in a predictable thermodynamic manner. Two cases will be discussed here; 1) the activity of atomic hydrogen in the lattice is equal to α_{max} and varies as α_{max} with temperature and 2) the value of atomic hydrogen in the palladium lattice is constant.

(Atomic Hydrogen Activity Equal to α_{\max}) - Consider the results in Figure 5.14 for a Pd membrane with a platinum plate on just the outside, or solution-metal interface. The solid line depicts the theoretical, thermodynamic potential response for the system at a measured pH of 2.4. Although the actual calculations are presented in the Appendix, a brief discussion here will elucidate the methodology.

Assuming the activity of hydrogen in the Pd lattice varies with increasing temperature and that the hydrogen activity is equal to the value at α_{\max} , then the rest potential for the Pd-H electrode can be calculated. Recalling the effects of Pd-H charging on the observed rest potential, it is reasonable to equate the activity of hydrogen in the lattice with α_{\max} . Also, according to Wicke and Nernst(30), though other workers(37,42) have derived similar equations, the H/Pd atom ratio can be related to the pressure of hydrogen in the lattice. Using this information, a predicted response curve for the Pd-H electrode can be generated. The predicted curve should increase with increasing temperature, whereas the actual plotted curve in the Figure 5.14 has a maximum around 110C. Another look at the actual system will explain the dilemma.

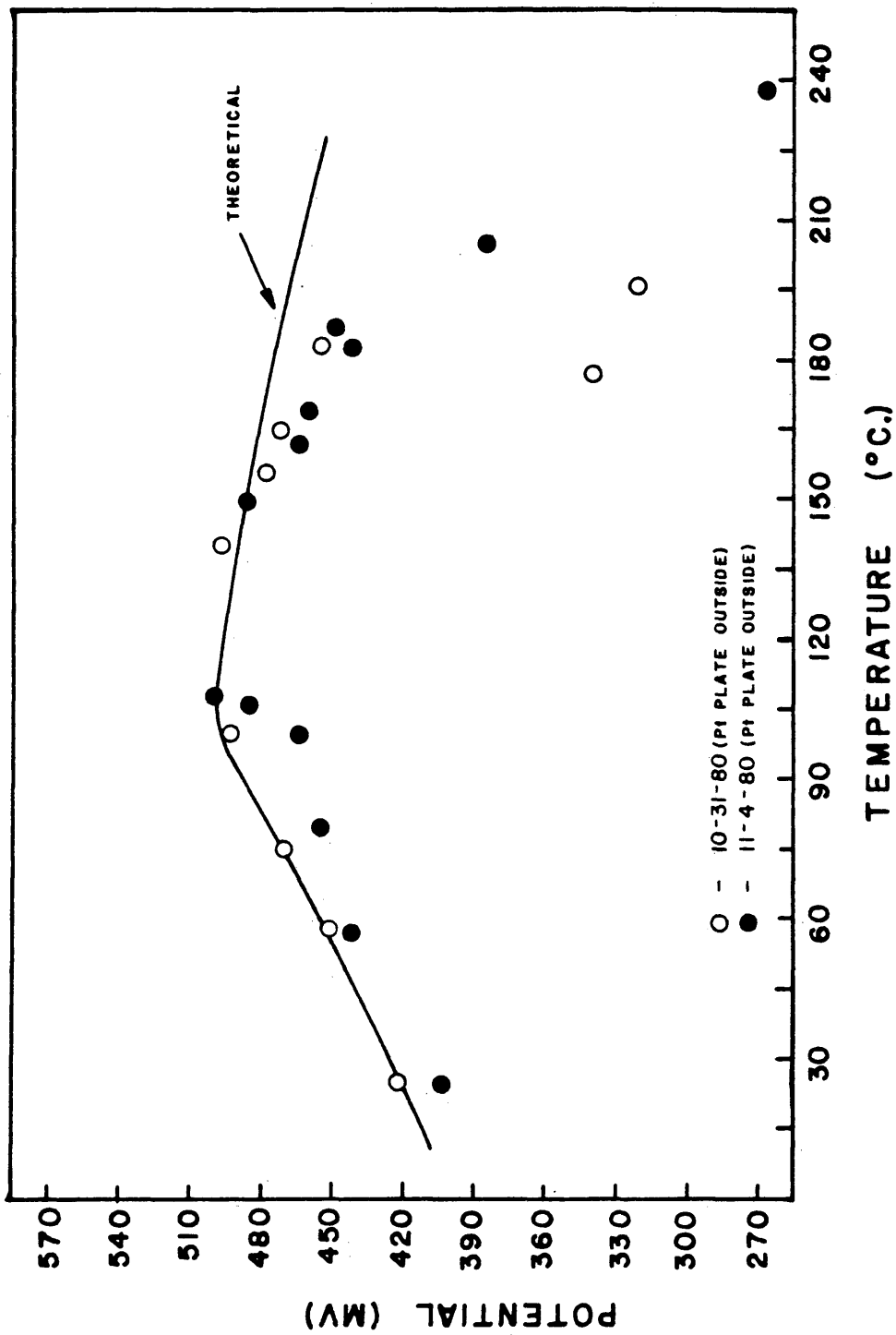


FIGURE 5.14 - MEASURED POTENTIALS OF THE AG/AGCL - PD-H/H₂ SYSTEM IN 0.1 M HCL AT ELEVATED TEMPERATURES (VARIABLE α_{max} PHASE)

Since all of the previous tests exhibited this parabolic potential response curve, it must be an inherent property of the Ag/AgCl-Pd-H system. Previous researchers have found that the lower limit for the potential difference between Pd-H and SHE is zero volts (i.e. the same reaction mechanisms are occurring on both electrodes) (33). They propose that when the electrode has established true equilibrium at the Pt and Pd surfaces, the rest potential is 0.00 V. (vs. SHE) and the stable hydride phase is the β phase. Any non-equilibrium condition in the Pd-H electrode will result in a positive or more noble rest potential with respect to the SHE and indicate the presence of the α phase. Therefore, at H/Pd ratios greater than 0.57 at 25C, or pure β phase, the electrode will exhibit a limiting potential of 0.00 V. on the SHE scale. At lower hydrogen contents, with the α phase present, the electrode will register a more noble, or positive potential. Referring back to the figure then, the theoretical curve represents a parabolic envelope or upper limit for the Pd-H electrode. At temperatures below 100C, notice that the calculated curve is for a changing hydrogen activity and assumes the presence of a stable α phase (i.e. possibly a non-equilibrium condition).

Figure 5.14 shows that the experimental results

agree fairly well with the proposed theoretical calculations, although there are some discrepancies. The results for test 11-4-80 fall below the theoretical curve at low temperatures. This could be due to the effects of larger grains on the rest potential; an observation which was noted earlier. Above 155C though, the data points deviate significantly from the theoretical curve. It was discovered that a Ag impurity had deposited at the Pd-H surface and poisoned the electrode. Ag ions were reduced by the atomic hydrogen at the Pd-H surface. An X-ray diffraction analysis of the deposit confirmed the presence of a pure Ag impurity (Refer back to Table 5.2). It may be significant to point out that the silver ions were the only known noble ion impurities in the system, yet other noble ions may also poison the Pd-H surface. In another system, utilizing a satd. calomel reference (Refer to Figure 5.15), the experimental results agreed fairly well with theoretical calculations below 80C. These results confirm the predictable, thermodynamic behavior of the Pd-H electrode.

(Constant Atomic Hydrogen Activity) - The results in Figure 5.16 show that this Pd-H electrode, with a platinum plate on the inside and outside surfaces, exhibited the same type of response as the SHE. This electrode, presumably with a fully equilibrated β phase,

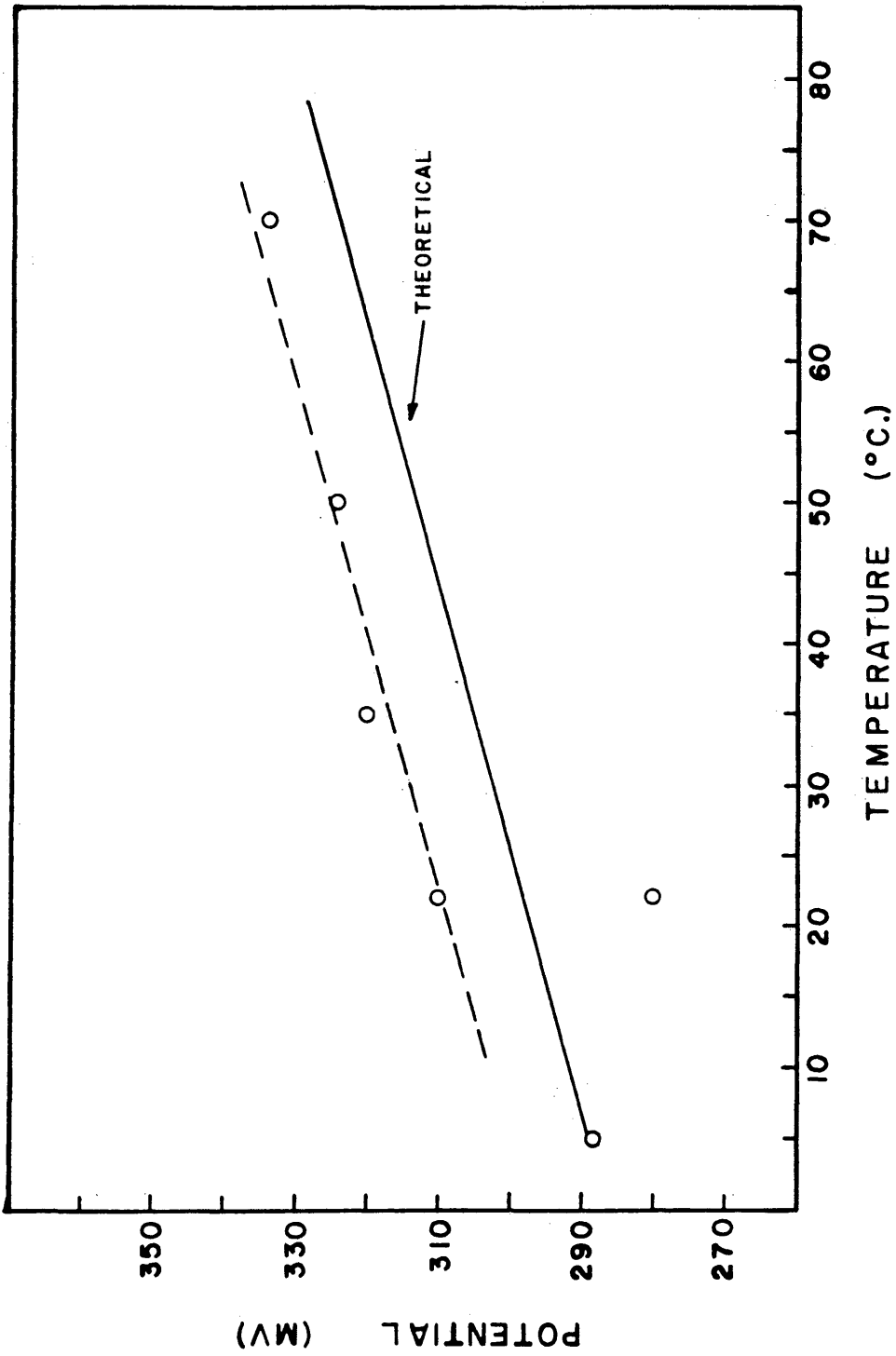


FIGURE 5.15 - POTENTIAL VERSUS TEMPERATURE FOR THE PD-H ELECTRODE IN 0.01 M HCL (ACTUAL PH = 2.4) SOLUTION (SATD, CALOMEL REF)

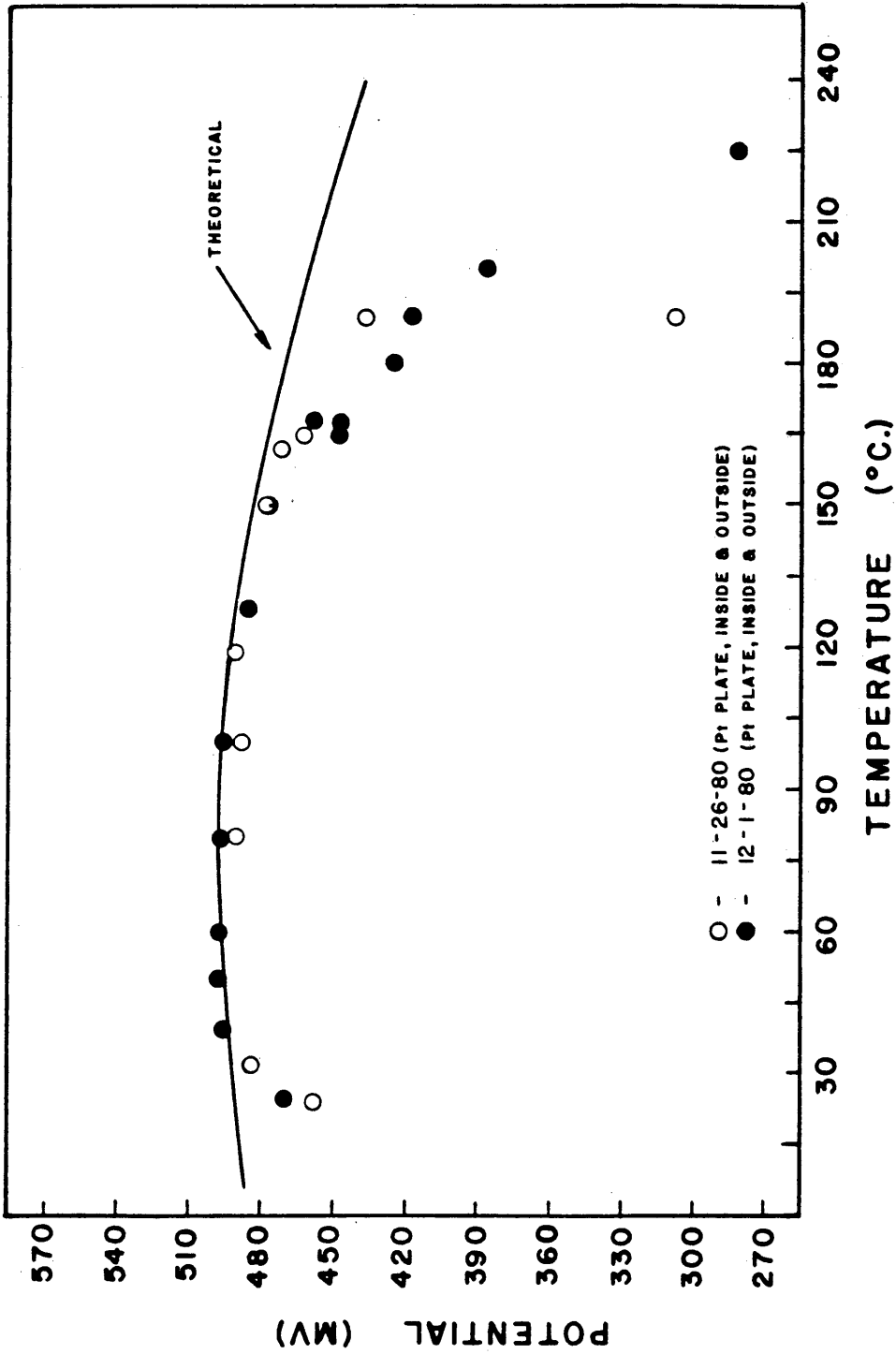


FIGURE 5.16 - MEASURED POTENTIALS OF THE AG/AGCL - PD-H/H₂ SYSTEM IN 0.01 M HCL AT ELEVATED TEMPERATURES (CONSTANT H₂)

agreed reasonably well with the theoretically predicted response of an electrode with a constant hydrogen activity. The actual constant value of hydrogen activity was arrived at through a curve fitting procedure. Ag, as in the previous test, poisoned the electrode surface. A test was run with a Ag/AgCl wire electrode and zirconia junction and the Pd-H electrode was stable up to at least 260C (Figure 5.17).

Though a study of the porosity of the platinum plate was not made, exposure of the Pd surface under the Pt plate may have contributed to the changing hydrogen activity in Figure 5.14 and temperatures below 100C, or to the constant hydrogen activity in this case (Figure 5.16). Schuldiner(35) has suggested that the local cell action between Pt and Pd will promote a 0.00 V. difference in the Pd-H - Pt/H₂ system. If a Pd-H electrode has both platinum and palladium sites exposed, suggesting some type of local cell action, then the results in Figure 5.16 would tend to indicate that the platinum plate on the Pd surface was porous.

5.4.5(b) Effect of pH - At 25C, the Pd-H rest potential is dependent on the pH of the solution. The linear relationship between potential (vs. SCE) and the logarithm of the hydrogen ion concentration is clearly shown in Figure 5.18. This result is not too surprising since the

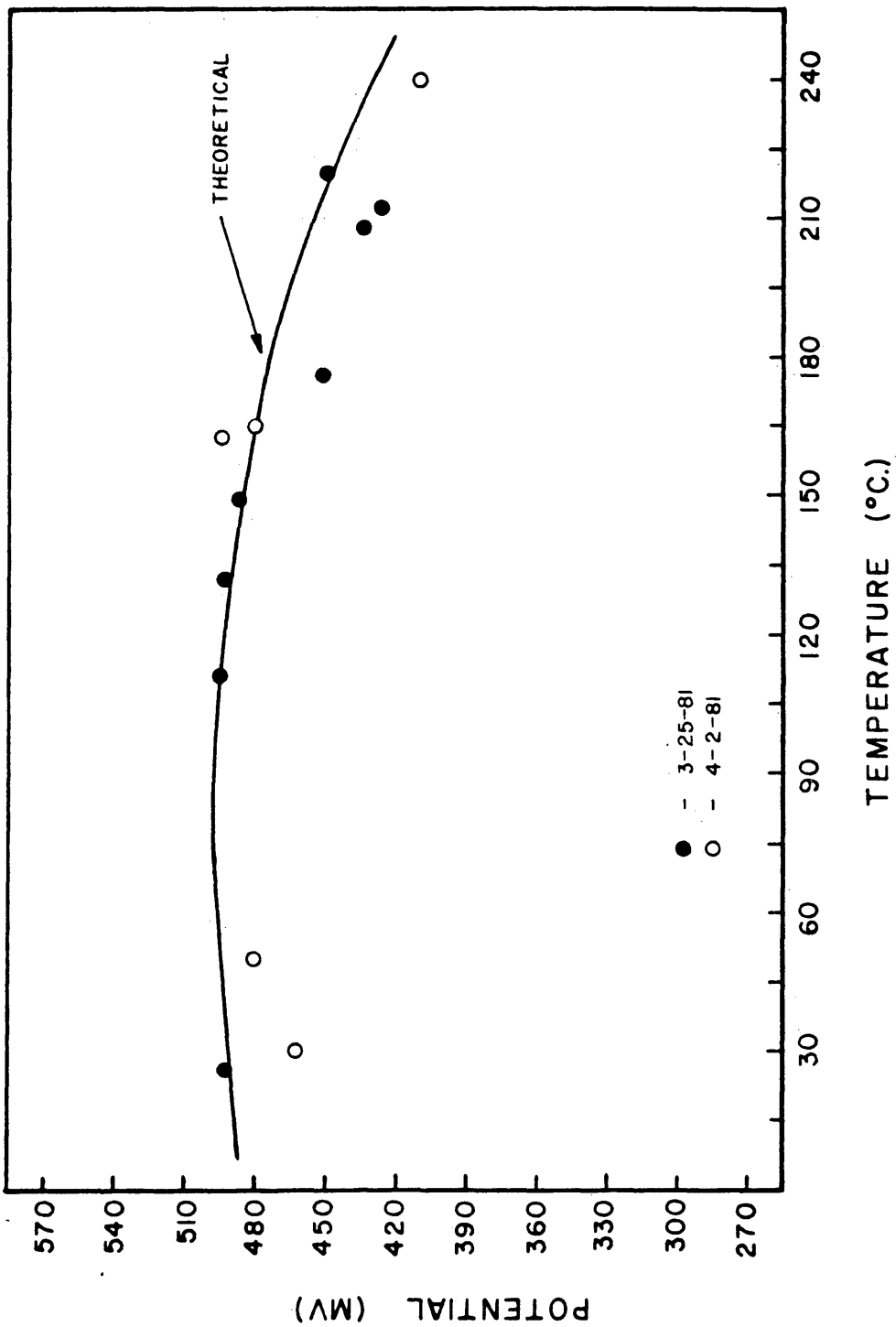


FIGURE 5.17 - MEASURED POTENTIALS OF THE AG/AGCL - PD-H/H₂ SYSTEM IN 0.01 M HCL AT ELEVATED TEMPERATURES (ZIRCONIA JUNCTION)

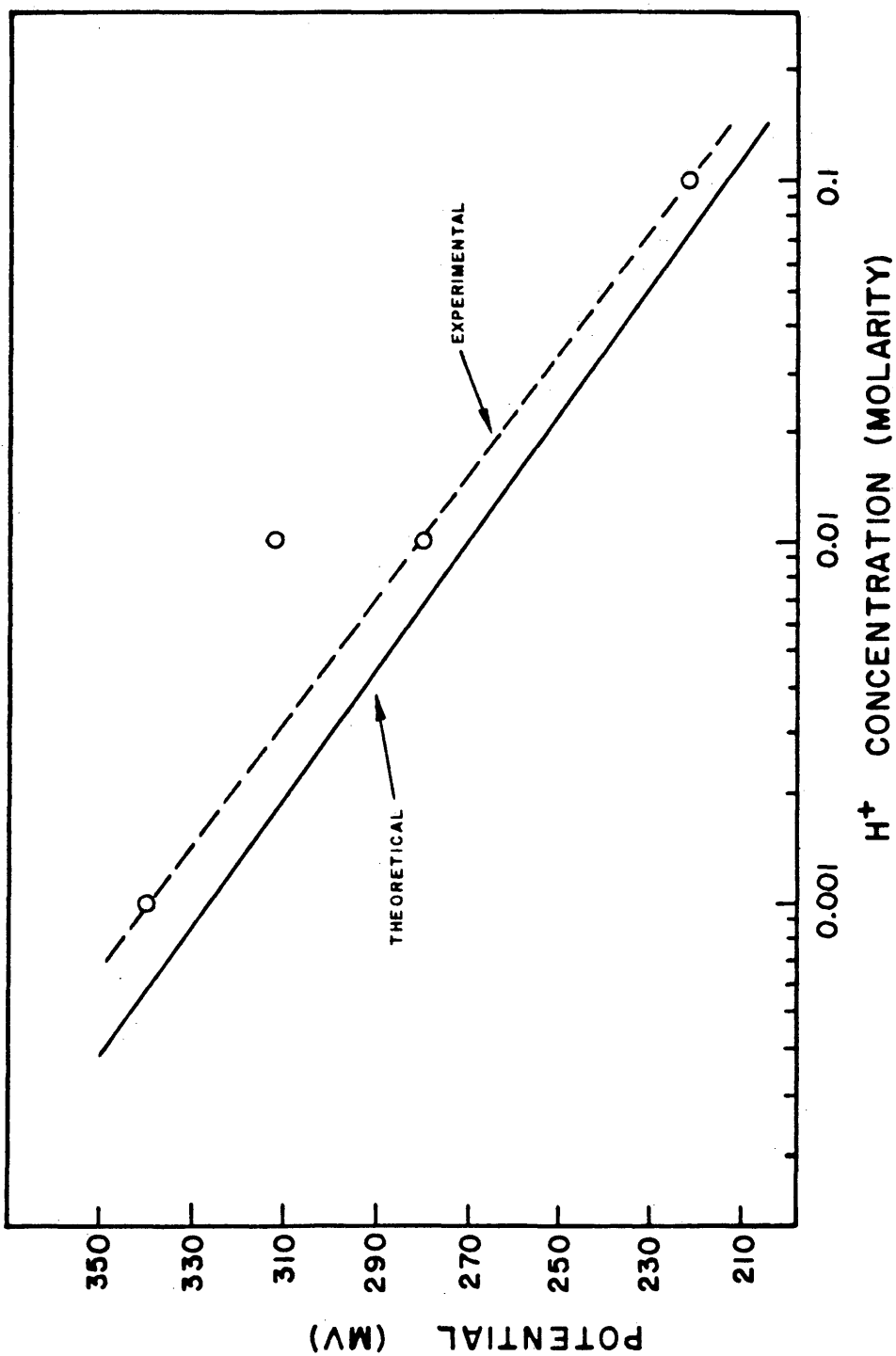


FIGURE 5.13 - pH DEPENDENCE OF THE PD-H ELECTRODE

potential, according to the Nernst equation, is a logarithmic function of the activity of the oxidized and reduced species in the reaction. Although two points were plotted for the 0.01 M $[H^+]$, the stray datum point was observed in another series of tests and has been included for comparison. Vasile and Enke(42) have observed, for a pure Pd wire cathodically charged with hydrogen, that the Pd-H electrode is pH independent in the two phase, 'plateau' region. On the other hand, a standard hydrogen electrode, by definition, is pH dependent. Therefore, a fully equilibrated Pd-H electrode will be pH dependent whereas, an electrode with the α phase present will not necessarily be pH dependent. The Pd-H electrode in this research was pH dependent at 25C though it may not have been a fully equilibrated electrode.

The results in section 5.4.5(a) and (b) have shown the stability of this Pd-H membrane electrode. Though this Pd-H electrode apparently behaves in a thermodynamic manner, it will be mentioned that the potential response of this electrode is analagous to the standard hydrogen electrode.

5.4.5(c) Reversibility - Unless an electrode can be polarized a few millivolts cathodically or anodically from the equilibrium rest potential, it will not meet the criteria for a practical reference electrode. Since

a practical measurement circuit cannot have infinite impedance, some current, however small, will flow and slightly polarize an electrode. The first set of potentiodynamic scans were run between 0 and 90C and a typical scan is shown in Figure 5.19. Notice the reversibility, including both anodic and cathodic scans, is for a range of ± 50 mv, yet Ives mentions that a reference electrode need only exhibit reversibility in a ± 3 mv range. The potentiodynamic scans of the Pd-H electrode in 0.001, 0.01, and 0.1 M HCl solutions were also reversible (Refer to Appendix). There was poor reversibility in the 0.1 M HCl solution, either due to the high chlorine concentration or hydrogen concentration. Except for the concentrated HCl solutions, the Pd-H electrode exhibited excellent reversible behavior in HCl solutions below 90C.

5.4.5(d) Pd-H Performance in Various Solutions -

The Pd-H electrode was tested in other solutions with specific cationic specie. In the presence of Cr^{+++} ions, the Pd-H electrode was poisoned and the results did not reflect theoretical predictions; there was a reddish-brown deposit on the electrode surface at the end of the test. Another cation, Ni^{++} , did not appear to impair the electrode performance although the results from this test also differed from theory. Because of the

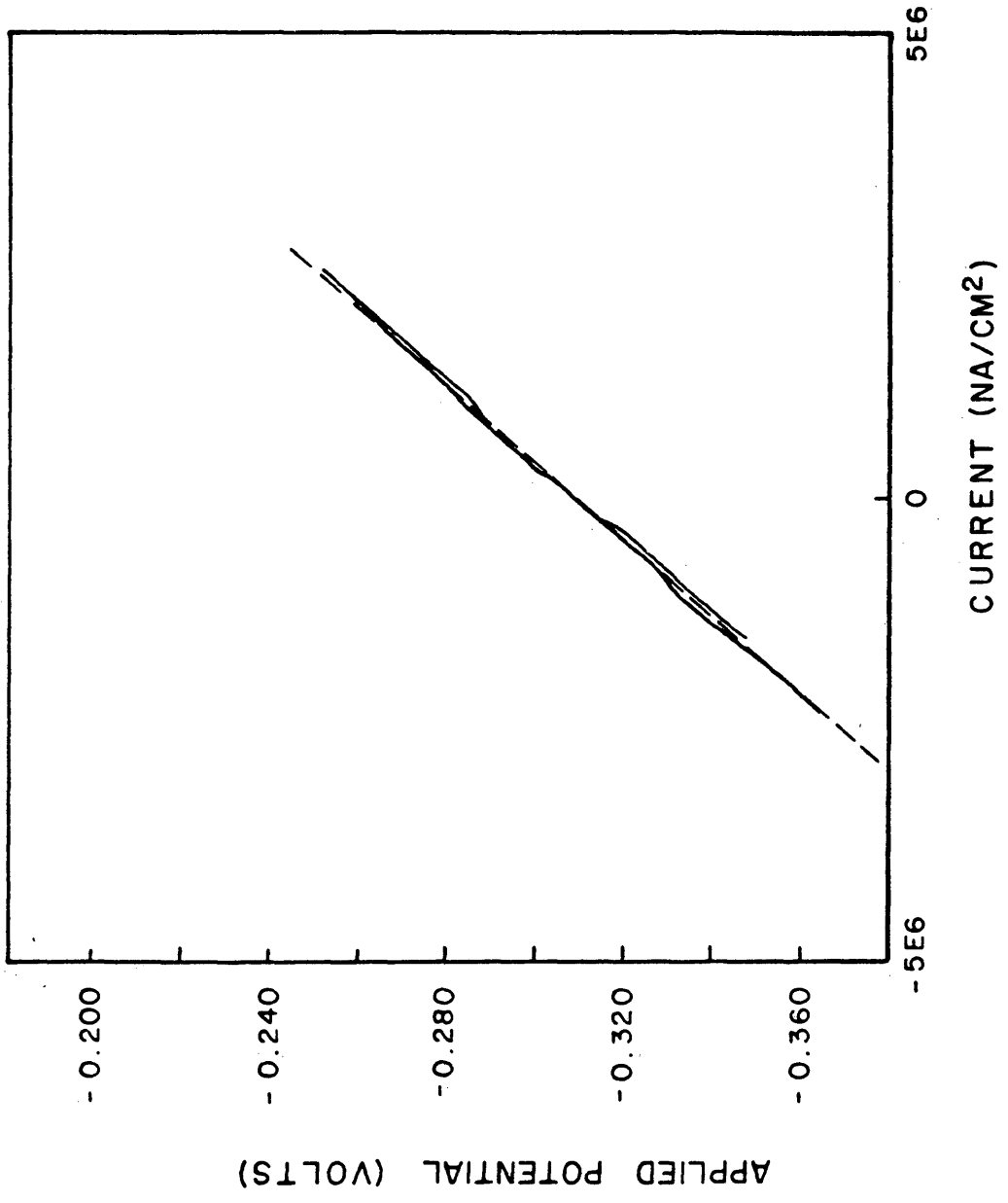
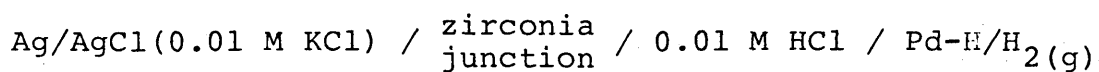


FIGURE 5.19 - TYPICAL LINEAR POLARIZATION SCAN OF THE PD-H ELECTRODE (CONDITIONS FOR THIS TEST: 0.01 M HCL AND 25C)

atomic hydrogen activity at the Pd-H surface, this electrode may fail similarly to the Pt/H₂ electrode. Hence, practical utilization of this electrode may require a junction or membrane, isolating the contaminants from the Pd-H surface.

5.4.5(e) Thermal Cycling - The observations from this research indicate that Pd-H responds quickly and favorably to temperature changes or cycles. The potential versus temperature response of the Pd-H - Ag/AgCl system was dependent on whether the temperature was increasing or decreasing. This noted temperature hysteresis was attributed to the slow equilibration rate of the Ag/AgCl electrode and not to the Pd-H electrode. A difference in equilibration times was observed in the potential difference between two identical Ag/AgCl electrodes. Allowing the Ag/AgCl sufficient time to equilibrate, the potential difference (vs. Pd-H) would eventually approach the theoretically calculated value.

Characterizing an electrode's susceptibility to thermal cycling effects is difficult since the response of an electrode is a function of the other components in the system. In these tests, the electrochemical cell was;



It has been found that a Ag/AgCl electrode will become unstable and fail after repeated thermal cycling(5). Consequently, fresh, stable Ag/AgCl electrodes were used for these measurements.

5.4.5(f) Determination (Proposal) of a Reaction Mechanism at the Pd-H Electrode -

Now that the apparent thermodynamic stability and reversibility of the Pd-H electrode have been established, it would be appropriate to comment on a possible reaction scheme. The following discussion assumes the discharge of hydrogen ions at the Pd-H surface rather than the reduction of water molecules (i.e. an acid media (H^+) instead of basic media). Since the Pd-H has already been shown to be a viable reference electrode in HCl media, this academic exercise is only intended to elucidate a possible hydrogen reaction mechanism and compare or contrast the results to the standard hydrogen reaction.

Considering the configuration for the Pd-H electrode, the following reaction process occurs. First, hydrogen gas enters the Pd membrane from the 'dry', gaseous side, and is absorbed into the palladium lattice. Then, hydrogen diffuses through the bulk palladium metal to the metal-solution interface. Though hydrogen was shown(28) to diffuse faster through the β phase

hydride than the α phase hydride, it should not limit the overall reaction mechanism. At the metal-solution interface, atomic hydrogen in the lattice transfers to the adsorbed state on the metal surface. Finally, the adsorbed hydrogen atom ionizes and is released into the solution. This reaction scheme and the calculations for the rate determining step have been included in the appendix. It will therefore suffice to mention that the hydrogen discharge mechanism has been proposed as the rate determining step for the overall Pd-H reaction scheme. This is analogous to the slow-discharge theory on the standard hydrogen electrode.

Assuming the hydrogen discharge step is rate limiting, then theory predicts an anodic tafel constant of 0.118 at 25C (298K). The actual experimental anodic tafel slope is approximately 0.12, or 0.12-0.112, at 24C for the Pd-H electrode. The good agreement between theoretical and experimental calculations supports the hydrogen discharge mechanism.

The stoichiometric number for this rate determining step has also been determined. By definition, the anodic tafel constant, β_a , is given by the following expression;

$$\beta_a = \frac{d \eta}{d(\log i)} = \frac{2.3 RT}{\alpha F}$$

Likewise, for the cathodic tafel constant:

$$\beta_c = \frac{d \eta}{d(\log i)} = \frac{2.3 RT}{\alpha^{\rightarrow} F}$$

where α^{\rightarrow} and α^{\leftarrow} are transfer coefficients.

Using the tafel constants from experimental results,

where $\beta_a = 0.112$ and $\beta_c = 0.104$, the following

transfer coefficients were calculated;

$$\alpha^{\leftarrow} = 0.483 ; \text{ and } \alpha^{\rightarrow} = 0.566$$

Finally, the stoichiometric number, ν , was calculated,

using the relation;

$$\nu = \frac{n}{\alpha^{\rightarrow} + \alpha^{\leftarrow}} = \frac{1}{0.566 + 0.483} = 0.953 \approx 1$$

where n is the number of electrons transferred.

These results show that the rate determining step occurs once for every single occurrence of the overall hydrogen reaction.

Since the proposed rate limiting step, the discharge of hydrogen ions, depends on the concentration of hydrogen ions, the electrochemical reaction order could be determined. At constant emf, but not constant overpotential, η , the current density, i , depends on the concentration C_{H^+} with a certain power, Z_{H^+} , the electrochemical reaction order. The electrochemical reaction order is given by the following equation;

$$Z_{H^+} = \left\{ \frac{\log i_+}{\log C_{H^+}} \right\}_{C_{Pd-H}, E}$$

For the hydrogen reaction at a Pd-H electrode, the activity of hydrogen atoms, or reduced species, is assumed to be constant at the Pd surface. The graphical determination of Z_{H^+} is shown in Figure 5.20.

The vertical distance between the two curves, represented by the dashed line (a), is the electrochemical reaction order. This value is approximately 1.05. Utilizing the law of mass action;

$$C_o = K_o [H^+]^{1.05} [Pd-H]^o = K_o [H^+]^1 .$$

To complete this exercise, the corresponding reduced species should have one more electron than the oxidized species. For example;

$$S_o = [H^+] \quad \text{and} \quad S_r = [Pd-H] ;$$

where S_o is the oxidized substance and S_r is the reduced substance. Therefore, the rate limiting step in the overall hydrogen reaction transfers one electron for every hydrogen ion discharged.

The above discussion suggests a possible reaction mechanism which occurs at the Pd-H electrode tested in this research. Considering all of the above results together, a simple, realistic reaction scheme was proposed. In other words, the rate limiting step discharges one hydrogen ion and transfers one electron for each

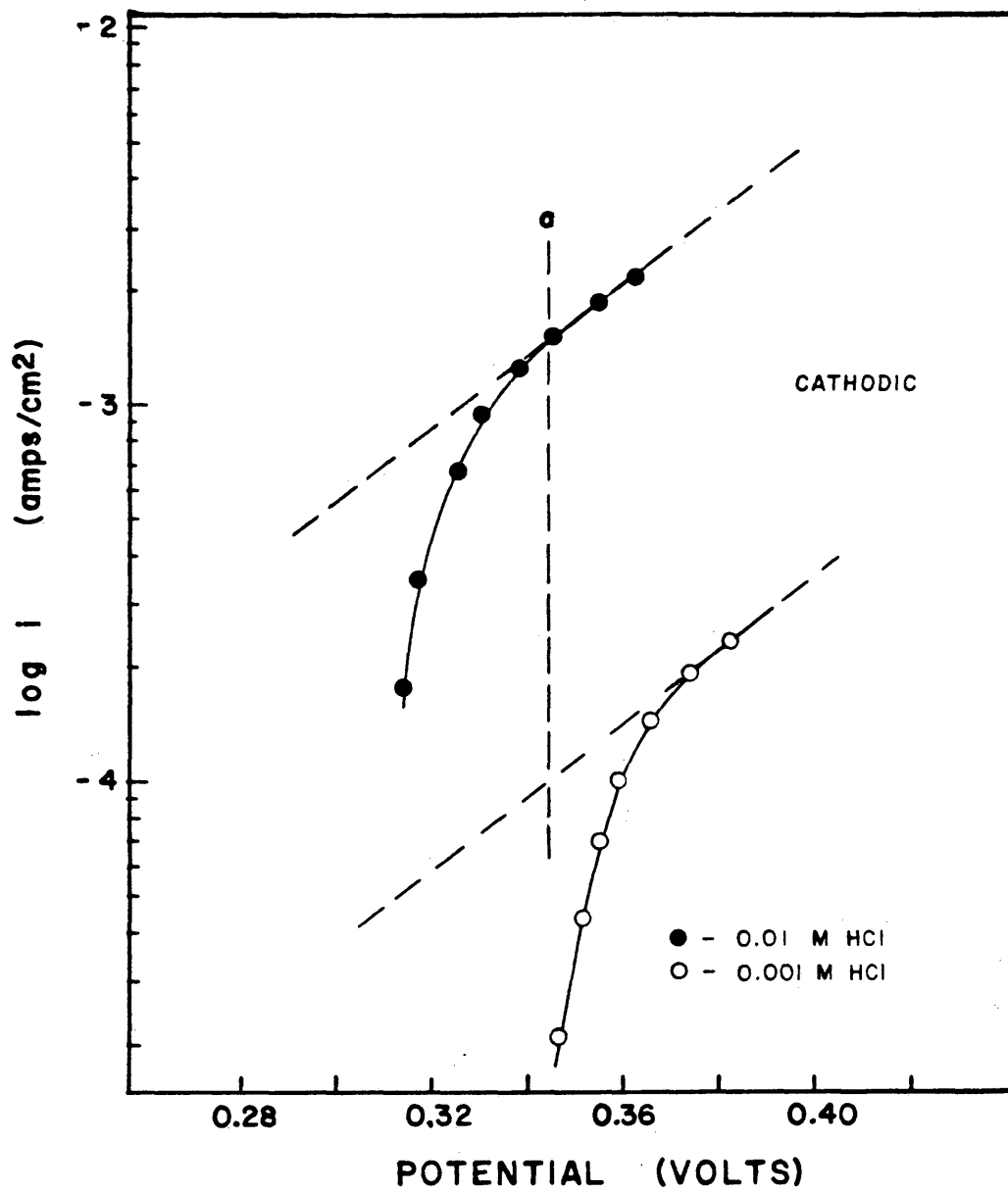


FIGURE 5.20 - CATHODIC CURRENT DENSITY VERSUS POTENTIAL FOR THE $H^+/Pd-H$ REDOX REACTION AT 25C

overall hydrogen reaction. These results, within experimental error, agree quite well with the theoretical calculations and therefore, provide a mechanistic look at the Pd-H electrode reaction.

CHAPTER 6

SUMMARY

As the demand on performance of economical containment materials is maximized, in future energy conversion systems, on-line corrosion monitoring, especially three electrode systems, will be even more critical in evaluating and preventing the failure mechanisms in these systems. It was the purpose of this study to survey and discover or develop a high temperature-pressure reference electrode(s), the limiting component in a three electrode system, for use in solar energy systems. The reference electrode(s) had to be serviceable up to at least 300C and in an aqueous pH range of 2-11. Silver-silver halide, copper-copper sulfate, and Pd-H were the primary candidate reference electrodes proposed for this study.

Because of its noted versatile and practical applications as a low temperature corrosion monitor, the Cu/CuSO₄ was tested at higher temperatures. The high solubility of CuSO₄, however, limit this electrode to approximately 90C. Since a Thalamid electrode is similarly limited to approximately 150C on account of the high solubility of its thalious chloride, the temperature limitations of high solubility salts certainly

supports Ives low solubility criteria for a reference electrode of the 'second kind'. Cu/CuSO_4 was tested in H_2SO_4 , NaCl , distilled water, and ethylene glycol-water solutions and did not appear to be limited to just sulfate solutions.

Various Ag/AgCl electrodes were tested in 0.01 M HCl solutions. Thermal Ag/AgCl electrodes prepared from pure AgCl powder, were sensitive to light and contaminants, such as the borosilicates in high alkali glassware and the response at higher temperatures above 100C was poor. In later tests with the electrolytic Ag/AgCl electrode, it was noted that the electrode configuration with teflon compartments and zirconia junction material, may have caused the instability in the Ag/AgCl response. A bare, thermally coated Ag/AgCl electrode was never tested since another Ag/AgCl electrode, the electrolytic-type, was much easier to prepare.

Analogous to the thermal-type electrode, the response of the electrolytic-type Ag/AgCl electrode was also unstable above 150C, yet the results were more predictable. This instability was attributed to the non-equilibrium condition of the electrode at higher temperatures and pressures. By using a 0.01 M $[\text{Cl}^-]$ concentration within the electrode compartment, this equilibration rate was intentionally enhanced although other adverse factors were predominating. The bare electrolytic

Ag/AgCl wire exhibited the most predictable stable response at higher temperatures. Above 150C, however, the solubility of Ag ion impurities from the Ag/AgCl wire was appreciable in a 2-liter vessel.

For high temperature aqueous environments, the Pd-H was observed to be a stable, viable reference electrode. The Pd-H electrode consisted of a Pd membrane with high surface area Pt plates on both the electrolytic and gaseous sides. Hydrogen gas was effectively removed from the system and isolated on one side of the membrane (gaseous side) and the test solution was in direct contact with the other side of the membrane (electrolytic side). With reference to the Ag/AgCl electrode in a 0.01 M HCl solution, this Pd-H electrode exhibited the same potential difference as the standard hydrogen electrode. The reaction mechanisms on this Pd-H electrode were even similar to the standard hydrogen electrode. Not only was the hydrogen discharge mechanism shown to be rate controlling, but it was also shown that one electron transfers for every hydrogen ion that is discharged in the overall reaction.

The catalytic activity of the palladium surface is susceptible to the same types of contaminants as the platinum surface. Silver ions were reduced at the Pd-H surface at higher temperatures and thereby 'poisoned' the electrode. Other noble metal ions may also selec-

tively reduce at the Pd-H surface. Over a period of at least seven days of testing, the response of the Pd-H electrode was not impaired by the presence of dissolved oxygen, carbon dioxide, or other impurities in the atmosphere. A variety of junction configurations though, could be devised to isolate the Pd-H membrane electrode from the test solution. Also, a flowing hydrogen gas stream rather than the static hydrogen atmosphere could be used to enhance hydrogen contact with the Pd-H membrane. This 'flowing' Pd-H electrode would consist of a U-tube arrangement with feed-throughs into and out of the test solution. As a corrosion monitor, this type of reference electrode is adaptable to many different types of applications.

Finally, the applications and projections for this reference electrode should be more accurately assessed in future research. The electrode appears limited to acid aqueous media (i.e. discharge of hydrogen ions), though stability may also prevail in basic media. The basic hydrogen absorption mechanisms within the Pd lattice are not quite understood and with an understanding of this phenomenon, a complete standard hydrogen electrode may be devised for a multitude of applications.

REFERENCES CITED

1. Bovankovich, J. C., "On-Line Corrosion Monitoring", Mater. Prot. Performance, 12 6 p. 20-3, (1973).
2. Fincher, D. R., Nestle, A. C., "New Developments in Monitoring Corrosion Control", Mater. Prot. Performance, 12 7 p. 17-22, (1973).
3. Glanville, R., Richards, P. H., and Tozer, B. A., "The Laser Corrosion Monitor", Combustion, 49 5 p. 18-22, (1977).
4. Callow, L. M., Richardson, J. A., and Dawson, J. L., "Corrosion Monitoring Using Polarization Resistance Measurements I. Techniques and Correlation and II. Sources of Error", Br. Corros. J., p. 123-139, (1976).
5. Ives, D. J. G., and Janz, G. J., Reference Electrodes, New York, Academic Press, (1961).
6. Audubert, R., Discussions Faraday Soc., 1, 72, (1974).
7. Biegler, T., and Woods, R., "The Standard Hydrogen Electrode: A Misrepresented Concept", J. of Chem. Educ., v. 50, no. 9, p. 604-5, (1973).
8. Case, B., and Bignold, G. J., J. Appl. Electrochem., v. 1, p. 141, (1971).
9. MacDonald, Digby D., "Reference Electrodes for High Temperature Aqueous Systems: A Review and Assessment", Corrosion, (NACE), v. 34, no. 3, p. 75-84, (1978).
10. Dobson, J. V., Snodin, P. R., and Thirsk, H. R., Electrochim Acta, v. 21, p. 527, (1976).
11. Jones, D. de G., and Masterson, H. G., "Techniques for the Measurement of Electrode Processes at Temperatures Above 100C", Advances in Corrosion Science and Technology, v. 1, p. 1, (1970).

12. Lietzke, M. H., and Stoughton, R. W., J. of Phys. Chem., v. 67, p. 2573, (1963).
13. Compton, K. G., "The Use of Reference Electrodes in Corrosion Studies", Materials Research and Standards, v. 10, no. 1, p. 13-15, 59-60, 64, (1970).
14. Greeley, R. S., Smith, W. T., Stoughton, R. W., and Lietzke, M. H., "Electromotive Force Studies in Aqueous Solutions at Elevated Temperatures I. The Standard Potential of the Silver-Silver Chloride Electrode", J. Phys. Chem., v. 64, p. 652, (1960).
15. Baucke, Friedrich G. K., "Thermodynamics of Solid-State Connected Ion-Sensitive Membrane Electrodes: the Silver-Silver Chloride System II. Standard Potentials (ϵ_0^+ to ϵ_j) between 5 and 90 deg. C. of the 2nd kind Silver-Silver Chloride Reference Electrode with 3.5 M and Saturated KCl Measured by Means of Membrane Electrodes", J. Electroanal. Chem. Interfacial Electrochem., Series: 67, Issue: 3, p. 291-9, (1976).
16. Baucke, Friedrich, G. K., "Electrode Hg, Tl(40 weight %) TlBr(s).dvr.... as Reference Electrode in Aqueous Solution. Reversibility of the System and Standard Potentials ($\epsilon_{deg.} + \epsilon_{silon.}$) of the Half Cell Between 5 and 90 deg", J. Electroanal. Chem. Interfacial Electrochem., Series: 39, Issue: 2, p. 263-73, (1972).
17. Baucke, Friedrich, G. K., "Standard Potentials (ϵ_0^+ to ϵ_j) of the Thalamid Reference Electrode, Hg, Tl(40 wt. %) TlCl(s) KCl(s).dvr....., in Aqueous Solution Between 5 and 90 deg.", J. Electroanal. Chem. Interfacial Electrochem., Series: 33, Issue: 1, p. 135-44, (1971).
18. Dobson, J. V., Chapman, B. R., and Thirsk, H. R., "The Palladium-Hydride Reference Electrode in Hydrogen-Free Electrolyte Solutions at Elevated Temperatures", Int. Corros. Conf. Ser., Series: NACE-4, Issue: High Temp. High Pressure Electrochem. Aqueous Solutions, Conf., p. 341-51, (1976).

19. Lewis, Derek, "Studies of Redox Equilibria at Elevated Temp. I. - The Estimation of Equilibrium Constants and Standard Potentials for Aqueous Systems up to 374C.", Arkiv for Kemi, p. 385-404, (1974).
20. Lewis, Derek, "Theoretical Studies of Aqueous Systems Above 25 deg.. I. Illustration of Data on Aqueous Equilibriums and Equilibrium Data for the System Oxygen(g)-water(l)-hydrogen(g)", Chem. Scr., 74, 6(2), p. 49-54, (1974).
21. Lewis, Derek, "Theoretical Studies of Aqueous Systems Above 25 deg.. I. Fundamental Concepts for Equilibrium Diagrams and Some General Features of the Water System", AB ATOMENERGI, NYKOPING Swed., (AB. Atomenergi, Stockholm (Rapp.)), 71, (AE-431), 23 p., (1971).
22. Greeley, R. S., Smith, W. T., Lietzke, M. H., and Stoughton, R. W., "Electromotive Force Measurements in Aqueous Solutions at Elevated Temperatures. II. Thermodynamic Properties of Hydrochloric Acid", J. Phys. Chem., v. 64, p. 1445, (1960).
23. Lindsay, W. T., and Pement, F. W., "Electrical Resistance of Alpha Hydrogen-Palladium", J. of Chem. Physics, v. 36, no. 5, p. 1229-1234, (1962).
24. Simons, J. W., and Flanagan, T. B., "Electrical Resistance of Dilute Solutions of Hydrogen in Palladium", J. of Chem. Physics, v. 44, no. 9, p. 3486-90, (1966).
25. Moon, K. A., "Pressure-Composition-Temperature Relations in the Palladium-Hydrogen System", J. Phys. Chem., v. 60, p. 502-4, (1956).
26. Barton, J. C., and Lewis, F. A., Z. Phys. Chem., N. F. 33, p. 99, (1962).
27. Bruning, H., and Sieverts, A., Z. Phys. Chem., 163A, p. 409, (1933).
28. Lewis, F. A., The Palladium Hydrogen System, London, Academic Press, (1967).

29. Gillespie, L. J., and Hall, F. P., "The Palladium-Hydrogen Equilibrium and Palladium Hydride", J. Am. Chem. Soc., 48, p. 1207, (1926).
30. Wicke, Von E., and Nernst, G. H., "Phase Diagram and Thermodynamic Behavior of the Systems Pd/H₂ and Pd/D₂ at Normal Temperatures: H/D Separation Effect", Z. Elektrochem., v. 68, no. 3, p. 224-35, (1964).
31. Smith, D. P., and Derge, G. J., "The Role of Intragranular Fissures in the Occlusion and Evolution of Hydrogen by Palladium", J. Amer. Chem. Soc., v. 56, p. 2513-25, (1934).
32. Levine, P. L., and Weale, K. E., Trans. Faraday Soc., 56, p. 357, (1960).
33. Krause, W., and Kahlenberg, L., Trans. Electrochem. Soc., 68, p. 449, (1935).
34. Aben, P. C., and Burgers, W. G., "Surface Structure and Electrochemical Potential of Palladium While Absorbing Hydrogen in Aqueous Solution", Trans. Faraday Soc., 58, p. 1989-1992, (1962).
35. Schuldiner, S., Castellan, G., and Hoare, J., "Electrochemical Behavior of the Palladium-Hydrogen System", J. of Chem. Physics, v. 28, no. 1, p. 16-24, (1958).
36. Fallon, J. R., and Castellan, G. W., "The Mechanism of Occlusion of Hydrogen by Palladium in Contact with Sulfuric Acid Solution", J. Phys. Chem., v. 64, p. 4-9, (1960).
37. Simons, J. W., and Flanagan, T. B., "Absorption Isotherms of Hydrogen in the α -phase of the Hydrogen Palladium System", J. of Phys. Chem., v. 69, no. 11, p. 3773-3781, (1965).
38. Flanagan, T. B., and Lewis, F. A., "Hydrogen Absorption by Palladium in Aqueous Solution", Trans. Faraday Soc., 55, p. 1400-1408, (1959).
39. Smith, Hydrogen in Metals, Chicago, Chicago Univ., (1940).

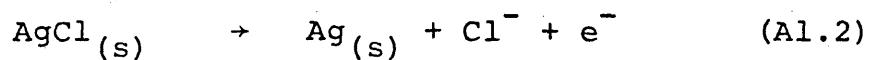
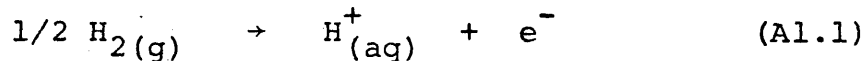
40. Dobson, J. V., "Potentials of the Palladium Hydride Reference Electrode Between 25 and 195 deg.", J. Electroanal. Chem. Interfacial Electrochem., Series: 35, p. 129-35, (1972).
41. Dobson, J. V., Dagless, M. N., and Thirsk, H. R., "Plateau Potentials of the $\alpha+\beta$ Palladium Hydride Electrode at Temperatures between 25 and 195C", J. Chem. Soc., Faraday Trans. 1, v. 68, p. 764, (1972).
42. Vasile, M. J., and Enke, C. G., "The Preparation and Thermodynamic Properties of a Palladium-Hydrogen Electrode", J. of Electrochemical Soc., v. 112, no. 8, p. 865-70, (1965).
43. Castellan, G. W., "The Transmission of Electrolytically Deposited Hydrogen through a Palladium Membrane Electrode", J. of Electrochemical Soc., v. 111, no. 11, p. 1273-83, (1964).
44. Silberg, P. A., and Bachman, C. H., J. Chem. Phys., v. 29, no. 4, p. 777, (1958).
45. Agrawal, A. K., and Staehle, R. W., "A Silver-Silver Chloride Reference Electrode for the High Temperature and High Pressure Electrochemistry", Corrosion (Houston), Series: 33, Issue: 11, p. 418-19, (1977).
46. Lederer, L., and Greene, N. D., "Electrochemical Behavior of a Palladium Hydrogen-Diffusion Electrode", Electrochimica Acta, v. 8, p. 883-886, (1963).
47. Cleary, H. J., and Greene, N. D., "Electrochemical Energy Conversion in a Palladium-Hydrogen Diffusion Electrode", Electrochimica Acta, v. 10, p. 1107-1115, (1965).
48. Barner, H. E., and Scheuerman, R. V., Handbook of Thermochemical Data for Compounds and Aqueous Species, New York, John Wiley & Sons, 156p. (1978).
49. Kubaschewski, O., Alcock, C. B., Metallurgical Thermochemistry, 5th ed., New York, Pergamon Press, 449 p., (1979).

50. Bockris, J. O'M., and Reddy, A. K. N., Modern Electrochemistry, New York, Plenum Press, 1432 p., (1970).
51. McKaveney, J.P., and Byrnes, C.J., "Analytical Monitors Using Electrodes of Semiconductors (Germanium, Indium-Antimonide, and Silicon)", Analytical Chemistry, v. 44, no. 2, p. 290-293, (1972).

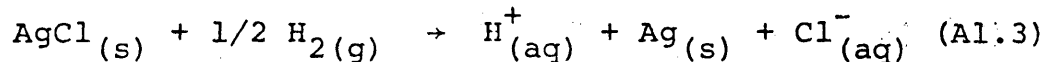
APPENDIX

A1 Estimation of Gibbs Free Energies at Elevated
Temperatures for the Ag/AgCl - H⁺/H₂ System -

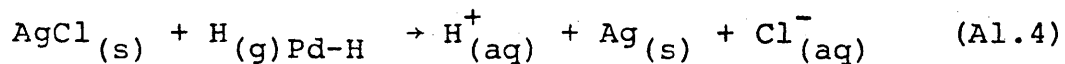
Consider first the two half cell reactions for the Ag/AgCl - H⁺/H₂ system;



The overall reaction would then be;



or for Pd-H;



The reference temperature and pressure will be 298.15K and 1 atm respectively for the following calculations. To calculate the standard Gibbs Free Energy change, ΔG_{298}° , for reaction A1.3, the following relationship was used;

$$\Delta G_{298}^{\circ} = \sum_{\text{prod}} \nu_p G_{p,T,P}^{\circ} - \sum_{\text{reac}} \nu_r G_{r,T,P}^{\circ} \quad (\text{A1.5})$$

and at 298K, $\Delta G_{298}^{\circ} = -5.1 \text{ Kcal/g-mole} \quad (48)$

Likewise, ΔH_{298}° and ΔS_{298}° were calculated with the following thermodynamic expressions;

$$\Delta H_{298}^{\circ} = \sum_{\text{prod}} \nu_p H_{p,T,P}^{\circ} - \sum_{\text{reac}} \nu_r H_{r,T,P}^{\circ} \quad (\text{A1.6})$$

$$\text{and } \Delta S_{298}^{\circ} = \frac{\Delta H_{298}^{\circ} - \Delta G_{298}^{\circ}}{T} \quad (\text{A1.7})$$

where T is in degrees Kelvin. The calculated values for ΔH_{298}° and ΔS_{298}° are -9.5 kcal/g-mole and -0.0148 kcal/g-mole- $^{\circ}\text{K}$ respectively.

Having calculated the standard Gibbs free energy change at 298K and 1 atm for reaction A1.3, this value for the reference state can be used to calculate the Gibbs free energy change at elevated temperatures. The Gibbs free energy function, ΔG_T° , is given by;

$$\Delta G_T^{\circ} = \Delta G_{298}^{\circ} - \Delta S_{298}^{\circ} \Delta T + \Delta \bar{C}_p^{\circ} \int_{298}^T \cdot \{T - T \ln(T/298)\} \quad (\text{A1.8})$$

where \bar{C}_p° is the average heat capacity of a specie.

The average heat capacities of nonionic species are calculated from existing C_p data. The two non-ionic specie in reaction A1.3 are $\text{Ag}_{(s)}$ and $\text{AgCl}_{(s)}$ and the C_p relationships are(49);

$$\text{For } \text{Ag}_{(s)}: C_p = 5.09 + 2.04 \times 10^{-3}T + 0.36 \times 10^5 T^{-2}$$

$$\text{and for } \text{AgCl}_{(s)}: C_p = 14.88 + 0.001T - 2.7 \times 10^5 T^{-2}$$

T is in degrees Kelvin and C_p is in cal/mole-deg.

Also, the average heat capacity of an ion was calculated using the following relation;

$$\bar{C}_p^{\circ} \Big|_{298}^T = (\bar{S}_T^{\circ} - \bar{S}_{298}^{\circ}) / \ln(T/298) \quad (\text{A1.9})$$

where \bar{S}_T° is equal to the partial molal entropy of an ion. The calculated Gibbs free energies at elevated temperatures, using equation A1.8 are presented in Table A1.

A2 Estimation of Potential Differences for the

Ag/AgCl - Pd-H System - Consider again the half cell reaction given in A1.1. The $H_2(g)$ refers to dissolved molecular hydrogen in solution. Later, in the mechanistic approach to the overall reaction scheme, the hydrogen at the Pd-H surface will be referred to as $H_{(Pd-H)}$, whereas $H_2(Pd-H)$ pressures (at α_{max}) will be used in the following thermodynamic calculations.

A2.1 Calculation of the Standard Electrode Potential (E_T°) -

For an electrode at equilibrium, the standard potential, E_T° , is related to the Gibbs free energy change of the cell reaction by the following expression;

$$E_T^{\circ} = -\Delta G_T^{\circ} / nF \quad (\text{A2.1})$$

The estimated E_T° values are given in Table A1.

	Temperature (°C.)				
	25	60	100	150	200
ΔG_T° (kcal/mole) Gibbs Free Energy	-5.1	-4.51	-3.69	-2.41	-0.808
E_T° (volts) Standard Potential	0.221	0.1956	0.1602	0.1046	0.0351

TABLE A1 - ESTIMATED GIBBS FREE ENERGIES AND STANDARD REST POTENTIALS FOR THE AG/AGCL - PD-H/H₂ SYSTEM AT ELEVATED TEMPERATURES

E_T (volts) Potential Difference	TEMPERATURE (°C.)				
	25	60	100	150	200
Constant H ₂ (g) (Sec. A2.2)	0.491	0.496	0.497	0.486	0.462
Variable H ₂ (g) (Sec. A2.3)	0.421	0.454	0.497	-	-

TABLE A2 - ESTIMATED POTENTIAL DIFFERENCES FOR THE AG/AGCL-PD-H/H₂ SYSTEM AT ELEVATED TEMPERATURES

A2.2 Calculation of Potential Difference Assuming

a Constant Hydrogen Pressure - The actual potential difference can be calculated from the Nernst equation;

$$E_T = E_T^{\circ} + (RT/nF) \ln(P_{H_2}) \quad (A2.2)$$

For the overall cell reaction in A1.3, and assuming dilute (<0.01 M) solutions, the potential difference is therefore;

$$E_T = E_T^{\circ} + (RT/nF) \ln \frac{[H^+][Cl^-]}{P_{H_2}^{1/2}(\text{Pd-H})} \quad (A2.3)$$

Recall that in a standard hydrogen evolution reaction, the hydrogen pressure is equal to 1 atm. This pressure, 1 atm, is actually the pressure of dissolved molecular hydrogen in the bulk of the solution and at the reaction surface, the pressure is less than 1 atm (i.e. diffusion and concentration gradients). In these calculations, the hydrogen pressure refers to the pressure of hydrogen in the α phase at the surface of the Pd-H electrode. It was found, with appropriate curve fitting, that a constant 0.353 atm was used in the calculation of the potential difference. Also, since the pH of the solution is ≈ 2.35 , or a $[H^+]$ concentration equal to 0.0045 M,

the $[Cl^-]$ concentration is equal to 0.0045 M. The calculated potential differences, using equation A2.3, are given in Table A2.

A2.3 Calculation of Potential Difference Assuming Hydrogen Pressure varies with α_{max}

Consider again equation A2.3, the Nernst equation for this system;

$$E_T = E_T^O + (RT/nF) \ln \frac{[H^+][Cl^-]}{P_{H_2}^{1/2}} \quad (A2.3)$$

Instead of assuming the hydrogen pressure is constant (Sec. A2.2) at the Pd-H surface, it will be assumed that the hydrogen pressure varies with α_{max} .

J.V. Dobson(41) has given values for the variation of α_{max} in terms of atom ratio, H/Pd, at increasing temperatures (Refer to Table A3). Also, according to Wicke and Nernst(30), the pressure of hydrogen in the α phase can be calculated from the atom ratio using the following expressions;

$$\ln P_{H_2}(\text{atm}) = -1/RT \cdot \Delta H_{H_2}(T,n) + 12.9 + 2 \ln \frac{n}{1-n} \quad (A2.4)$$

$$\text{and } \Delta H_{H_2}(T,n) = [4620 + 9000(1 + 445/T) \cdot n - 150] \quad (A2.5)$$

where $\Delta H_{H_2}(T,n)$ is in cal/mole.

The variation of hydrogen pressure in α_{\max} Pd-H with temperature is given in Table A3. With the information in Table A3, and using equation A2.3, the potential differences for the system were calculated and presented in Table A2.

A3 Estimation of Activity Coefficients with the

Debye- Huckel Limiting Law - To correct for the non-ideality of the system, calculations of the activity coefficients were made for 0.01 M HCl solutions at elevated temperatures. The Debye- Huckel Limiting Law was used to roughly estimate the activity coefficients for H^+ and Cl^- ions and comment on its use in calculating the potential differences in Section A2. The Debye- Huckel relation is given as;

$$-\log \gamma_i = \frac{AZ_i^2(I)^{1/2}}{1 + a_i^O B(I)^{1/2}} \quad (A3.1)$$

I, the ionic strength, is equal to $1/2 \sum m_i Z_i^2$, m_i is the molality of the i^{th} ion, Z_i is the charge of the i^{th} ion, A and B are constants which are characteristic of the solvent, and a_i^O has a value dependent on the effective diameter of the ion. This equation

TEMPERATURE (°C.)	$\eta_{\alpha_{\max}}$	P_{H_2} (atm)	$P_{H_{Pd-H}}$ (atm)
5	0.015	0.0115	0.023
25	0.016	0.0237	0.0474
35	0.017	0.0343	0.0686
60	0.02	0.0823	0.1646
70	0.0215	0.115	0.23
100	0.031	0.353	0.706
120	0.04	0.702	1.404
150	0.06	1.794	3.588
200	0.1	5.66	11.32

TABLE A3 - α_{\max} HYDROGEN PRESSURES AT ELEVATED TEMPERATURES

is valid in dilute solutions and has been extended to 0.01 M solutions. The activity coefficients, γ_i , for the H^+ and Cl^- ions were calculated and presented in Table A4.

Having calculated the activity coefficients in Table A4, the potential differences in Section A2 were re-determined. The amount of error incurred by not using non-ideality corrections was less than 1 percent at 22C and less than 2.3 percent at 200C. Since there were slight uncertainties in the actual measured potentials and pH of the system, it was felt that this non-ideality correction was not significant in the calculations in Section A2.

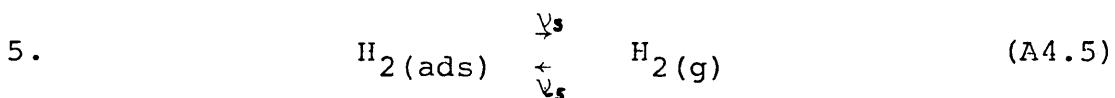
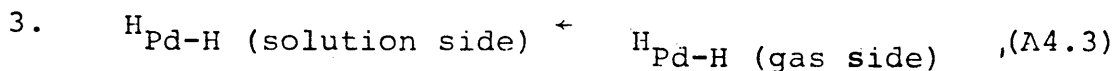
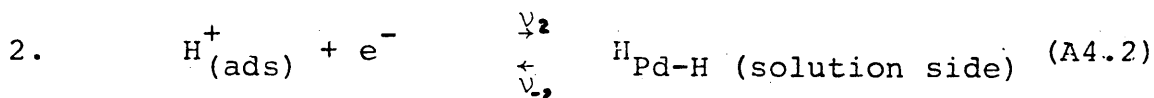
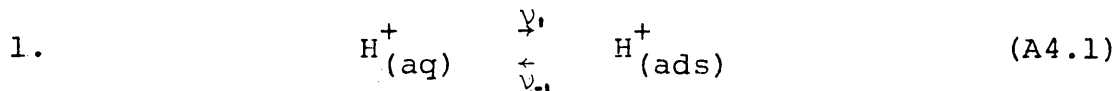
A4 Determination of Pd-H Rate Determining Step -

In setting up the overall reaction scheme for the Pd-H electrode, it is difficult to ascertain which particular steps are at equilibrium or at steady state. The sequence of reaction steps which simulate the standard hydrogen reaction would have to be in equilibrium. Although an entire reaction scheme will be presented, representing both the 'entrance' and 'exit' planes of the Pd-H membrane, one or two steps may control the entire hydrogen reaction mechanism.

TEMPERATURE (°C.)	A (kg ^{1/2} mole ^{1/2})	B (x10 ⁻³) (kg ^{1/2} cm·mole ^{1/2})	γ_{H^+} ($\bar{a}=9 \times 10^{-8}$)	γ_{Cl^-} ($\bar{a}=3 \times 10^{-8}$)
22	0.515	0.3285	0.9125	0.898
60	0.548	0.3343	0.9076	0.892
100	0.596	0.3416	0.9	0.883
150	0.686	0.350	0.887	0.863
200	0.81	0.358	0.868	0.845

TABLE A4 - ACTIVITY COEFFICIENTS FOR (Cl⁻) AND (H⁺)
IONS IN 0.01 M HCL AT ELEVATED TEMPERATURES

The assumed reaction scheme is as follows (Refer also to Figure);



Bockris and Reddy (50) use a step by step procedure to arrive at the Butler-Volmer equation for multi-step reactions and this procedure will be followed here.

Assuming Step 2 (A4.2) is the rate determining step (rds);

$$\begin{aligned} i &= F(v_{-2} - v_2) \\ &= F[k_{-2}(1-\theta_{\text{H}^+})e^{(1-\beta)F\Delta\phi/RT} - k_2\theta_{\text{H}^+}e^{-\beta F\Delta\phi/RT}] \end{aligned}$$

where v_2 is the reaction rate in the cathodic direction, v_{-2} is the reaction rate in the anodic direction, and θ_{H^+} is the fraction of surface covered by adsorbed H^+ ions.

Next, assuming that $\theta_{H^+} \ll 1$, then $(1 - \theta_{H^+}) \approx 1$, and;

$$i = F[k_{-2}e^{(1-\beta)F\Delta\phi/RT} - k_2\theta_{H^+}C_{H^+}e^{-\beta F\Delta\phi/RT}]$$

At this point, suppose $\Delta\phi$ is sufficiently positive with respect to the equilibrium potential, then;

$$i = F[k_{-2}e^{(1-\beta)F\Delta\phi/RT}]$$

Now $\Delta\phi$ can be solved for in terms of $\log i$;

$$\Delta\phi = -\frac{2.3RT}{(1-\beta)F} \log(Fk_{-2}) + \frac{2.3RT}{(1-\beta)F} \log i$$

or
$$\Delta\phi = \frac{2.3RT}{(1-\beta)F} \log i + \text{constant}$$

Assuming $\beta=0.5$, the slope (anodic tafel constant) of a $\Delta\phi$, or overpotential, versus $\log i$ plot would be;

$$\text{slope} = \beta_a = \frac{2.3(8.31)(298)}{(0.5)(96,500)} = 0.118$$

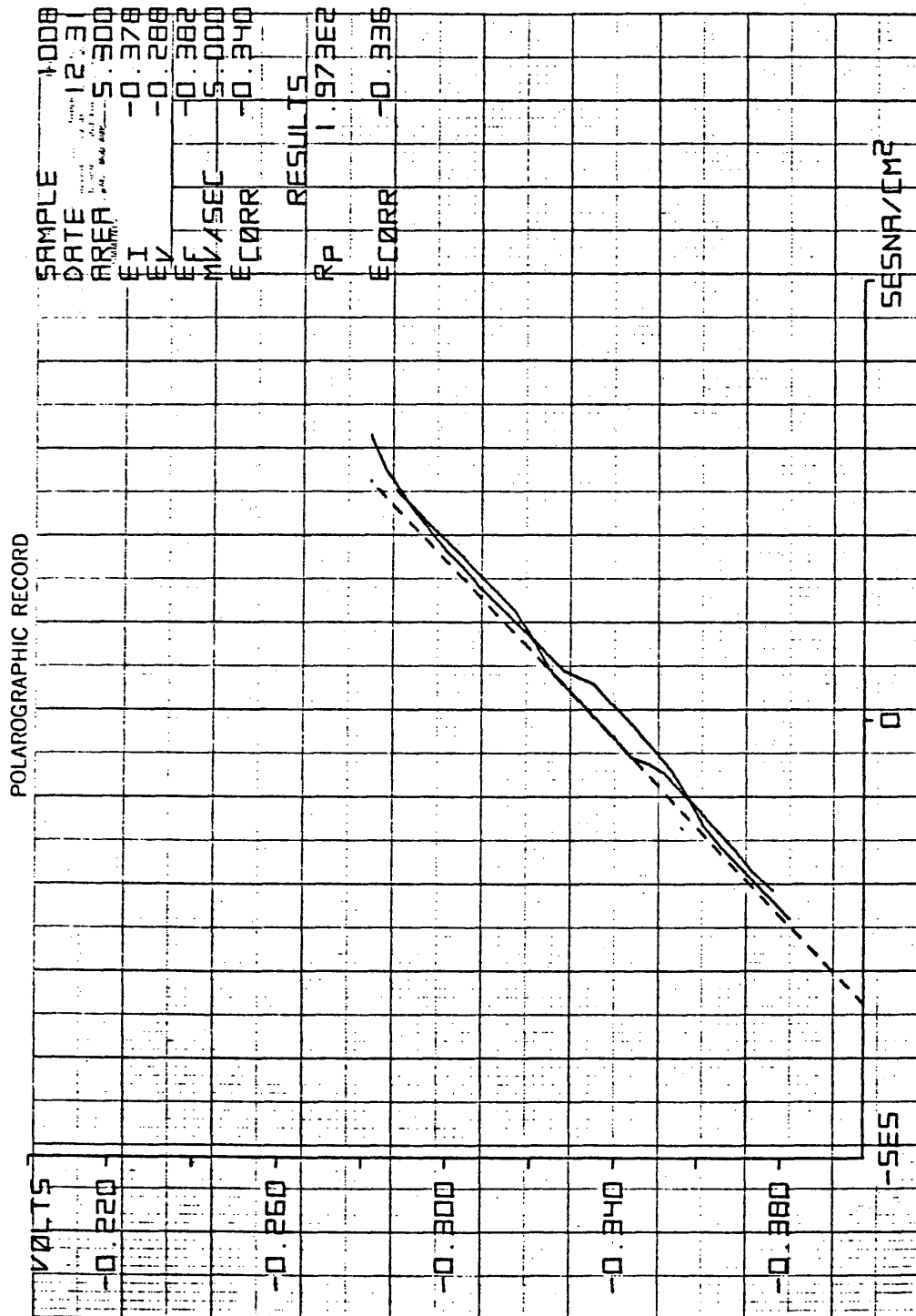
Therefore, if the actual anodic tafel constant, β_a , were equal to 0.118, then this would verify Step 2, or;



as the rate determining step within the realm of the original assumptions.

A5 Polarization Measurements - The actual linear polarization scans for Pd-H and the potentiodynamic

scans for pure Ag are presented in the proceeding figures. Although anodic and cathodic scans were run at the Ag surface to determine exchange current densities, the information was not presented in this thesis. The location of the vertical line on the anodic Ag scan does pinpoint the necessary current density for AgCl deposition (i.e. $\approx 1.0 \text{ ma/cm}^2$ in 0.01 M HCl solution). The information from the other figures, however, was used in the presentation of this thesis.



Figures A1 - Linear polarization scan of Pd-H electrode in 0.001 M HCl at 25C.

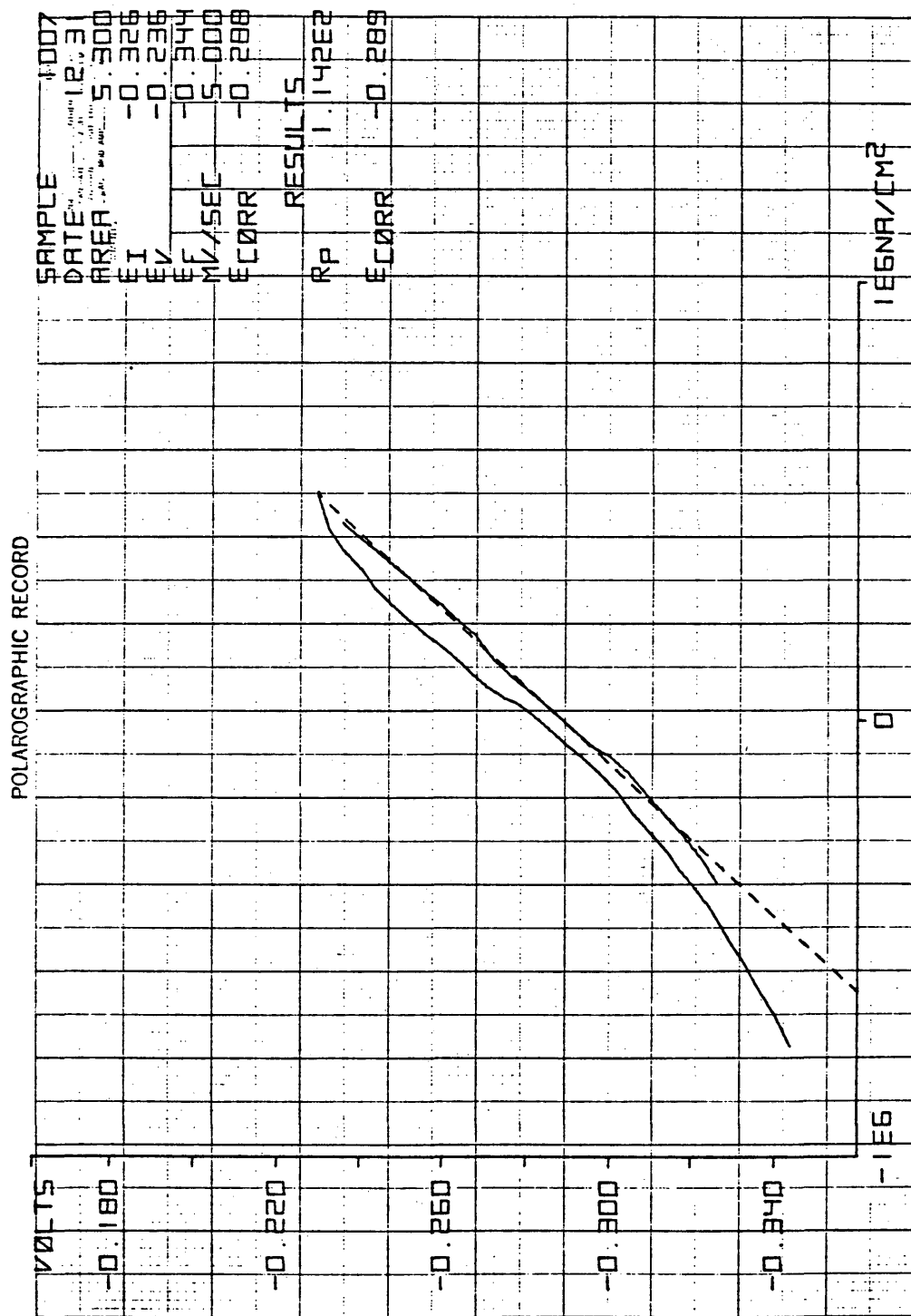


Figure A2 - Linear polarization scan of Pd-H electrode in 0.01 M HCl at 5C.

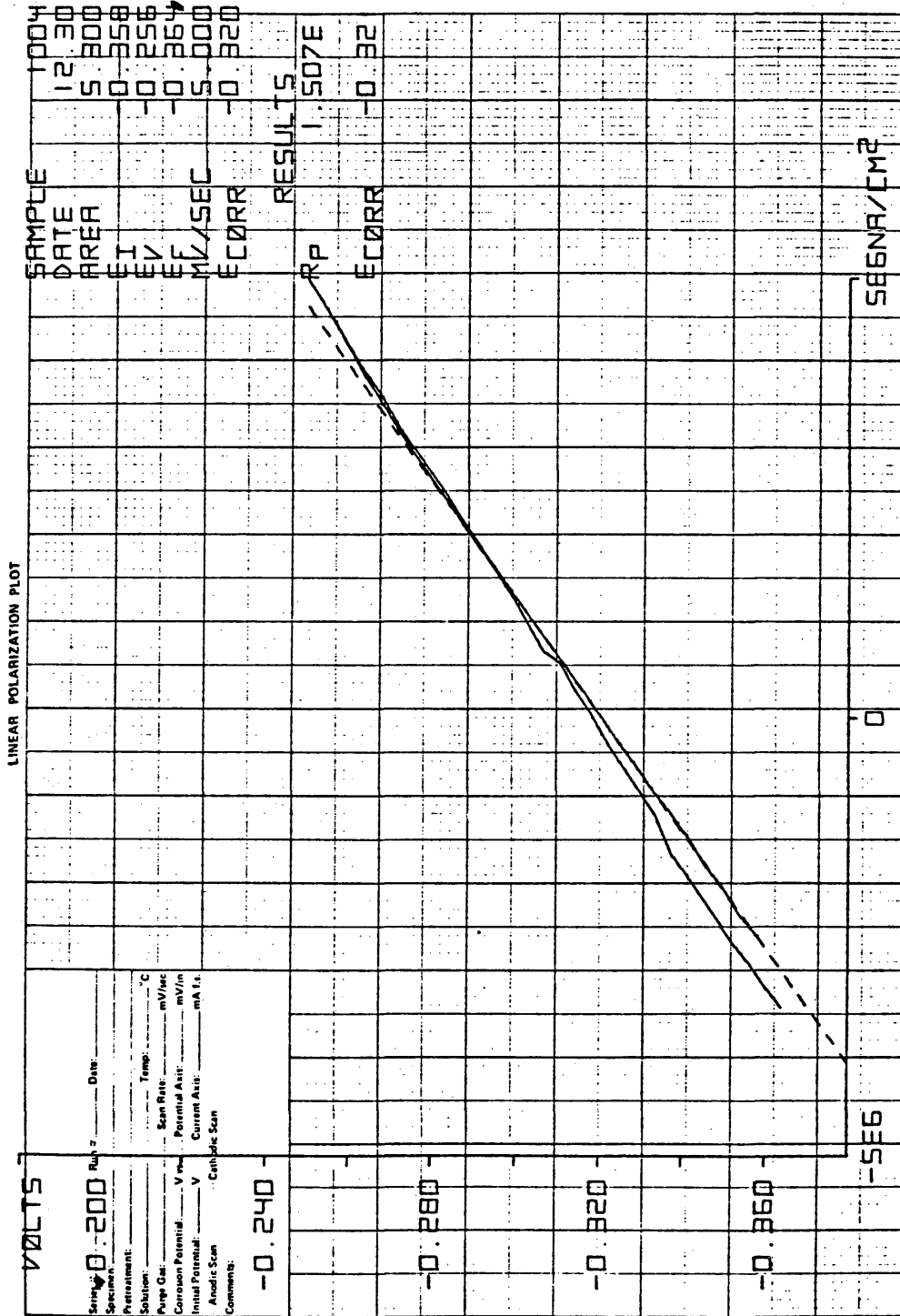


Figure A3 - Linear polarization scan of Pd-H electrode in 0.01 M HCl at 35°C.

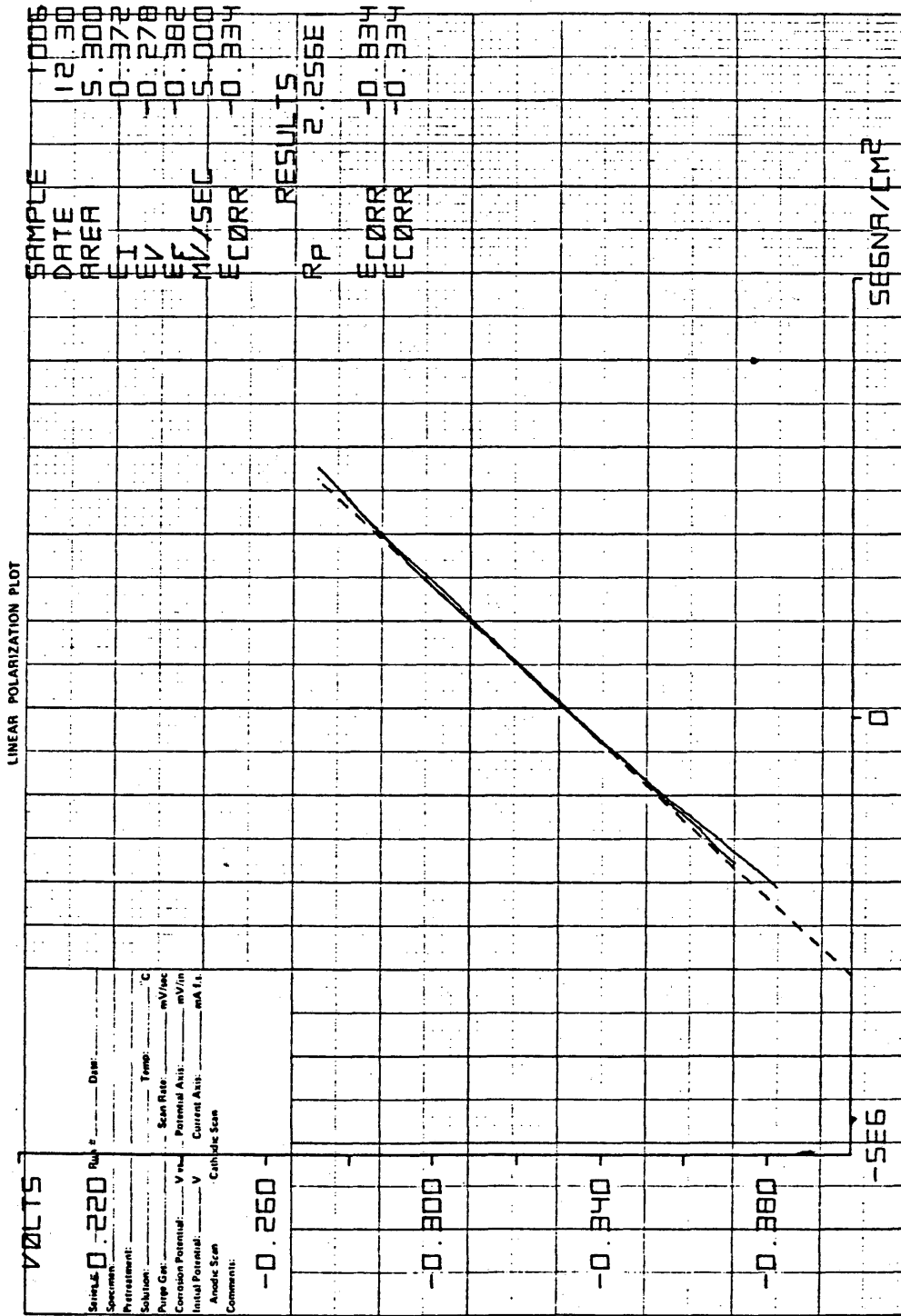


Figure A4 - Linear polarization scan of Pd-H electrode in 0.01 M HCl at 70C.

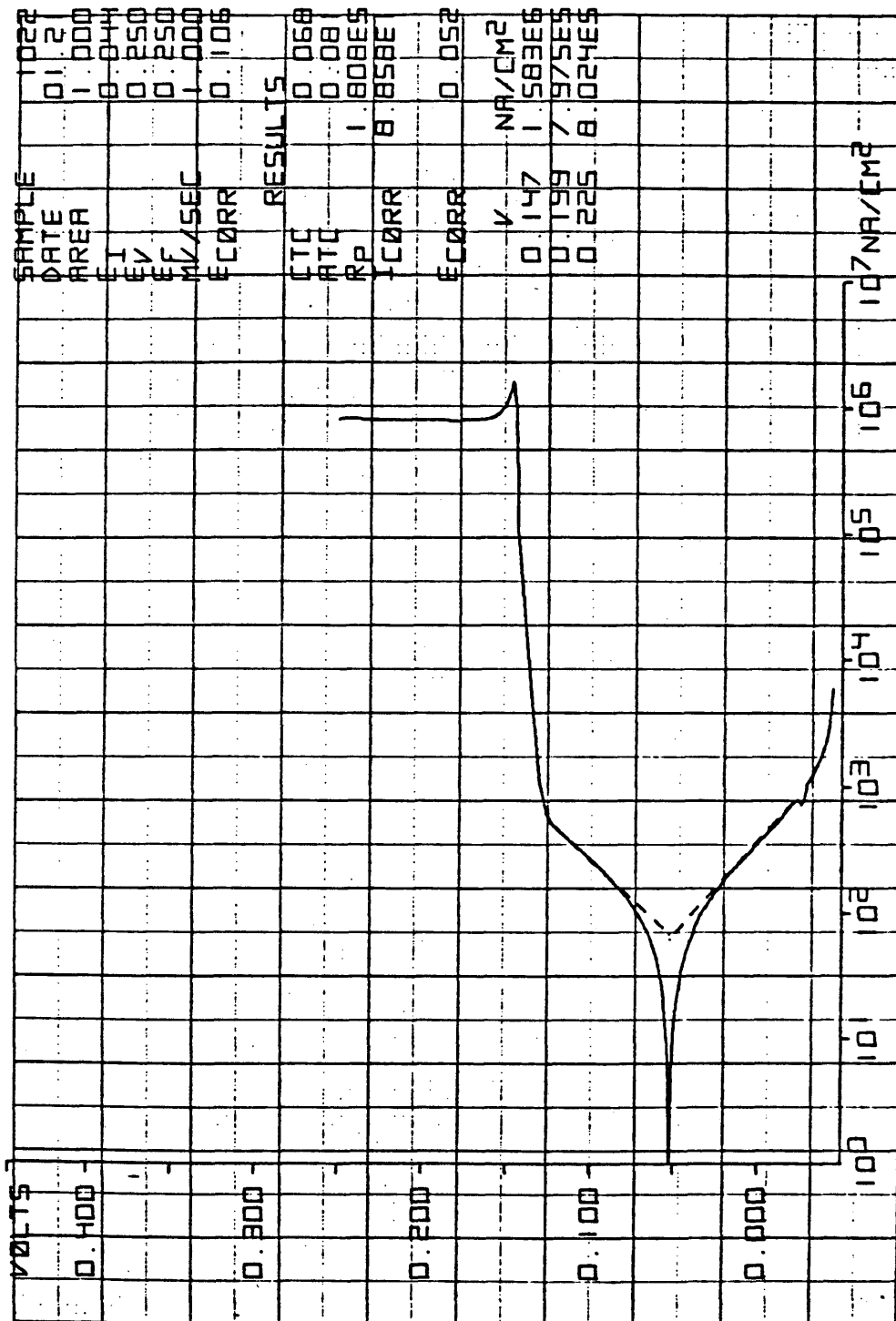


Figure A7 - Potentiodynamic scan of Ag metal in 0.01 M HCl at 40C.

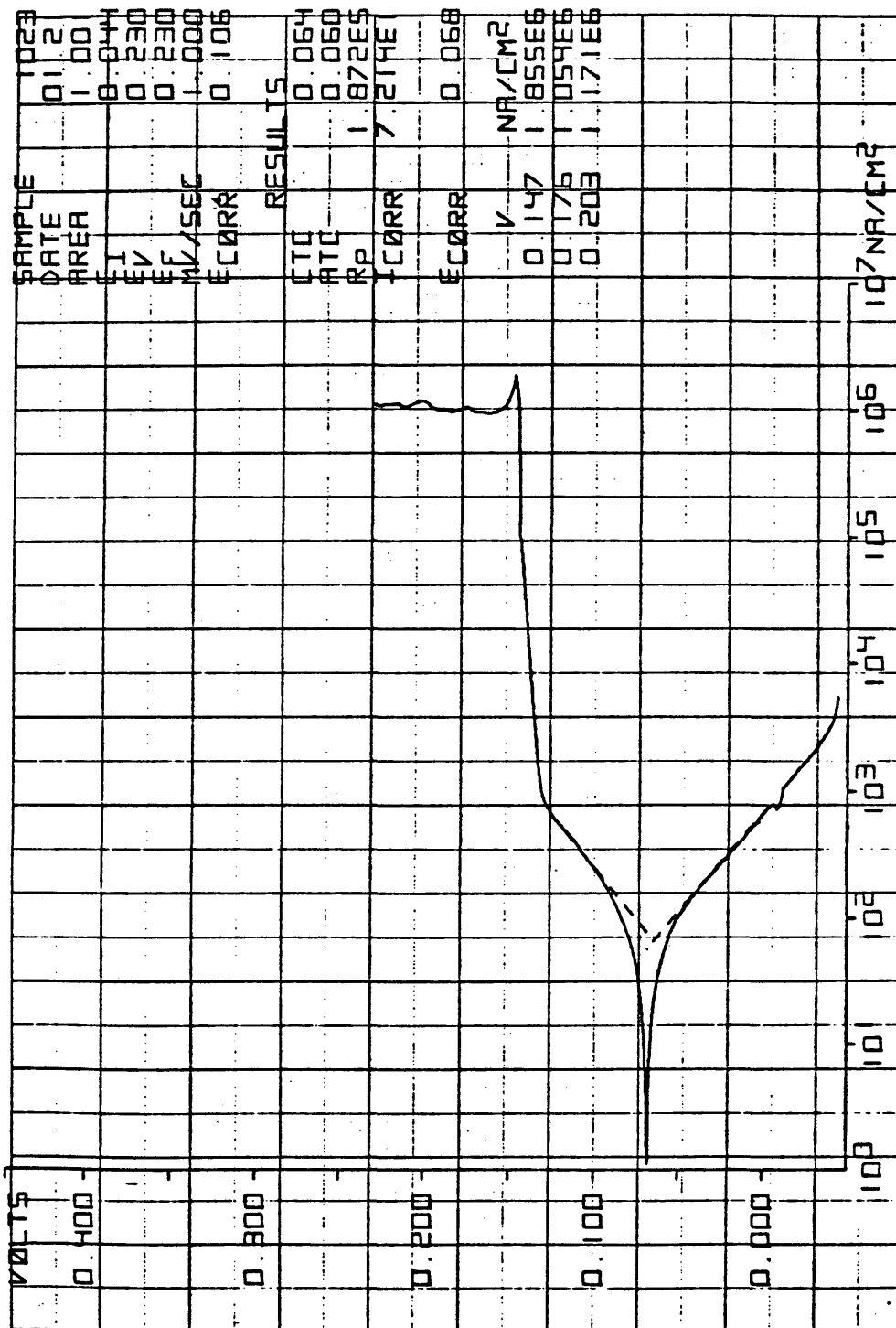


Figure A8 - Potentiodynamic scan of Ag metal in 0.01 M HCl at 60C.

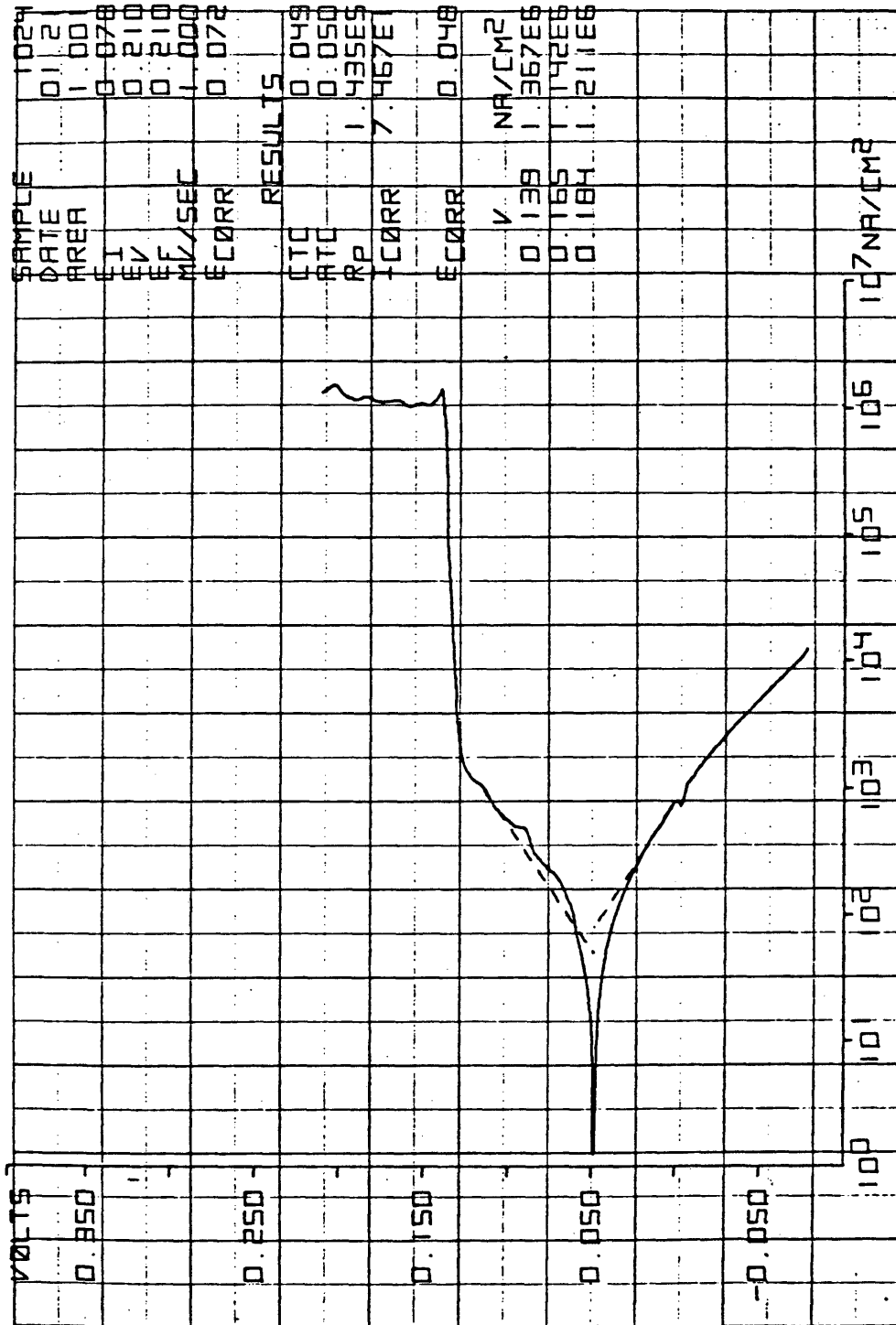


Figure A9 - Potentiodynamic scan of Ag metal in 0.01 M HCl at 77.2°C.